TRANSCEND

Transformative Science and Engineering for Nuclear Decommissioning

Small Modular Radiation Experimental Systems: Development and Future Application

Christopher Anderson (and many more), Dalton Cumbrian Facility, University of Manchester

Theme 4: Nuclear Materials

03/12/20
Location: Sunny Cumbria

Energy
For a Low Carbon Future

Presentation Schedule

Section 1: Background and doctrine

Section 2: Current developments

Section 3: Future applications and plans

What is this project?

Small MOdular Radiation Experimental Systems

SMORES

Not as delicious

Based at DCF, West Cumbria

Project has expanded into a community of contributors

The idea of SMORES is in the name..

With the primary aim being:

- **Building a suite of modular components suitable for radiation experiments**

This component development will include but is not limited too..

Microcontrollers

Sensing technology

Infrastructure

Mechanical accessories

But why develop these systems?

- DCF has a history of building one off systems to serve one project before being abandoned
- Externals don't always have the ability to fully utilise the equipment at DCF
- Extant systems aren't always compatible with each-other
- There is a significant lack of gas related radiation experimental equipment (important because of Sellafield storage).
- Current methods and equipment for radiation experiments could be vastly improved upon with the right components

SMORES aims to remedy all of these issues by adhering to the following..

Core philosophy of SMORES

Modularity

Automation

Eventual Active lab Compatibility

In-Situ Sensing

Component Standardisation
(where possible)

Remote Accessibility

Section 2: Current developments in SMORES

Time to be more specific..

The core of SMORES will be based upon a newly designed gas manifold that incorporates the key ideals of the previous slide (first iteration will focus on this).

The manifold is standardised to the following:

- Primarily Swagelok ¼” tubing and fittings connecting components
- Pressure ratings exceeding 28.4 bar (agreed in the DCF-NNL-Sellafield meeting)
- Arduinos as the microcontrollers (but with CANopen and python interfaces)
- Made of stainless steel

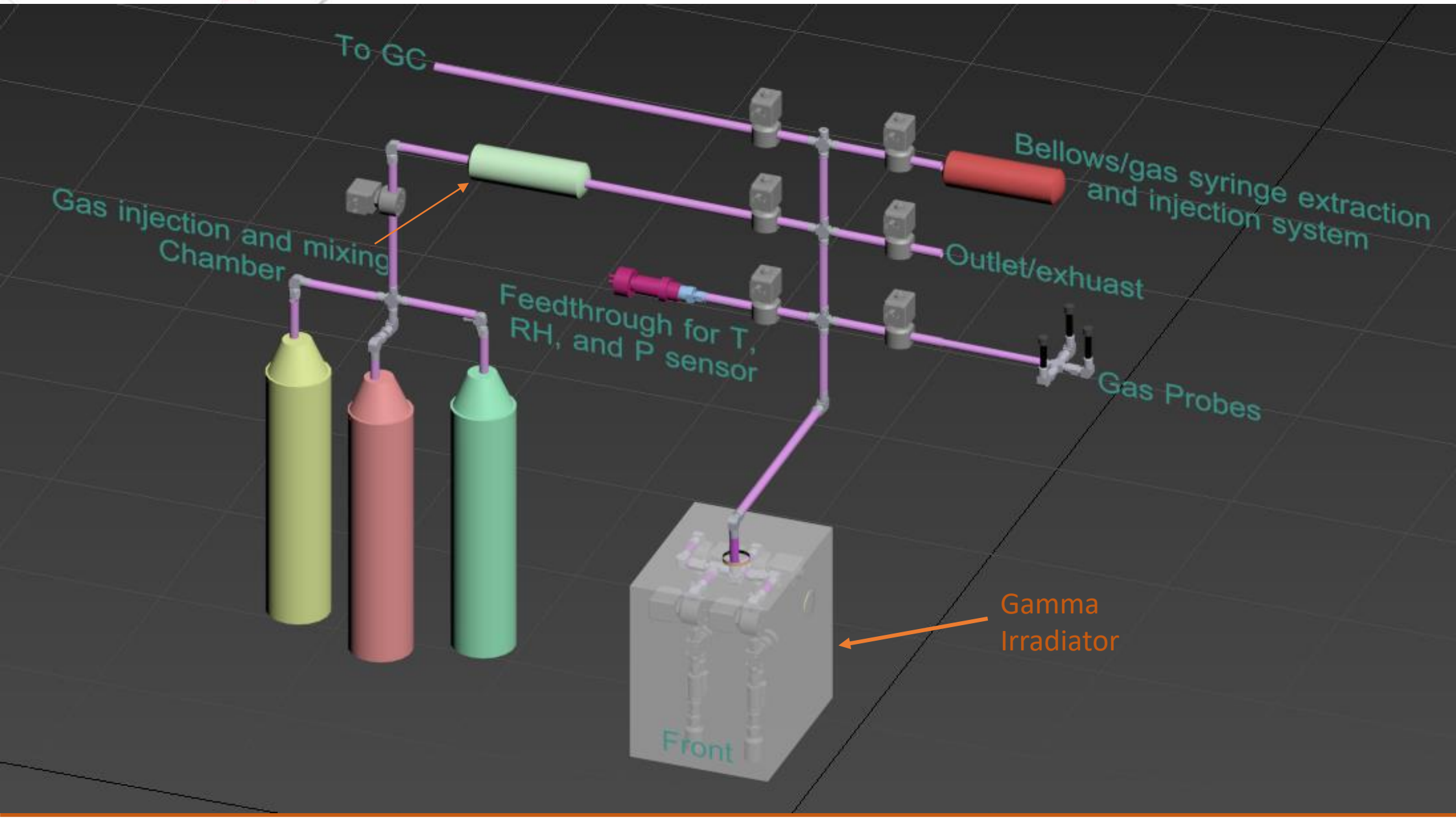
To GC
Bellows/gas syringe extraction and injection system
Gas injection and mixing Chamber
Outlet/exhuast
Feedthrough for T, RH, and P sensor
Gas Probes
Gamma Irradiator
Front

Repeating Sample Units (RSU's)

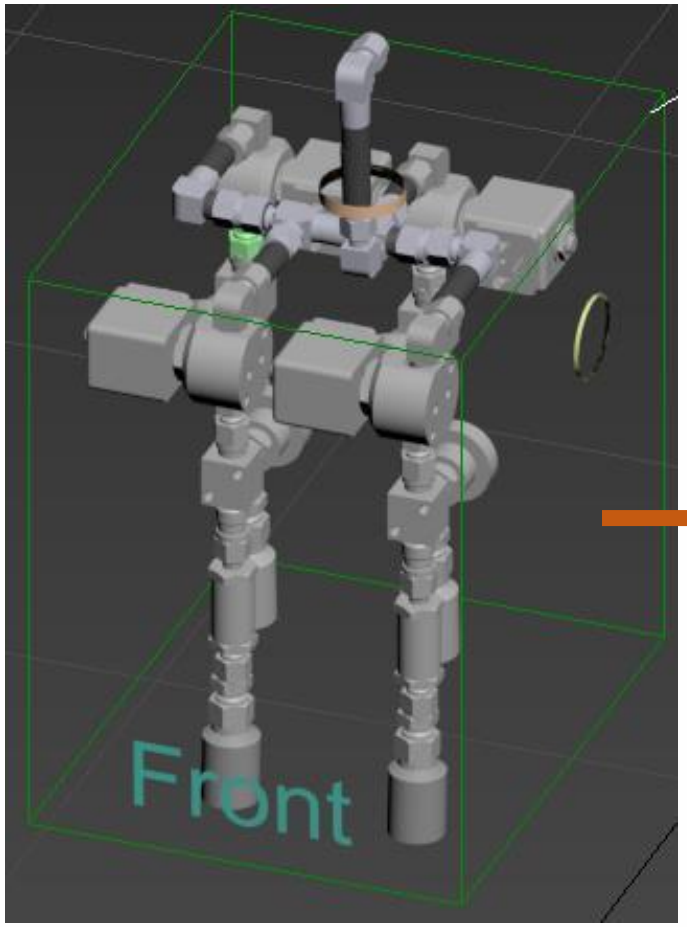

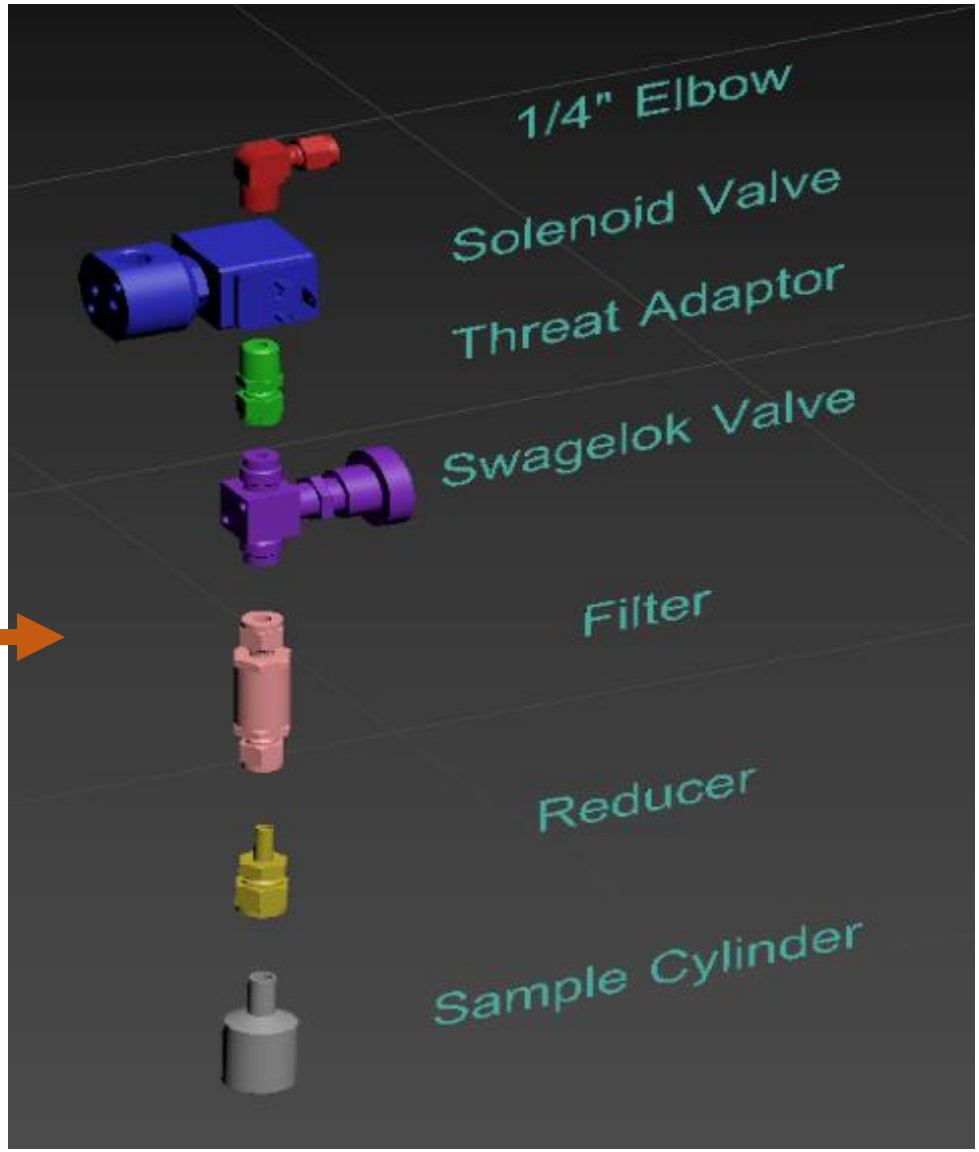

Repeating Sample Units (RSU's)

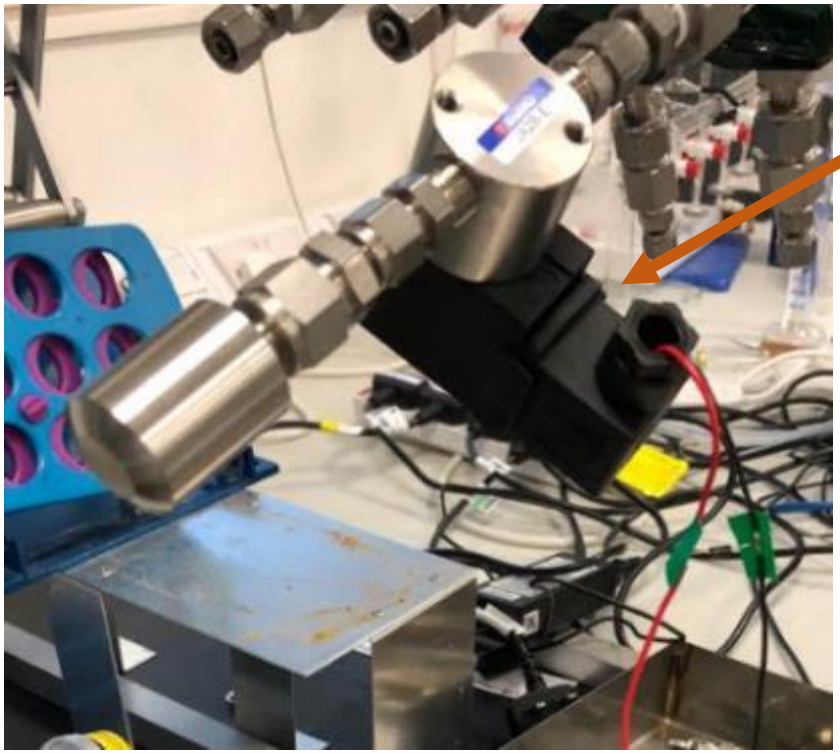

Solenoid Valve
(can be controlled via Arduino)

Swagelok Valves

SMORES Valves

Manual

Solenoids

Why different types?

Cost difference is pretty huge!!

Stainless steel seal will be available eventually

Awaiting delivery to begin testing

Seal: Steel | EPDM | Ruby

ethylene propylene diene monomer rubber

SMORES Valves

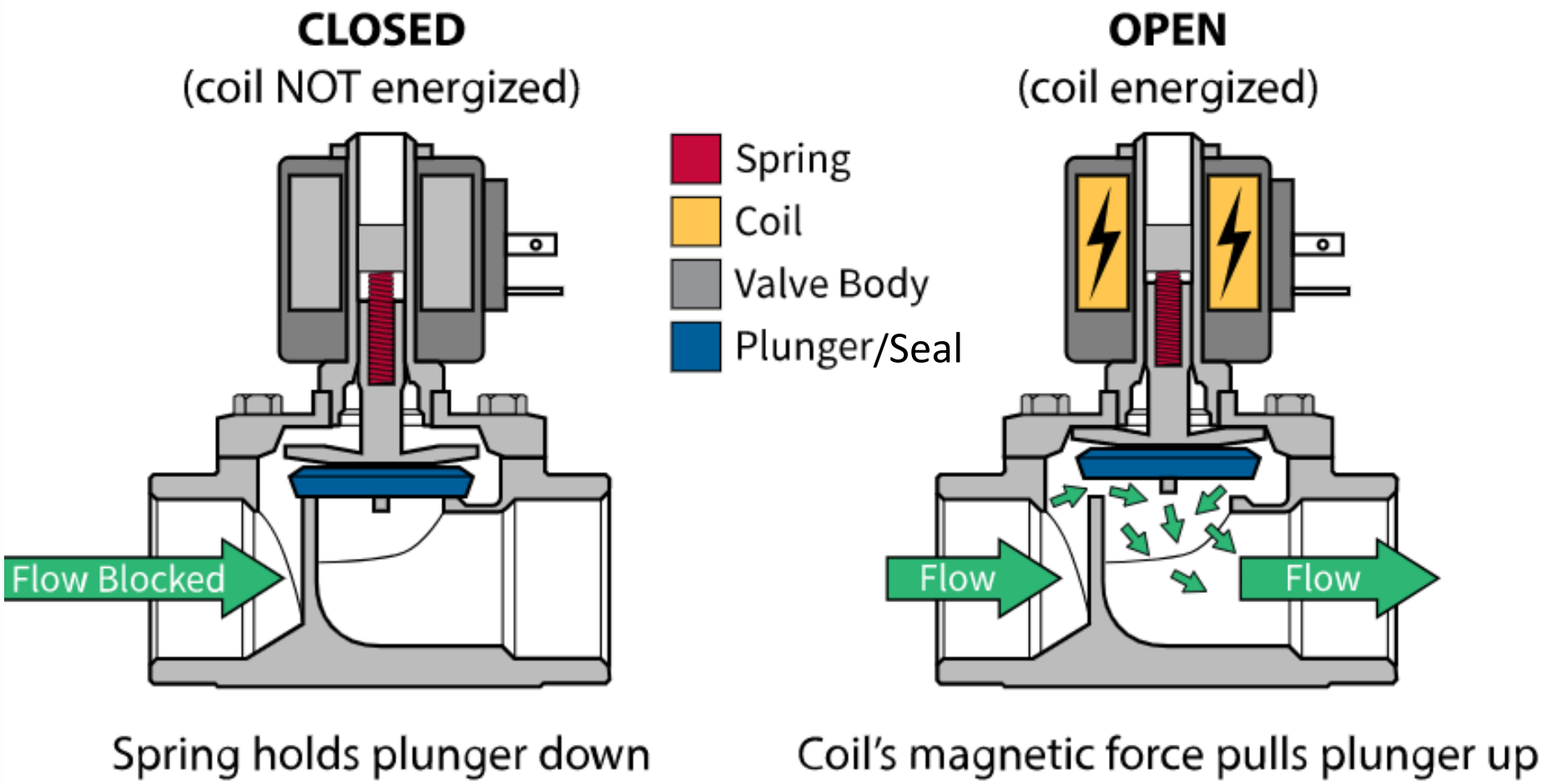

Picture from: https://assuredautomation.com/actuated-valve-training/types-of-valves.php

Controlling SMORES valves

+

=

Controlling SMORES valves

```
int solenoidPin = 9;                    //This is the output pin on the Arduino

void setup()
{
  pinMode(solenoidPin, OUTPUT);          //Sets that pin as an output
}

void loop()
{
  digitalWrite(solenoidPin, HIGH);      //Switch Solenoid ON
  delay(1000);                          //Wait 1 Second
  digitalWrite(solenoidPin, LOW);       //Switch Solenoid OFF
  delay(1000);                          //Wait 1 Second
}
```

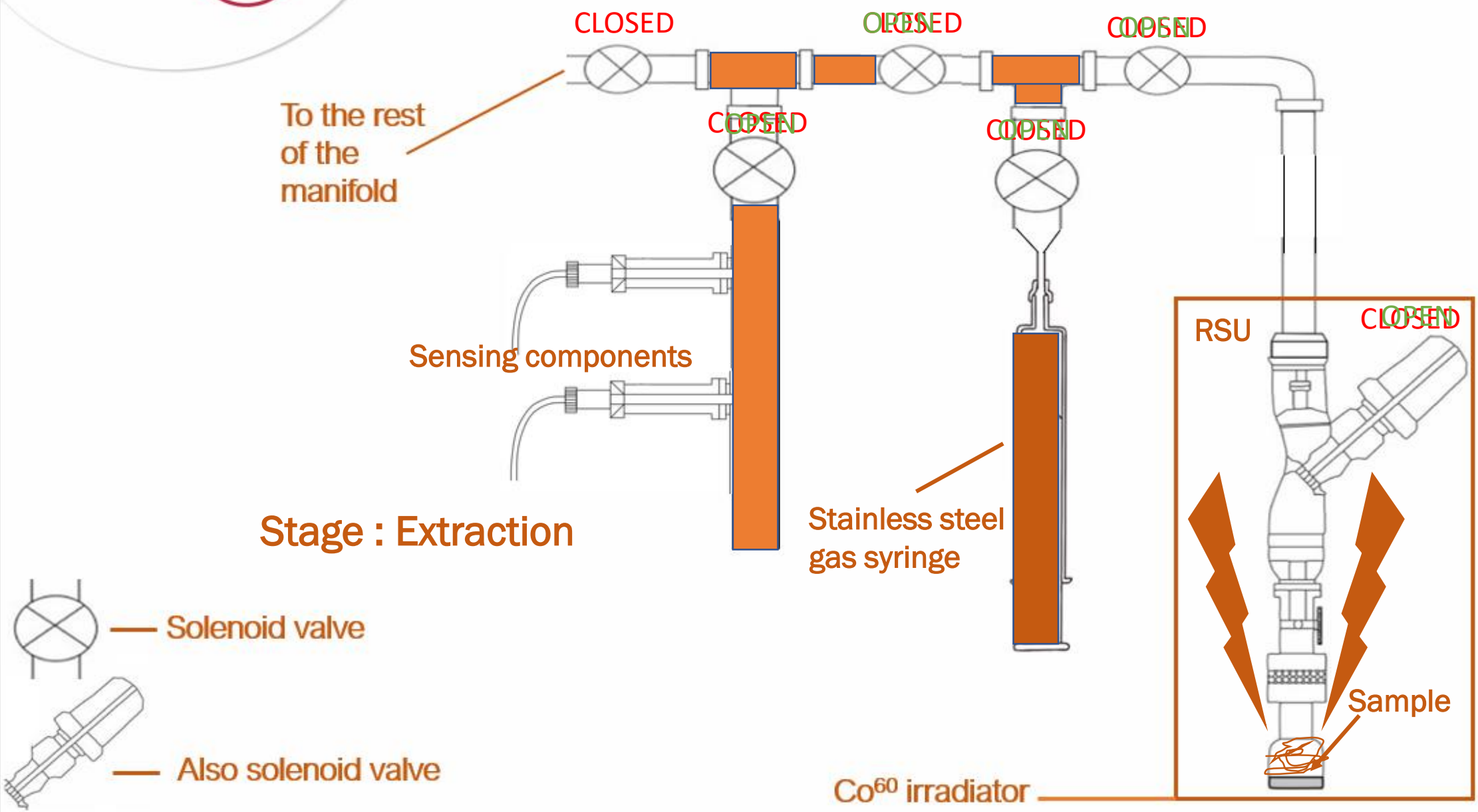

Stage : Extraction

Sensing capabilities

Most sensors will be out of the radiation field

O_2, H_2, NO, N_2O, through Unisense probe sensors

CO_2, CO, and CH_4 through Edinburgh Sensors infra-red gas cards

RH/T/P through BME280 microsensors

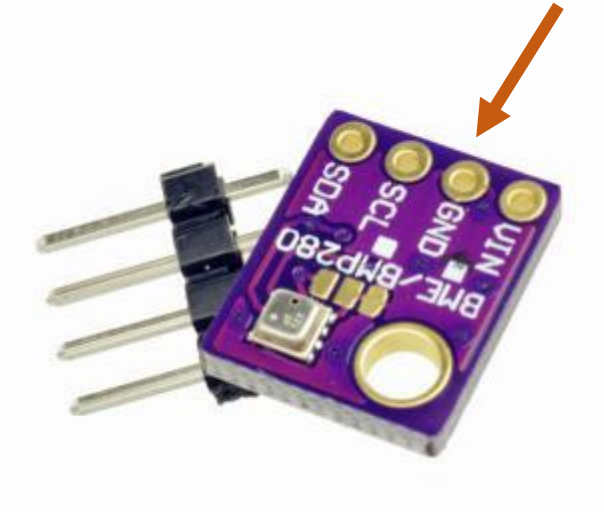

Radiation hardness testing

299,520 Gy

Actual sensor part

Irradiated

Not Irradiated

```
#include <Wire.h>
#include <SPI.h>
#include <Adafruit_Sensor.h>
#include <Adafruit_BME280.h>
unsigned long time;
#define BME_SCK 13
#define BME_MISO 12
#define BME_MOSI 11
#define BME_CS 10

Adafruit_BME280 bme;
 Serial.println(F("BME280 test"));
 bool status;
 status = bme.begin(0x76);
   if (!status) {
      Serial.println("Could not find a valid BME280 sensor, check wiring!");
      while (1);
   }
   Serial.println("-- Default Test --");
   delayTime = 1000;
   Serial.println();
}
Serial.println("-- Default Test --");
   delayTime = 1000;
   Serial.println();
}
void loop() {
   printValues();
   delay(delayTime);
}
void printValues() {
   Serial.print("Temperature = ");
   Serial.print(bme.readTemperature());
   Serial.println(" *C");
   Serial.print("Pressure = ");
   Serial.print(bme.readPressure() / 100.0F);
   Serial.println(" hPa");
Serial.println(" m");
   Serial.print("Humidity = ");
   Serial.print(bme.readHumidity());
   Serial.println(" %");
   Serial.print("Time: ");
   time = millis();
   Serial.println(time);
   Serial.println();
}
```

File Edit Format View Help

```
10:33:02.319 ->
10:33:32.274 -> Temperature = 22.58 *C
10:33:32.274 -> Pressure = 989.65 hPa
10:33:32.321 -> Humidity = 25.30 %
10:33:32.368 -> Time: 29
10:33:32.368 ->
10:34:02.289 -> Temperature = 23.21 *C
10:34:02.336 -> Pressure = 989.69 hPa
10:34:02.383 -> Humidity = 24.48 %
10:34:02.429 -> Time: 30
10:34:02.429 ->
10:34:32.351 -> Temperature = 23.84 *C
10:34:32.398 -> Pressure = 989.54 hPa
10:34:32.445 -> Humidity = 23.74 %
10:34:32.445 -> Time: 31
10:34:32.445 ->
10:35:02.412 -> Temperature = 24.26 *C
10:35:02.412 -> Pressure = 989.33 hPa
10:35:02.459 -> Humidity = 23.09 %
10:35:02.506 -> Time: 32
10:35:02.506 ->
10:35:32.458 -> Temperature = 24.88 *C
10:35:32.458 -> Pressure = 989.49 hPa
10:35:32.552 -> Humidity = 22.36 %
10:35:32.552 -> Time: 33
10:35:32.552 ->
10:36:02.489 -> Temperature = 25.65 *C
10:36:02.536 -> Pressure = 989.24 hPa
10:36:02.583 -> Humidity = 21.63 %
10:36:02.583 -> Time: 34
10:36:02.630 ->
10:36:32.535 -> Temperature = 26.15 *C
10:36:32.582 -> Pressure = 989.59 hPa
10:36:32.629 -> Humidity = 20.90 %
10:36:32.629 -> Time: 35
10:36:32.676 ->
10:37:02.597 -> Temperature = 26.91 *C
10:37:02.643 -> Pressure = 992.87 hPa
10:37:02.690 -> Humidity = 20.21 %
10:37:02.690 -> Time: 36
10:37:02.690 ->
10:37:32.642 -> Temperature = 27.59 *C
10:37:32.689 -> Pressure = 995.87 hPa
```

Sensor	Dose Rate (Gy/min)	Dose for Critical Damage
A	312	~5.03 kGy
B	312	~2.49 kGy

So they didn't

- Low dose expe
- On the manifol
- Sacrificial sens ... le surface

```
File   Edit   Format   View   Help
10:37:32.736 ->
10:38:02.688 -> Temperature = 28.37 *C
10:38:02.735 -> Pressure = 1001.18 hPa
10:38:02.782 -> Humidity = 18.87 %
10:38:02.782 -> Time: 38
10:38:02.829 ->
10:38:32.750 -> Temperature = 29.05 *C
10:38:32.750 -> Pressure = 1022.39 hPa
10:38:32.844 -> Humidity = 18.22 %
10:38:32.844 -> Time: 39
10:38:32.844 ->
10:39:02.811 -> Temperature = -146.45 *C
10:39:02.811 -> Pressure = 1123.62 hPa
10:39:02.858 -> Humidity = 100.00 %
10:39:02.905 -> Time: 40
10:39:02.905 ->
10:39:32.873 -> Temperature = -146.45 *C
10:39:32.873 -> Pressure = 1123.62 hPa
10:39:32.920 -> Humidity = 100.00 %
10:39:32.967 -> Time: 41
10:39:32.967 ->
10:40:02.924 -> Temperature = nan *C
10:40:02.924 -> Pressure = nan hPa
10:40:02.971 -> Humidity = nan %
10:40:02.971 -> Time: 42
10:40:03.018 ->
10:40:32.954 -> Temperature = nan *C
10:40:32.954 -> Pressure = nan hPa
10:40:33.001 -> Humidity = nan %
10:40:33.048 -> Time: 43
10:40:33.048 ->
10:41:02.985 -> Temperature = nan *C
10:41:02.985 -> Pressure = nan hPa
10:41:03.031 -> Humidity = nan %
10:41:03.078 -> Time: 44
10:41:03.078 ->
10:41:33.031 -> Temperature = nan *C
10:41:33.031 -> Pressure = nan hPa
10:41:33.077 -> Humidity = nan %
10:41:33.124 -> Time: 45
```

What about the solenoid irradiation?

200 kGy overnight

ce Proceedings

Influence of gamma radiation on EPDM compounds properties for use in nuclear plants

Cite as: AIP Conference Proceedings **1779**, 080015 (2016); https://doi.org/10.1063/1.4965559
Published Online: 31 October 2016

Sandra Regina Scagliusi, Elisabeth Carvalho Leite Cardoso, Traian Zaharescu, and Ademar Benévolo Lugão

EPDM irradiated at 25, 50, 75, 100, 200 kGy

Suggests that mechanical properties become significantly worsened at 200 kGy

I very much agree

More to come in the following weeks..

Future applications and plans

- Radiolysis and recombination experiments

  Especially those looking to measure gasses during/after irradiations

  Direct beneficiary of SMORES is my personal project:

Gas generation from the radiolysis of water on Uranium and Thorium oxides

- Testing more equipment

  Sensing equipment

  More Solenoid valves

  Mass flow controllers, automated gas syringes, starting the manifold body, and more!

- Experiments with alpha

  An adaptation of the manifold that is compatible for use with the accelerator at DCF is being designed

  Will allow two types of radiation on the same samples to be explored with the same system

TRANSCEND

Transformative Science and Engineering for Nuclear Decommissioning

Thank you

Contact Details: christopher.anderson-3@postgrad.manchester.ac.uk
07857420556

TRANSCEND

Transformative Science and Engineering for Nuclear Decommissioning

Safe Interim Storage of plutonium: Water absorption onto thin-layer plutonium analogues

Transcend Research Consortium

Dr. Dominic Laventine, Prof. Colin Boxall
Lancaster University

Energy For a Low Carbon Future

Lancaster University

NATIONAL NUCLEAR LABORATORY

Lloyd's Register Foundation

- Introduction to UK plutonium interim storage
- Synthesis of thin-layer actinide coatings
- Contact angle measurements
- Piezo-crystal nano-balance experiments

- **Introduction to UK plutonium interim storage**
- Synthesis of thin-layer actinide coatings
- Contact angle measurements
- Piezo-crystal nano-balance experiments

Separation and Reprocessing in the UK

- Reprocessing of spent fuel allows the separation of plutonium from uranium and other species
- PUREX process co-extracts Pu and U as nitrates into an acidified raffinate.
- In the UK, further separation of Pu from the U performed at:
  - THORP reprocessing plant (due to close 2018) by hydrazine reduction of the plutonium
  - Magnox reprocessing plant (due to close 2020)

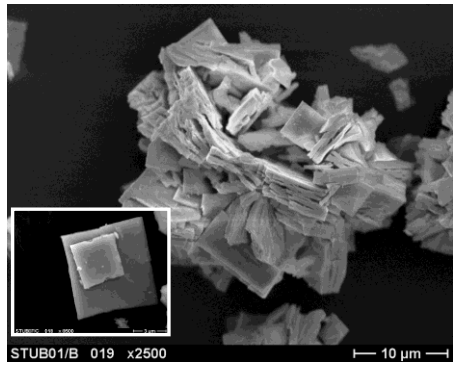

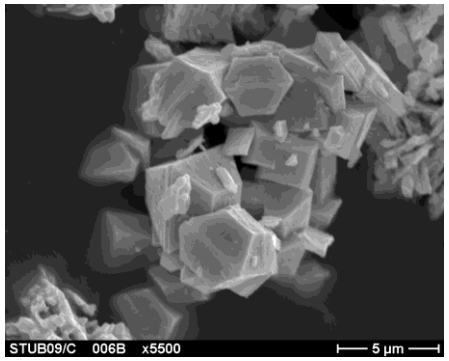

- *Ca.* 250 tonnes of separated Pu currently stockpiled worldwide. Approx. 137 tonnes is in interim storage in UK whilst the Government "develops its options".

Plutonium interim storage in the UK

Interim storage of PuO_2 involves sealing in nested steel containers, under a partial argon atmosphere with (PVC) packing material.

During storage the radioactivity of the plutonium results in heating of the canisters to an estimated central line temperature of 600°C.

PuO_2 is hydroscopic and picks up water during the packaging process. The disposition of this water under the storage conditions is unclear: It may exists in a gaseous state, or be weakly or strongly bound to the PuO_2 surface. Radiolytic and catalytic processes may also result in formation of radicals and other chemical species.

Need to understand how the structure and properties of PuO_2 change with time under storage condition and how this affects water absorption.

Cannister pressurisation

Over time a small number of cannisters have been observed to deform due to pressurisation: this makes storage and efficient heat transfer difficult 5 routes to gas production have been suggested that could contribute to this pressurisation:

(i) Helium accumulation from a decay
(ii) Decomposition of polymeric packing material
(iii) H_2O desorption (steam) from hygroscopic PuO_2
(iv) Radiolysis of adsorbed water
(v) Generation of H_2 by chemical reaction of PuO_2 with H_2O, producing a PuO_{2+x} phase.

The last 3 processes all involve PuO_2/H_2O interactions and are complex, inter-connected & poorly understood.

- Experimental methods have been employed to determine extent of H_2O adsorption, typically through measurement of pressure changes and use of the ideal gas equation to indirectly determine water adsorption at the plutonium oxide surface.

- Current models suggest water is initially absorbed onto metal oxides as a chemi-absorbed monolayer followed by multiple, physi-sorbed layers (with possible intermediate layers of differing binding energies).

- Introduction to UK plutonium interim storage
- **Synthesis of thin-layer actinide coatings**
- Contact angle measurements
- Piezo-crystal nano-balance experiments

Actinide thin layer synthesis

Thin (10-100s nm thick) layers of metal oxide synthesised by drop-coating of salt solutions with surfactant followed by evaporation and calination. Allows surface characteristics to be investigated while using only small amounts of radioactive material.

Cerium, Thorium, and Uranium oxides used as analogues of plutonium oxide due to their similar structures and atomic radii.

50 ug $Ce(NO_3)_3$
10 uL H_2O
10 uL MeOH
5% Triton-X
Calc.: 350°C

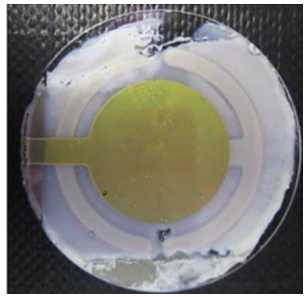

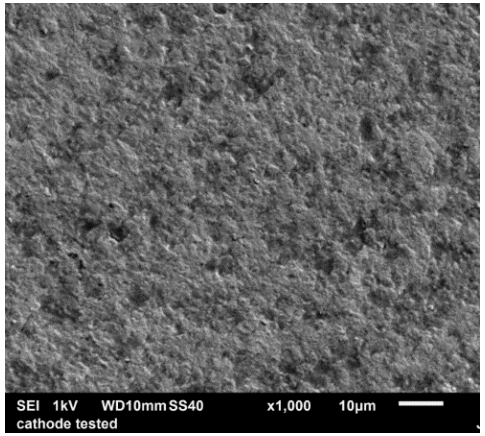

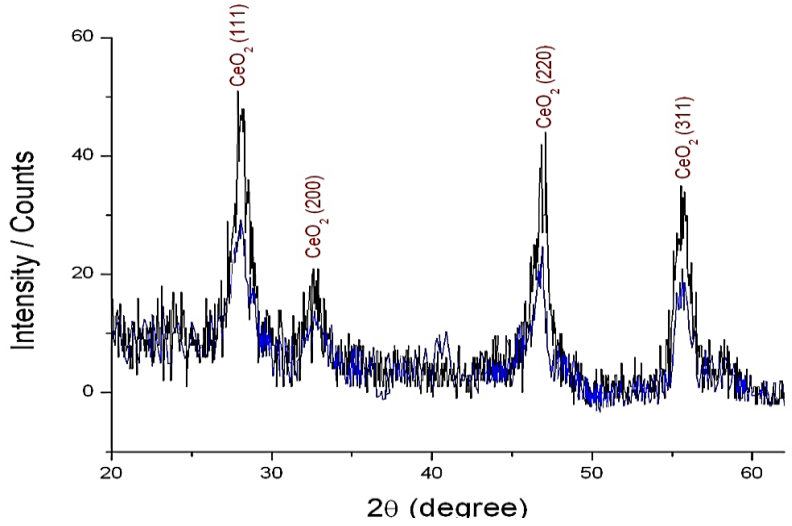

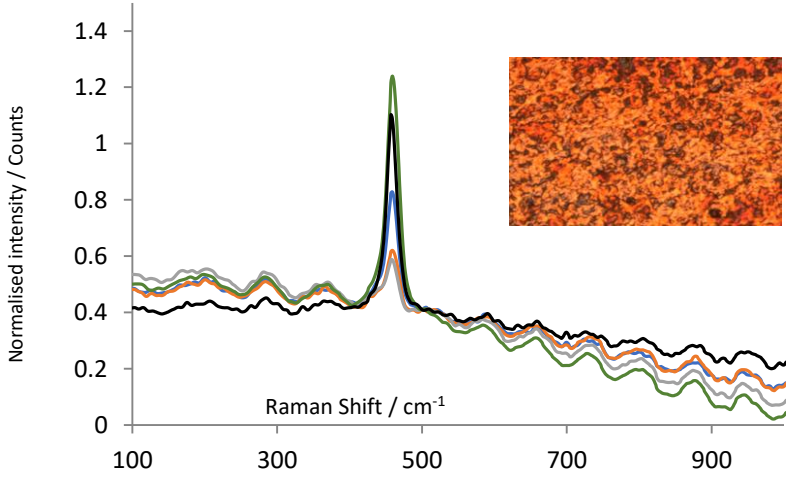

Thin layer depth analyses

Uncoated crystal $F_{25°C}$ = 5833918 Hz
Coated crystal $F_{25°C}$ = 5826468 Hz
D $F_{25°C}$ = –7450 Hz
D m = 42 ug
vol = 5.5 x 10^{-6} cm^3
Thickness = 125 nm

$$\Delta f = -\left(\frac{n{f_0}^2}{A\sqrt{\rho_q \mu_q}}\right)\Delta m$$

ρ_q = 3.570 $g.cm^{-1}$ n = 1
μ_q = 2.147 x 10^{11} $g.cm^{-1}s^{-2}$
Coated area = 1.33 cm^2
Active area = 0.46 cm^2
d_{CeO_2} = 7.65 $g.cm^{-3}$

XRD thickness is ~250 nm, indicating a porisity of 50%

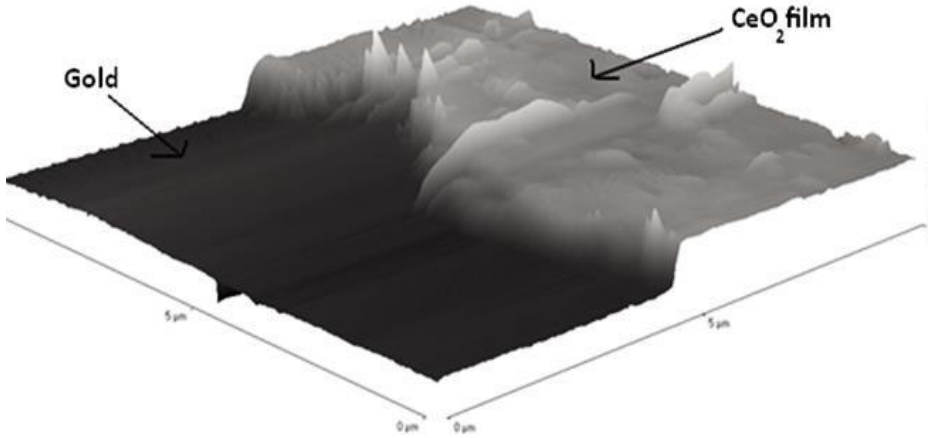

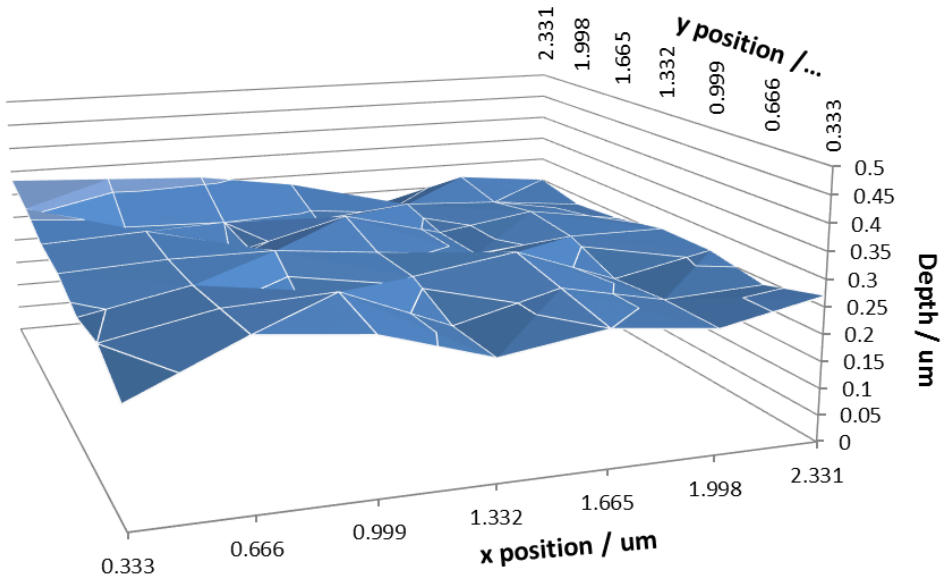

- Introduction to UK plutonium interim storage
- Synthesis of thin-layer actinide coatings
- Contact angle measurements
- **Piezo-crystal nano-balance experiments**

Microbalance water absorption

- Study the interactions of plutonium oxide and analogues with water.
  - -- Ceria (CeO_2)
  - -- Thoria (ThO_2)
  - -- Urania (UO_2 / U_3O_8)
  - -- Plutonium oxide (PuO_2) @ NNL Central Lab

- Use of quartz crystal microbalance methodology to experimentally determine:
  - -- The number of monolayers of water bound to the surface
  - -- The enthalpy of binding of the different layers.

- The QCM measures in-situ mass changes at the surface of a piezoelectrode. Changes in mass due to absorption or desorption at the electrode surface result in resonant frequency changes of the quartz crystal, and can be directly related via the Sauerbrey equation:

$$\Delta f = -\left(\frac{n{f_0}^2}{A\sqrt{\rho_q \mu_q}}\right)\Delta m$$

- Through control of temperature and partial pressure of the absorbed gas, the amount of water and enthalpy of absorption can be calculated.

Piezo-crystal nano-balance

Metal crystal transducer and $GaPO_4$ piezo-electric crystals allow higher temperature measurements compared to typical QCM.

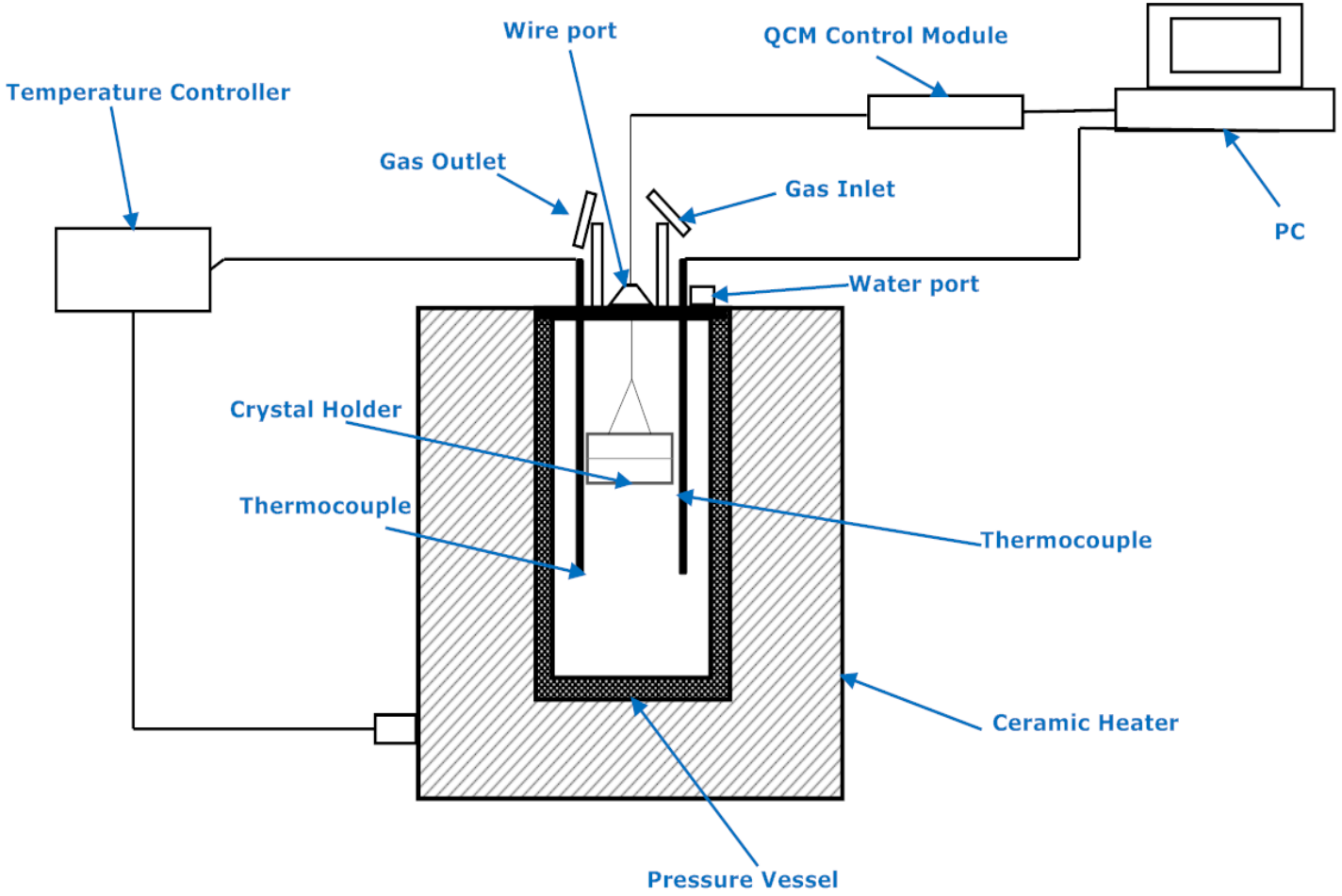

Water absorption: Pilot experiments

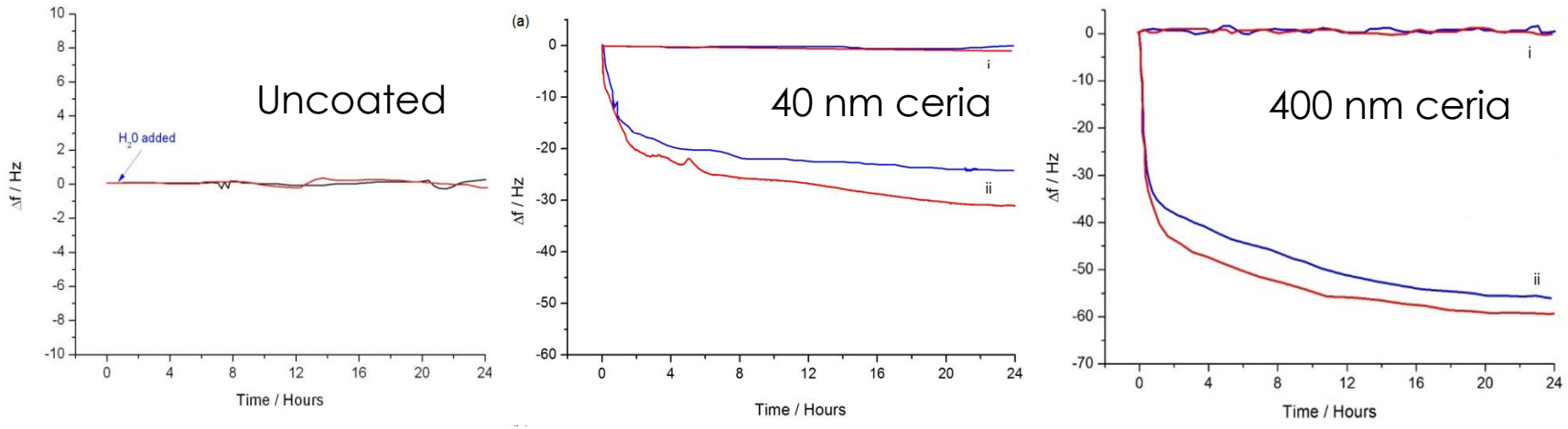

Frequency changes due water adsorption onto quartz crystals at 25°C, 10% humidity.
Uncoated crystals showed no appreciable water absorption.
Ceria-coated crystals showed a reduction in frequency due to absorption of water.

Different amounts of water were added to the pre-dried system at RT and equilibrated for 4 hours.

The change in frequency is proportional to the mass of water absorbed onto the ceria, and increased as the amount of water increased.

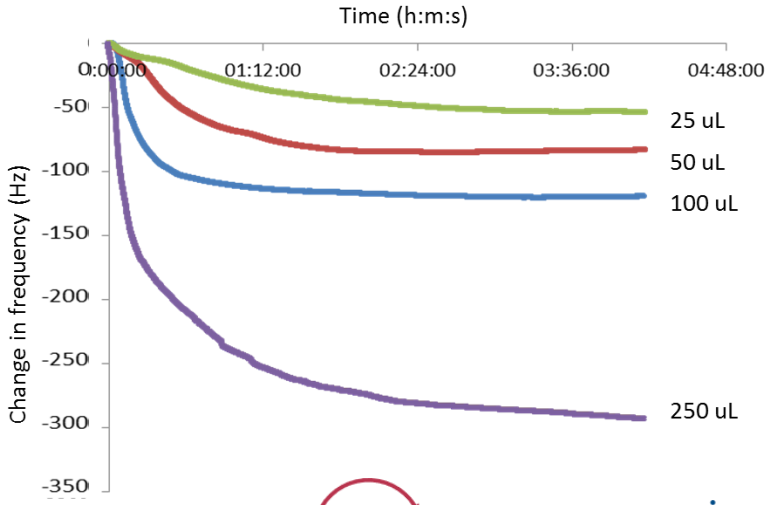

TRANSCEND
NATIONAL NUCLEAR LABORATORY
Lancaster University

Ceria films on $GaPO_4$ crystals: Humidity variation(old)

The BET equation allows the volume of a monolayer and the enthalpy of absorption to be calculated:

$$1/\left[Va\left(\frac{P0}{P}-1\right)\right] = \left(\frac{C-1}{V_M C}\right)\left(\frac{P}{P_0}\right) + \frac{1}{VmC} \qquad C = e^{(\Delta H_{ads} - \Delta H_{liq}/RT)}.$$

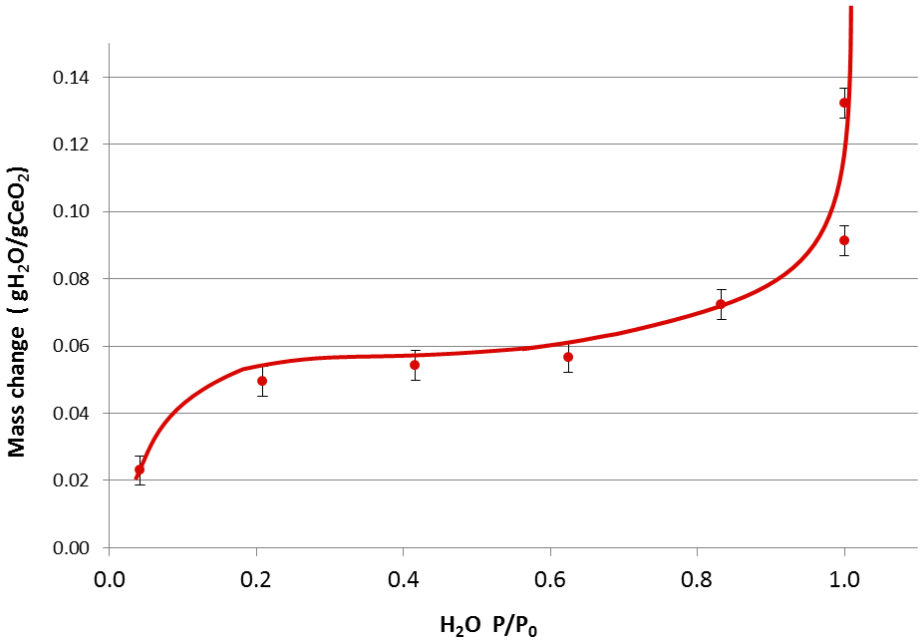

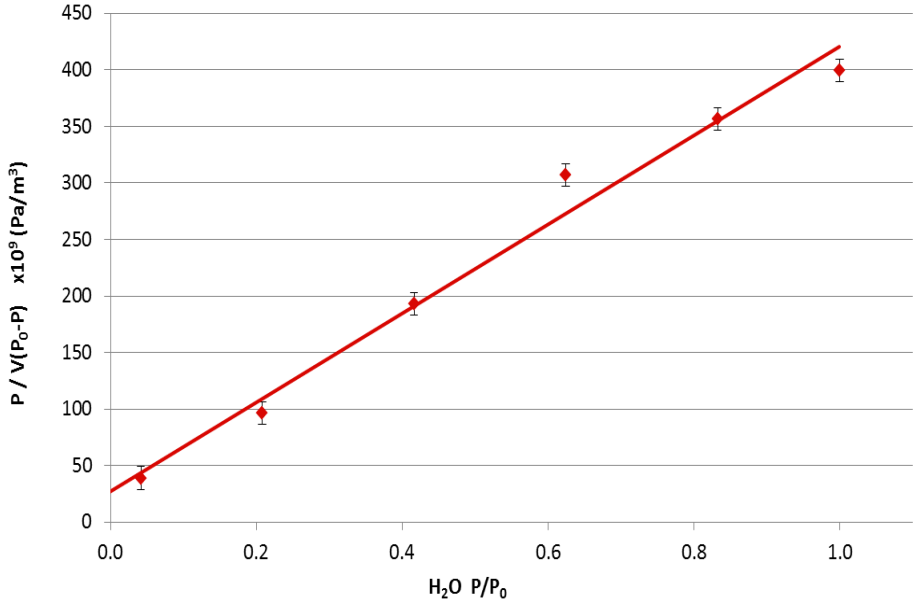

A plot of $P/V(P_0\text{-}P)$ against P/P_0 gives an intercept of $1/V_mC$ and a gradient of $(C-1)/(V_M C)$, therefore we can calculate:

V_m = 2.43 x 10^{-12} m^3 SA = 28 m^2g^{-1}

ΔH_{abs} = 44.3 $kJmol^{-1}$ ΔH_{bind} = 2.5 $kJmol^{-1}$

TRANSCEND NATIONAL NUCLEAR LABORATORY Lancaster University

Ceria films on $GaPO_4$ crystals: Humidity variation(old)

The BET equation allows the volume of a monolayer and the enthalpy of absorption to be calculated:

$$1/\left[Va\left(\frac{P0}{P}-1\right)\right] = \left(\frac{C-1}{V_M C}\right)\left(\frac{P}{P_0}\right) + \frac{1}{VmC}$$

$$C = e^{(\Delta H_{ads} - \Delta H_{liq}/RT)}.$$

Sensitivity factor of supplier wrong (by factor of ~1/3²

BET equation breaks down at P/P0 > 0.35

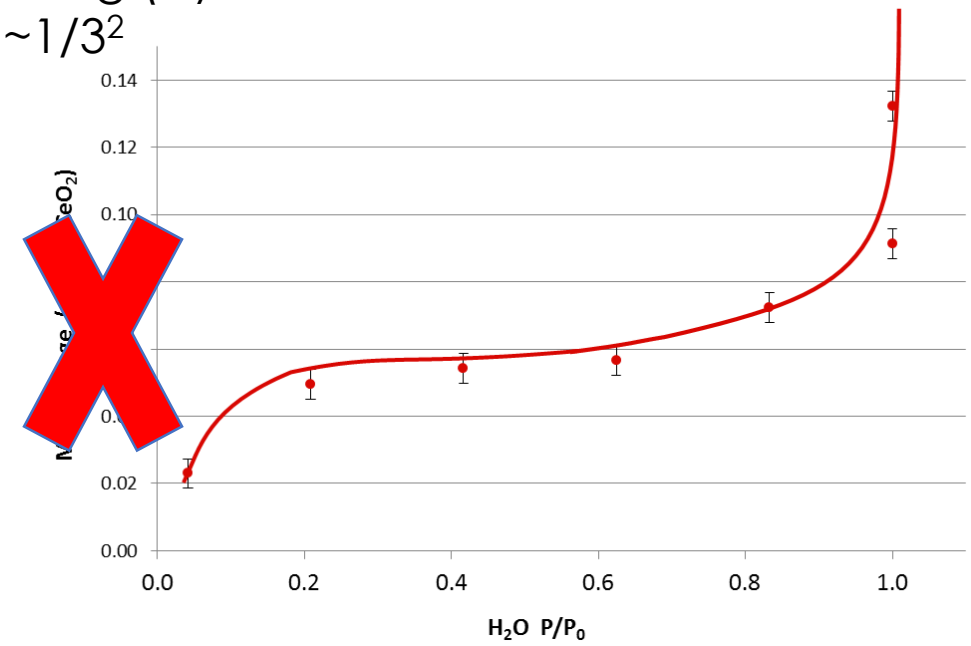

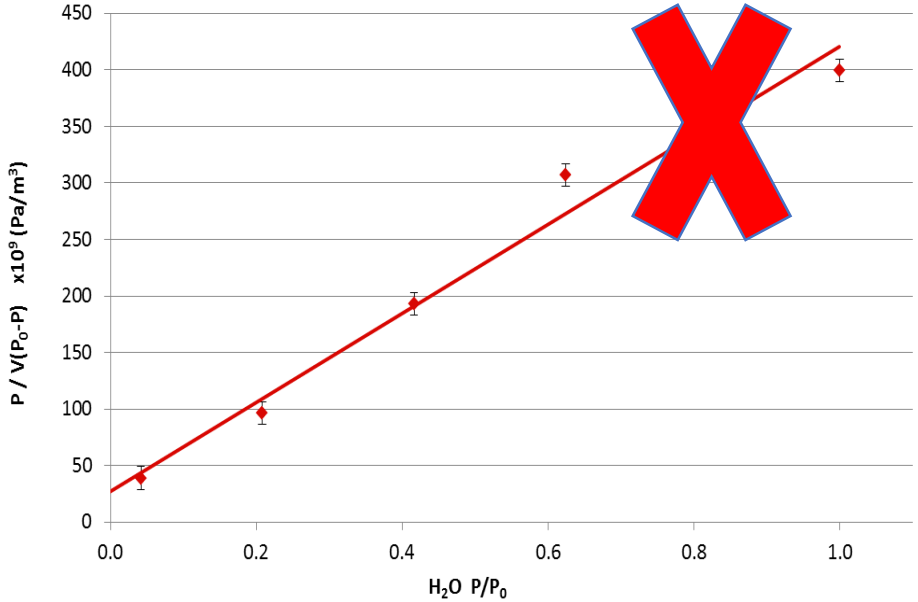

A plot of $P/V(P_0\text{-}P)$ against P/P_0 gives an intercept of $1/V_mC$ and a gradient of $(C-1)/(V_M C)$, therefore we can calculate:

V_m = 2.43 x 10^{-12} m^3 SA = 28 m^2g^{-1}

ΔH_{abs} = 44.3 $kJmol^{-1}$ ΔH_{bind} = 2.5 $kJmol^{-1}$

TRANSCEND NATIONAL NUCLEAR LABORATORY Lancaster University

Ceria films on $GaPO_4$ crystals: Humidity variation

The BET equation allows the volume of a monolayer and the enthalpy of absorption to be calculated:

$$1/\left[Va\left(\frac{P0}{P}-1\right)\right] = \left(\frac{C-1}{V_M C}\right)\left(\frac{P}{P_0}\right) + \frac{1}{VmC}$$

$$C = e^{(\Delta H_{ads} - \Delta H_{liq}/RT)}.$$

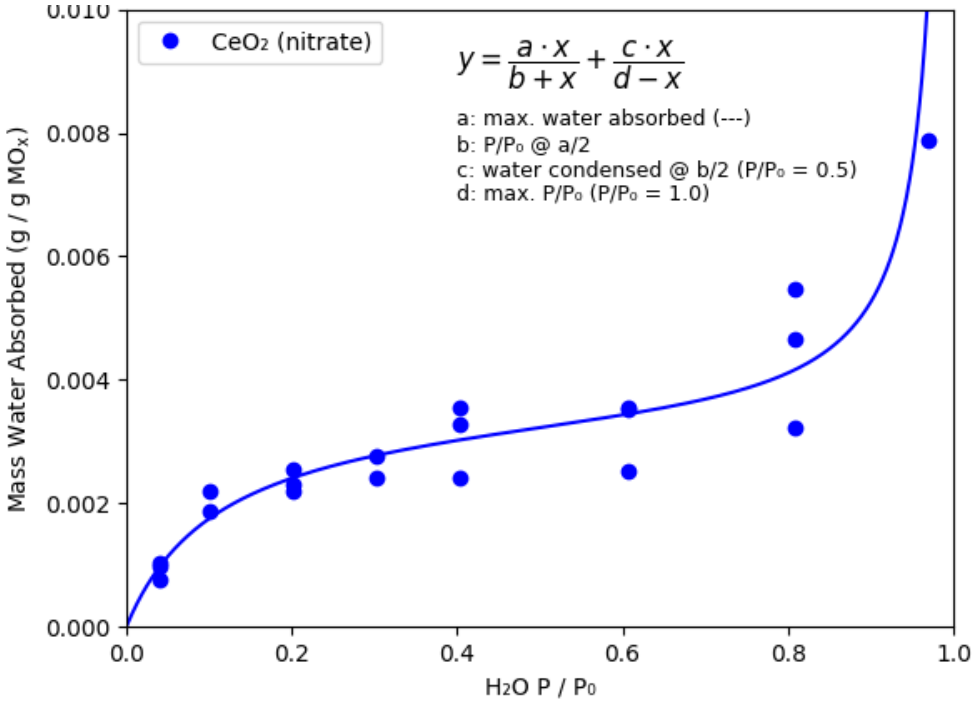

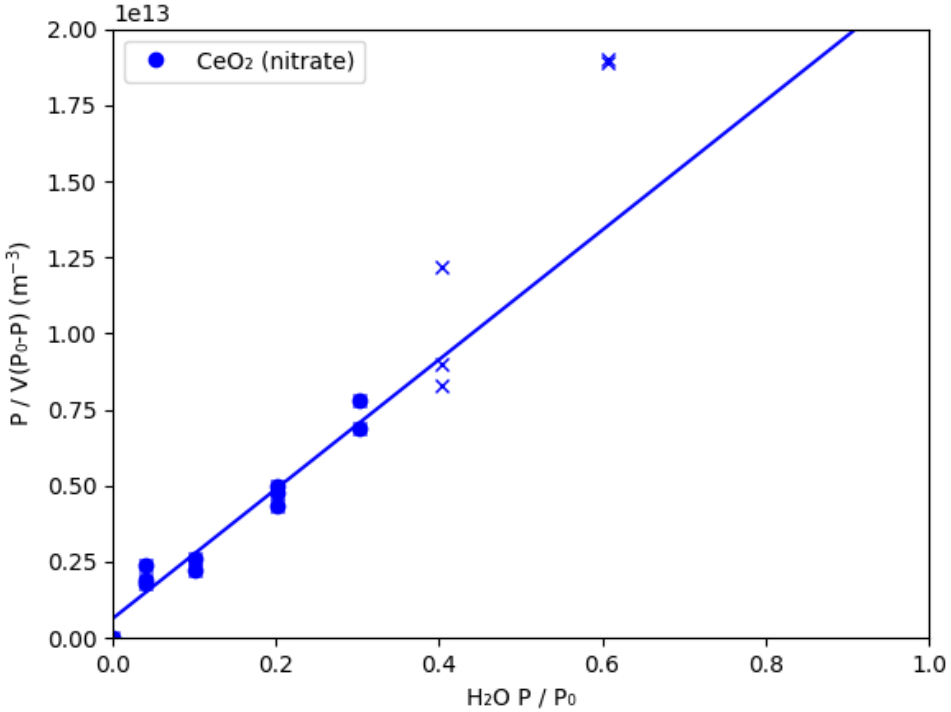

A plot of $P/V(P_0\text{-}P)$ against P/P_0 gives an intercept of 1/VmC and a gradient of $(C-1)/(V_M C)$, therefore we can calculate:

V_m = 9.13×10^{-14} m^3 SA = 10.6 m^2g^{-1}

ΔH_{abs} = 52.0 $kJmol^{-1}$ ΔH_{bind} = 10.2 $kJmol^{-1}$

TRANSCEND NATIONAL NUCLEAR LABORATORY Lancaster University

Ceria films on $GaPO_4$ crystals: Humidity variation

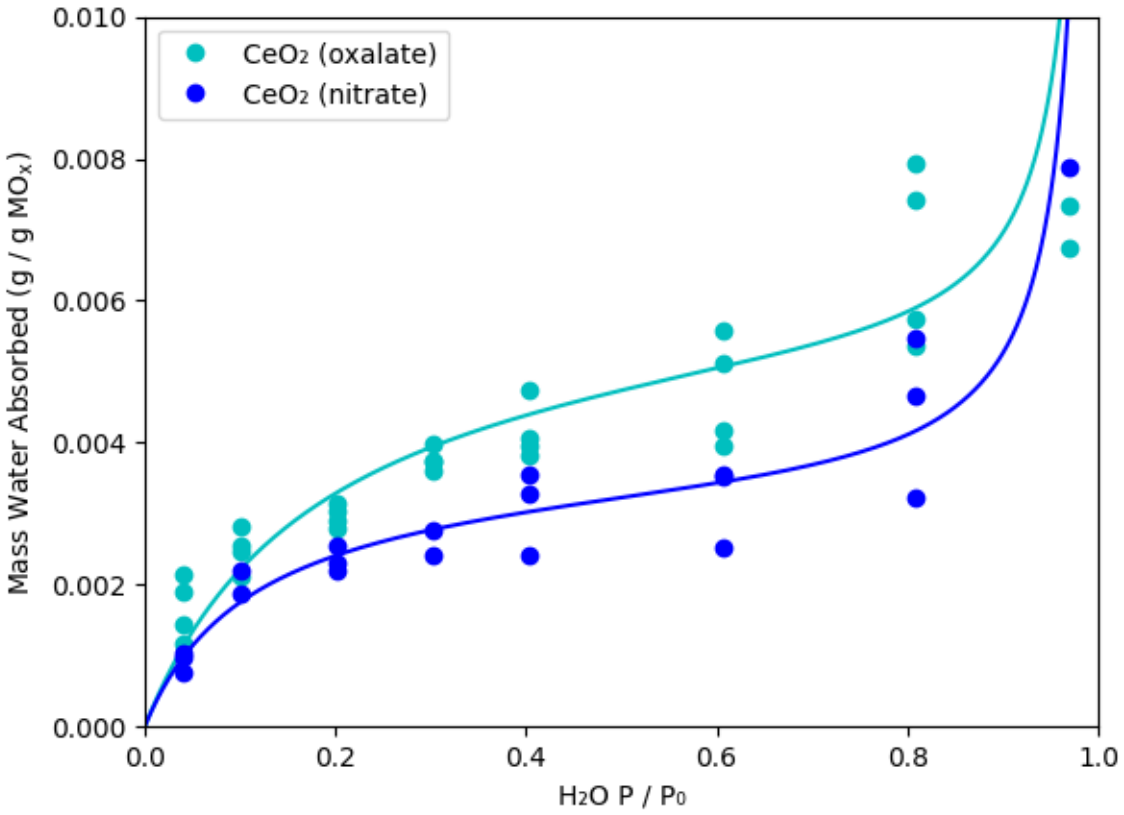

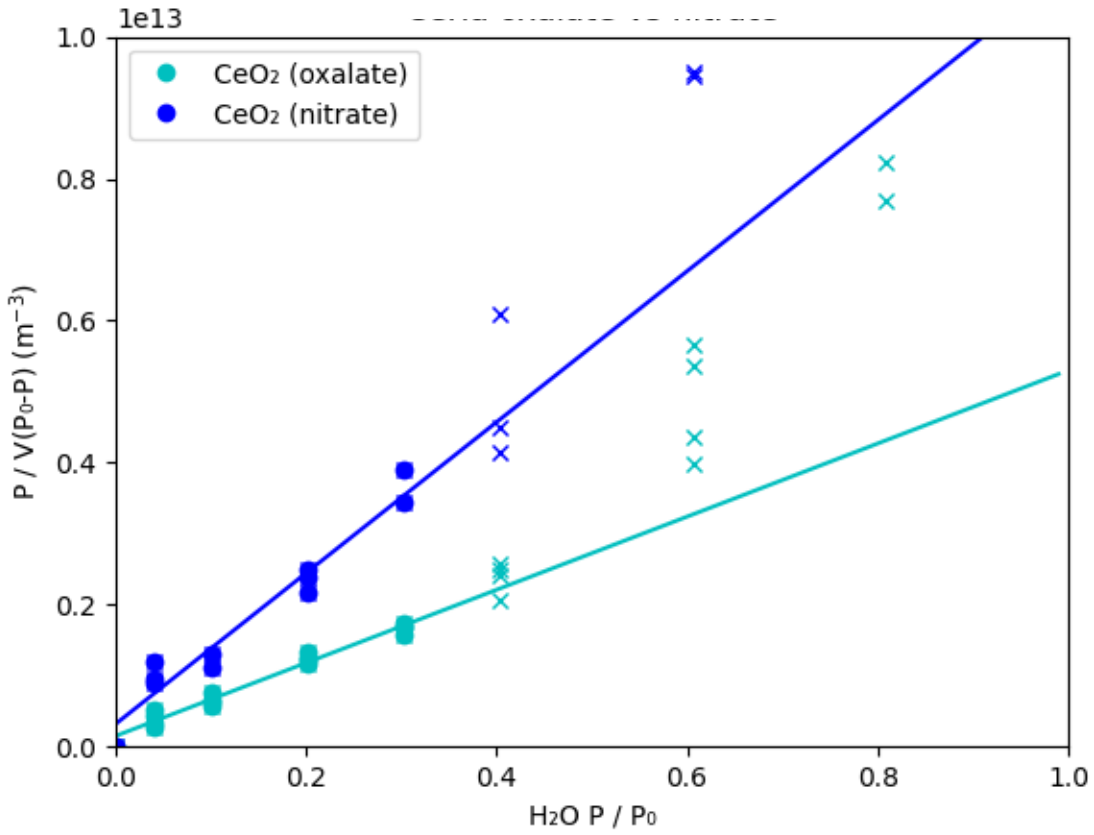

Oxide	Prec. Salt	BET slope X 10^{13}	BET incpt. x 10^{12}	SA m^3 / g	Hads kJ / mol
CeO_2	nitrate	1.06	0.318	10.6	52.0
CeO_2	oxalate	0.515	0.149	14.6	52.1

Urania films on $GaPO_4$ crystals: Humidity variation

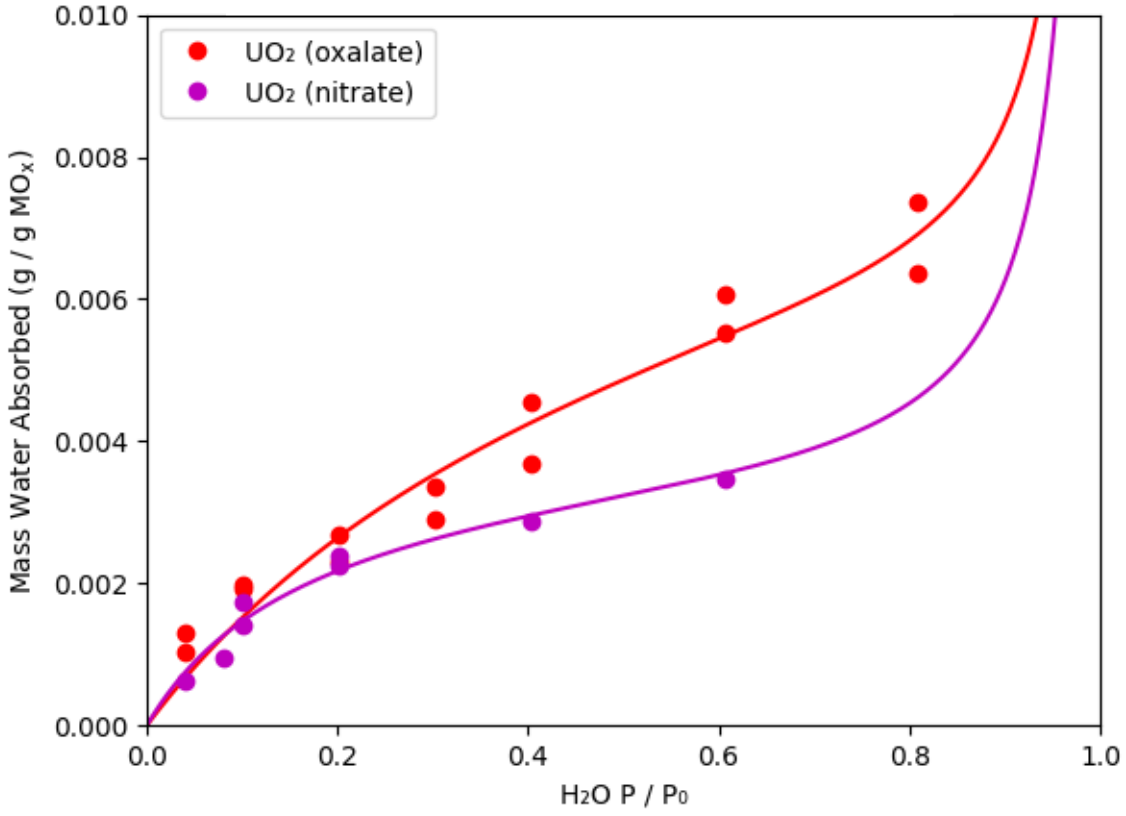

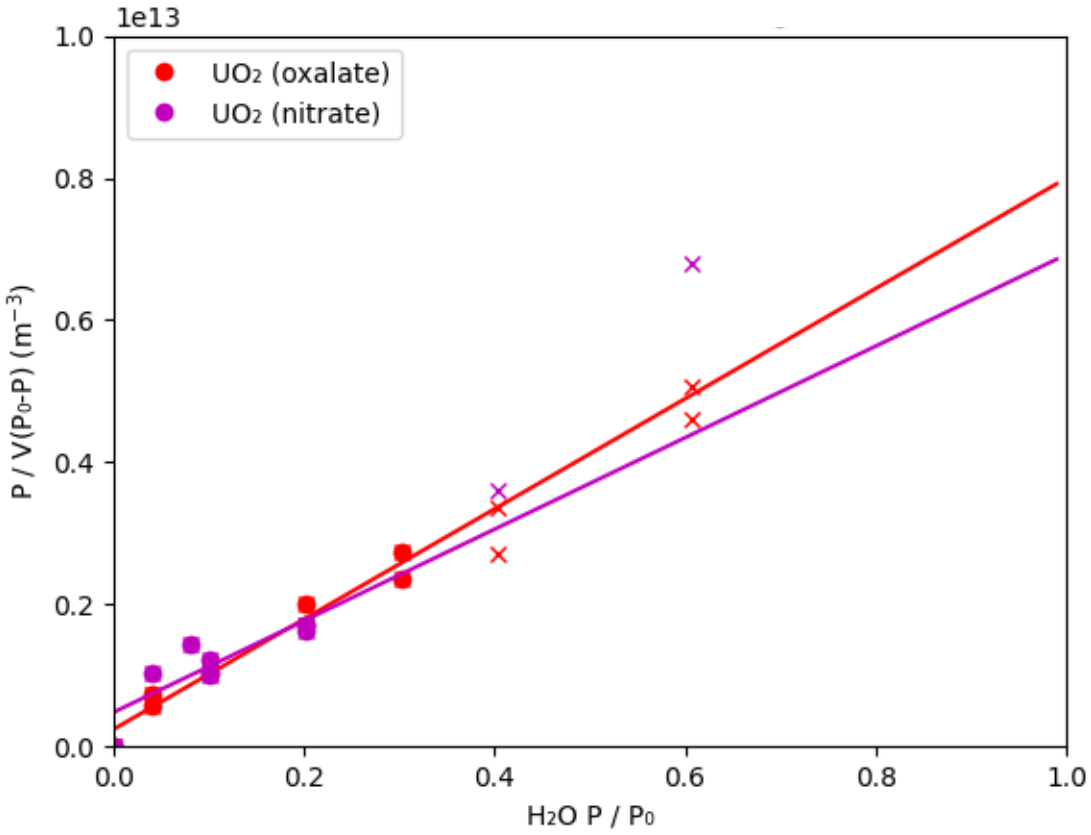

Oxide	Prec. Salt	BET slope X 10^{13}	BET incpt. x 10^{12}	SA m^3 / g	Hads kJ / mol
UO_2	nitrate	0.644	0.481	11.9	49.5
UO_2	oxalate	0.775	0.214	12.2	50.4

Thoria films on $GaPO_4$ crystals: Humidity variation

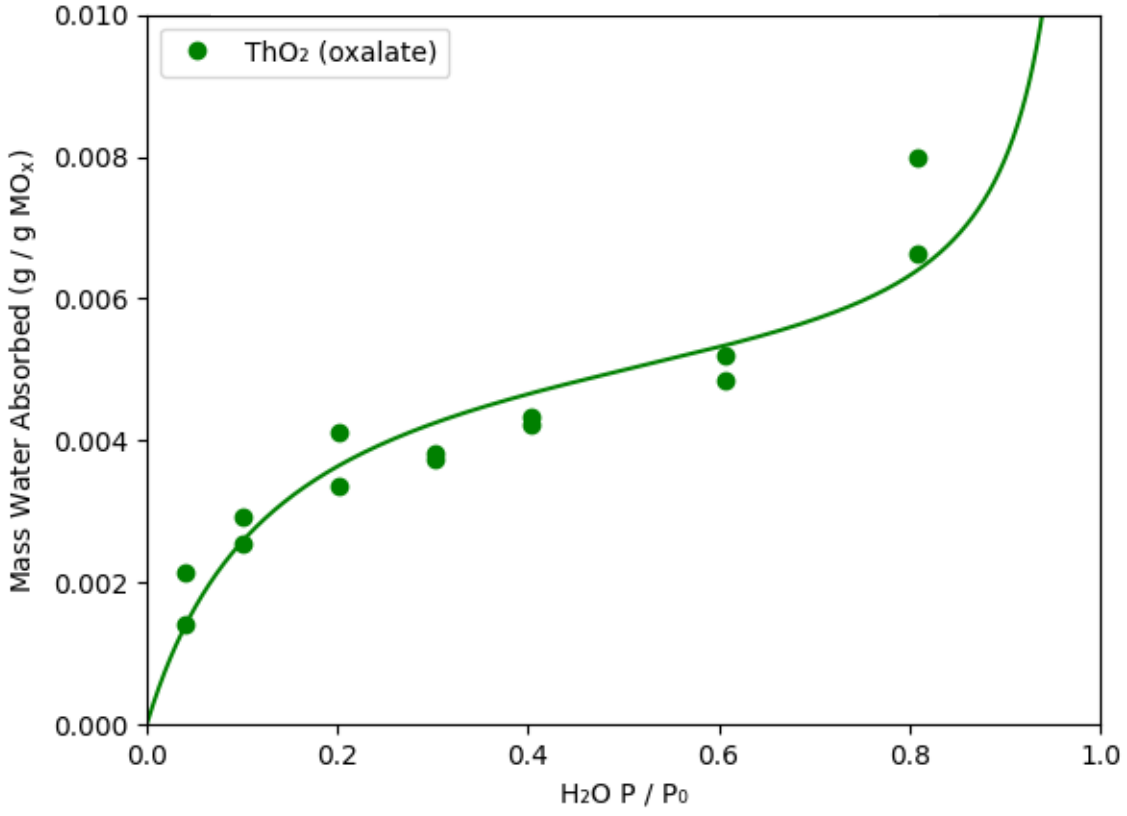

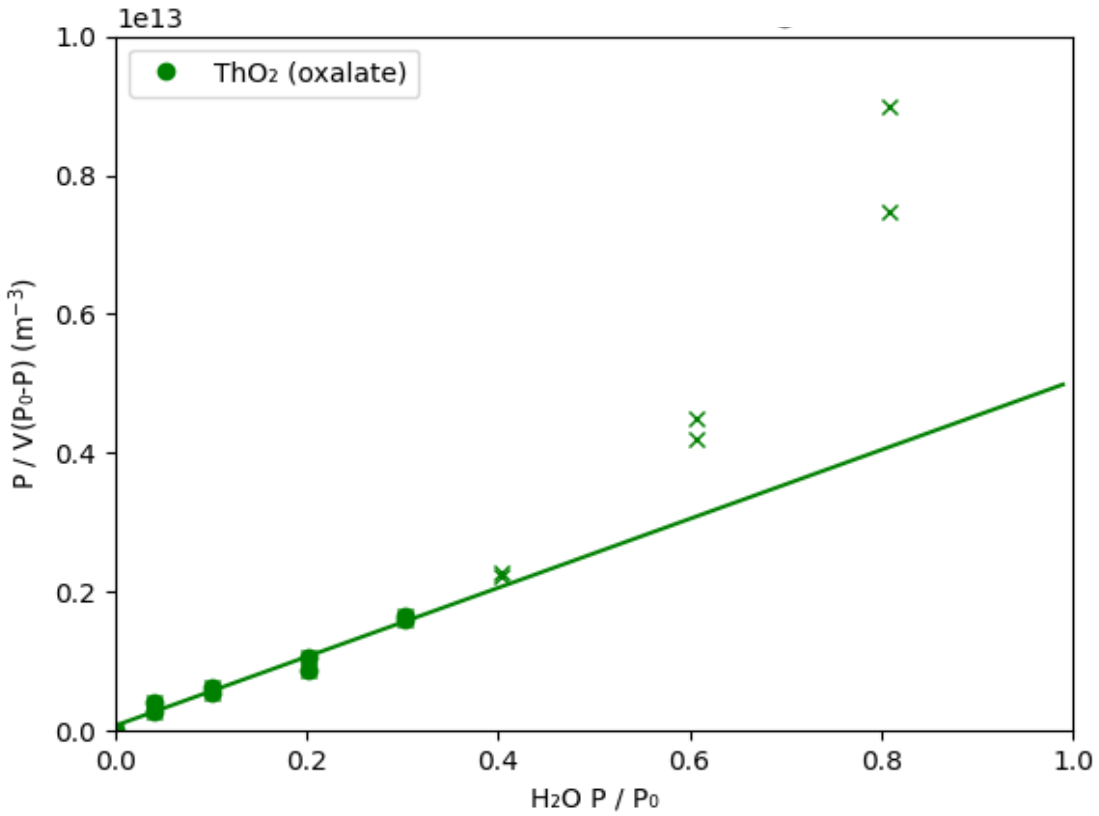

Oxide	Prec. Salt	BET slope X 10^{13}	BET incpt. x 10^{12}	SA m^3 / g	Hads kJ / mol
ThO_2	nitrate	TBD			
ThO_2	oxalate	0.496	0.741	15.1	54.0

Films from oxalate on $GaPO_4$ crystals: Humidity variation

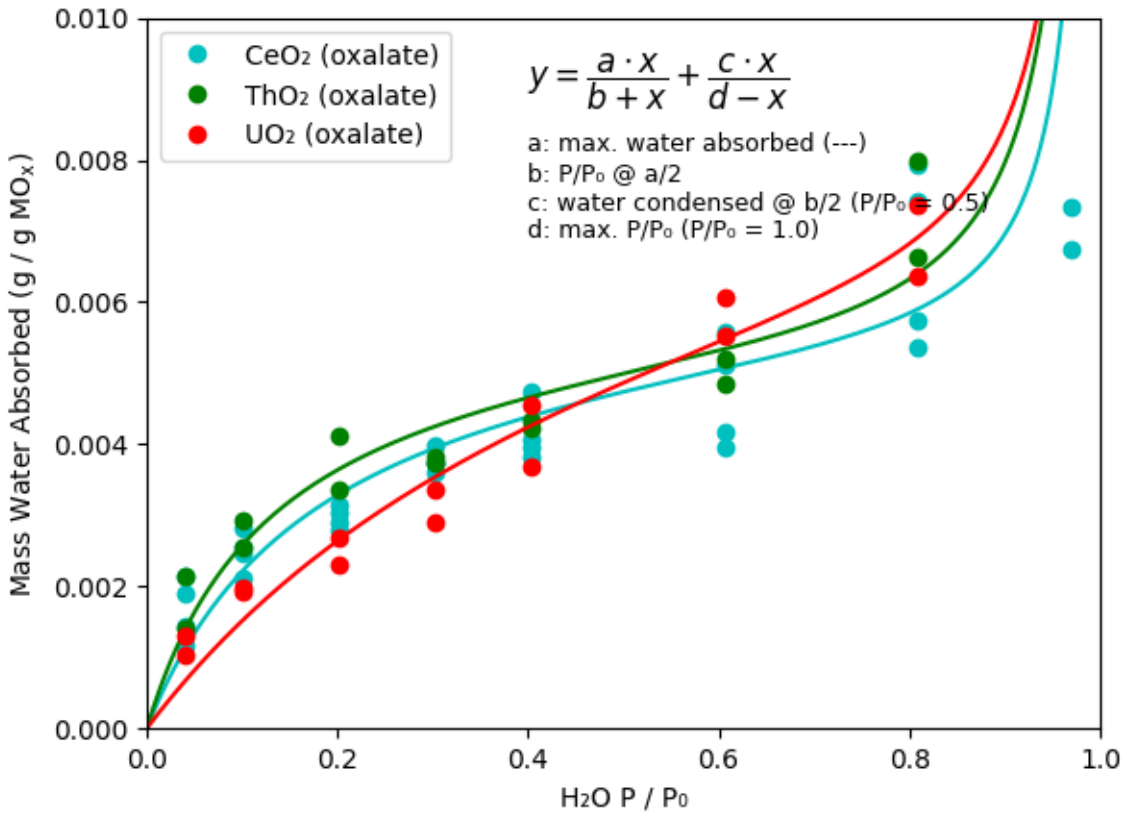

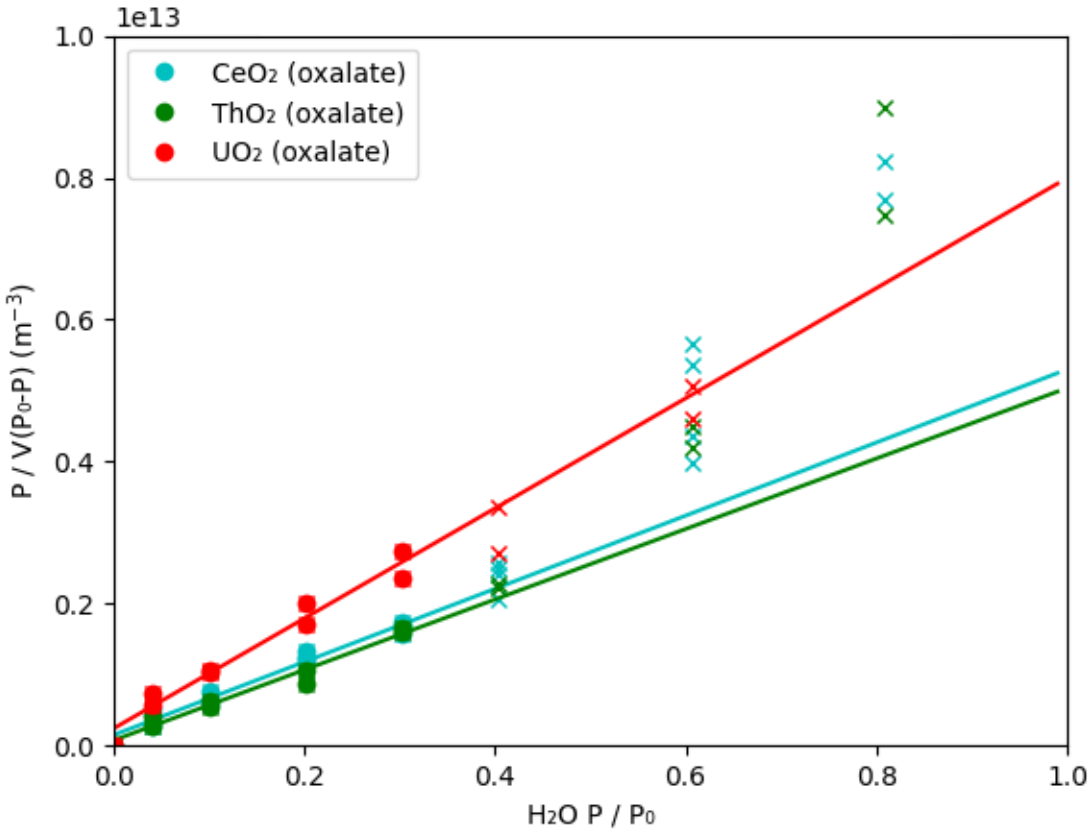

Oxide	Prec. Salt	BET slope X 10^{13}	BET incpt. x 10^{12}	SA m^3 / g	Hads kJ / mol
CeO_2	oxalate	0.515	0.149	14.6	52.1
UO_2	oxalate	0.775	0.214	12.2	50.4
ThO_2	oxalate	0.496	0.741	15.1	54.0

Ceria water absorption: Temperature variation

The water saturated system (75°C, 100% rel. humidity) was then heated to approx. 400°C, causing the bound water to desorb as the relative humidity drops.

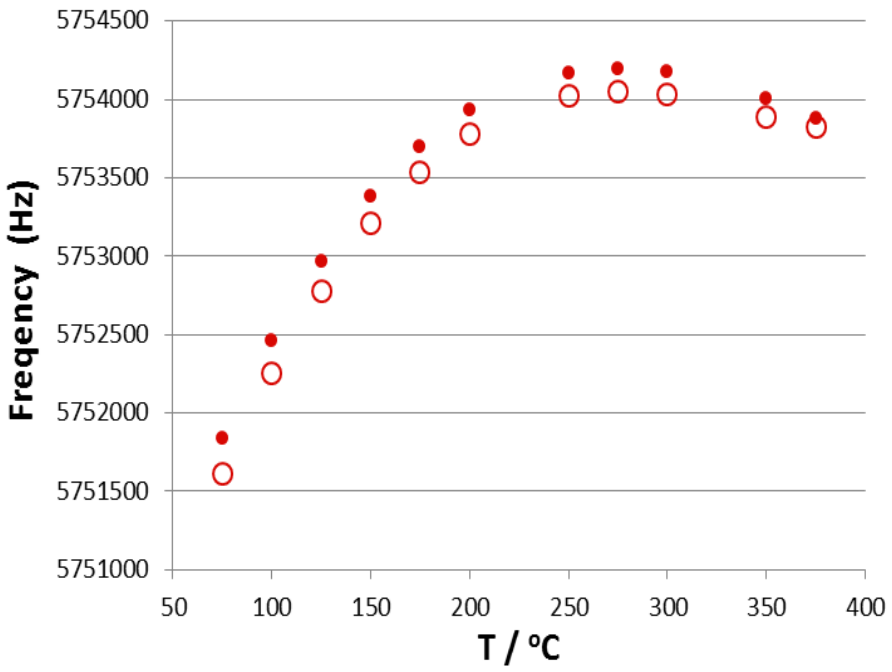

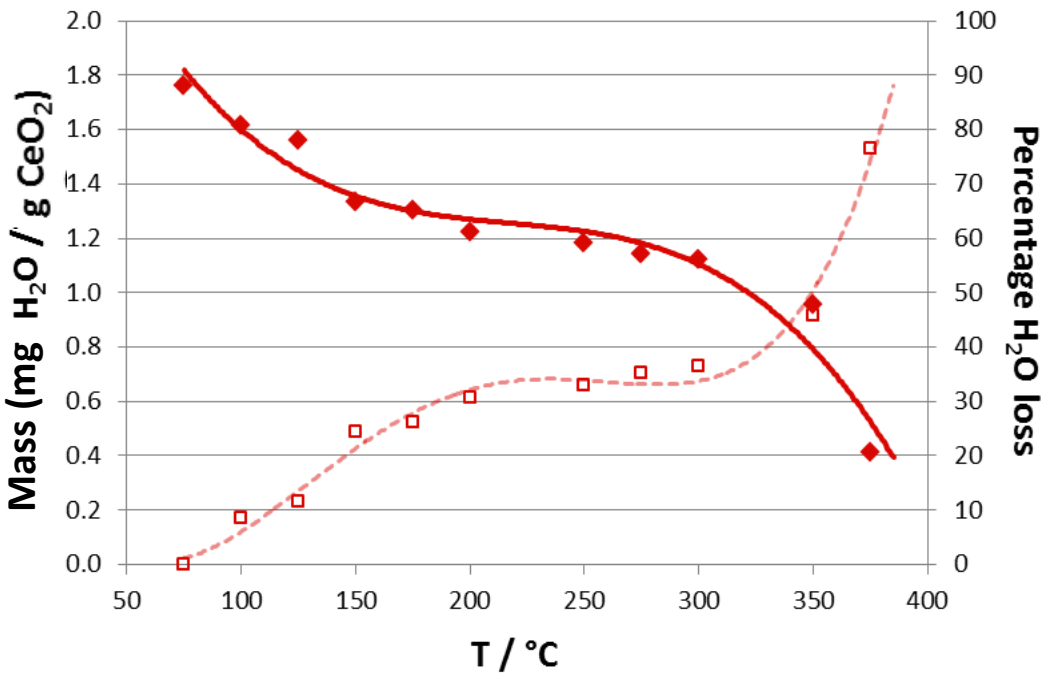

Approximately 20% of the water remains bound to the surface at 375°C.

Urania & Thoria films on $GaPO_4$ crystals

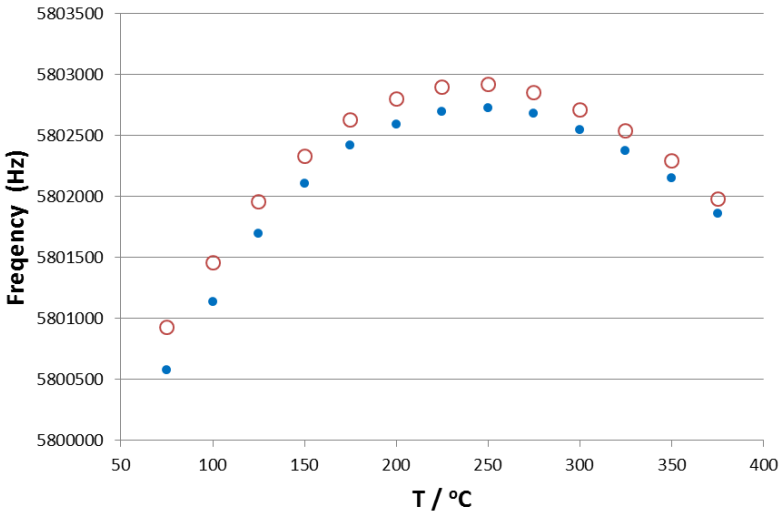

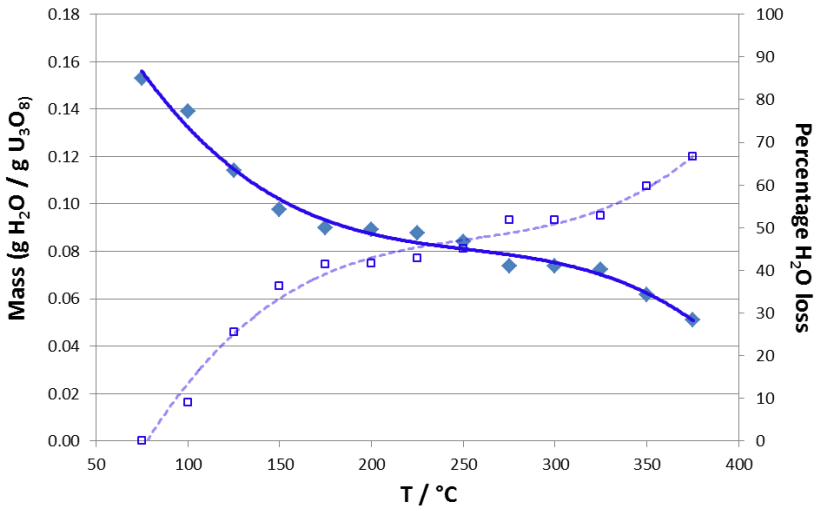

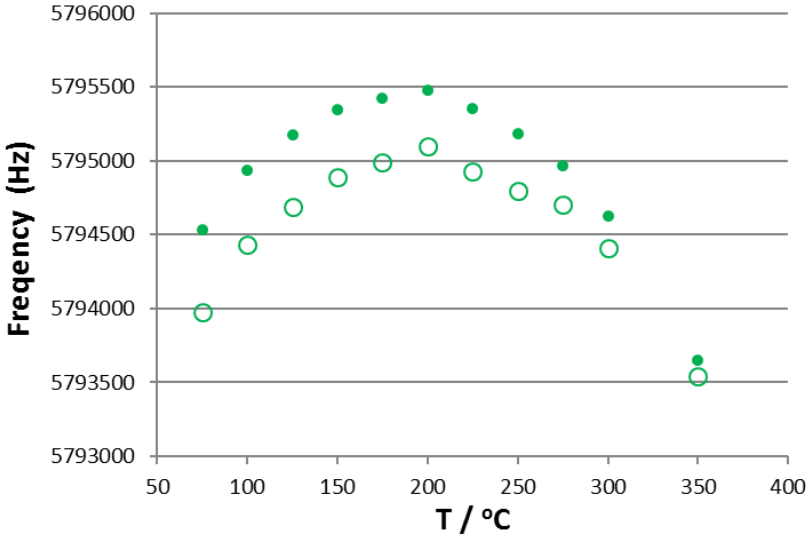

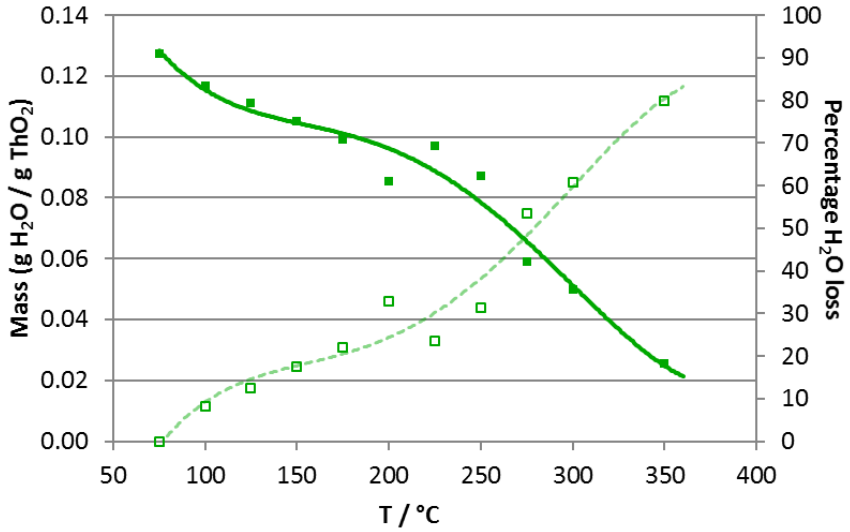

TRANSCEND

NATIONAL NUCLEAR LABORATORY

Lancaster University

- Introduction to UK plutonium interim storage
- Synthesis of thin-layer actinide coatings
- **Contact angle measurements**
- Piezo-crystal nano-balance experiments

Macroscopic water absorption: contact angle measurements

- Contact angle measurements of liquids on surfaces give an indication of the wettability of the surface.
- Surface irregularities disrupt droplet cohesion, increasing the wettability of a surface. Chemical characteristics also effect wettability.
- Therefore the surface finish resulting from different processing methods will alter the wettability.
- Plutonium's intrinsic radioactivity and high levels of decay heat causes surface damage during storage to an unknown extent.

$r.\cos\Theta_c = \cos\Theta_m$

$\gamma_{LG}.\cos\Theta_c = \gamma_{SL} - \gamma_{SG}$

Θ_c = *contact angle*

r: roughness factor

γ_{LG}: surface tension

γ_{SL}: solid-liq IE

γ_{SG}: solid-gas IE

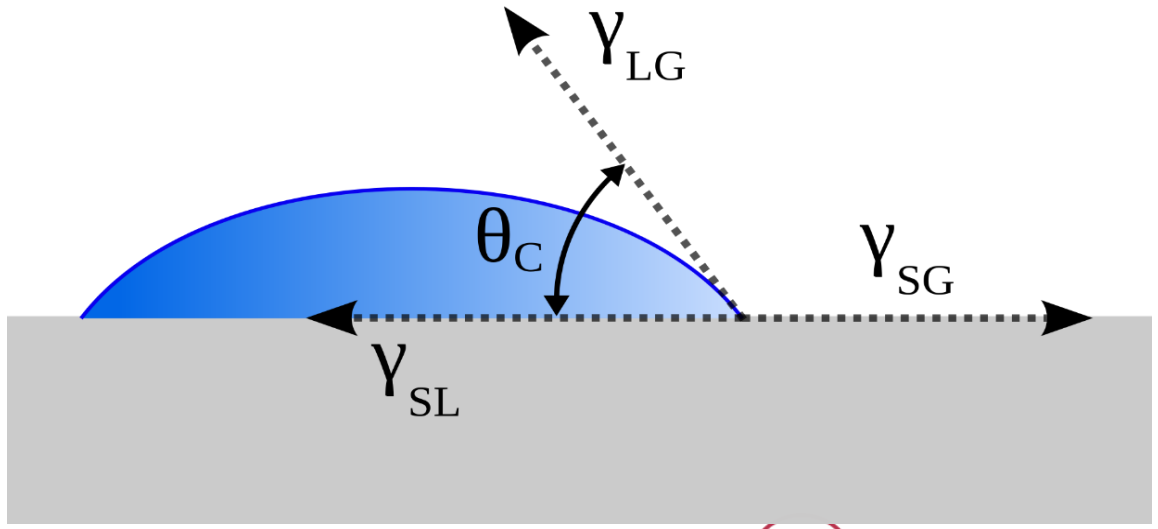

24

Contact angle measurements: method

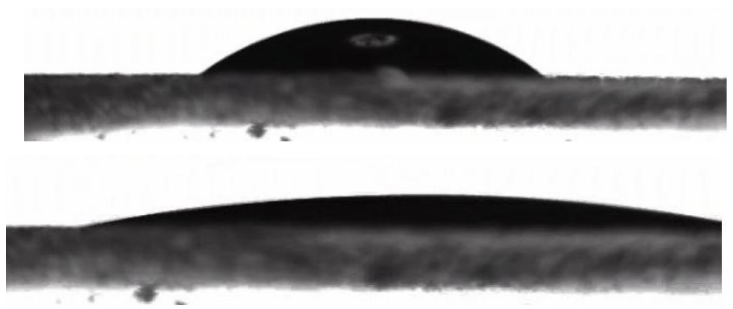

Water droplet on oxide nano-thick layer at 100% humidity, before and after UV irradiation.

- Measure contact angles of plutonium oxide analogues (CeO_2, ThO_2, UO_2, $Ce_{1-x}Eu_xO_2$) produced at a range of calcination temperatures.
- Vary humidity of the environment.
- Measure initial contact angles and variation in contact angle during evaporation.
- Automate droplet measurements using image recognition / machine learning.

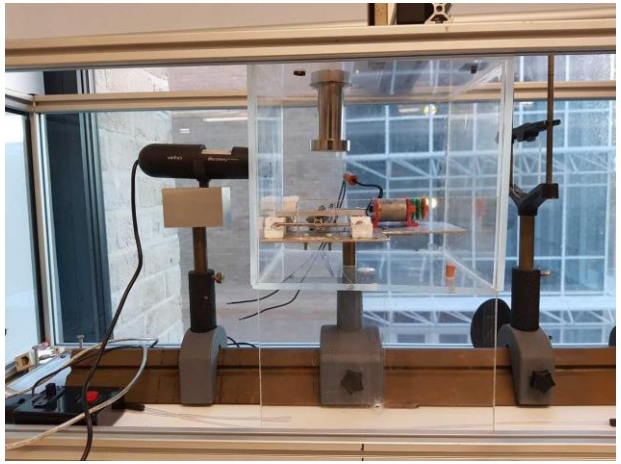

Contact angle measurements calcination temperature

- Higher calcination temperatures result in more hydrophilic surfaces, and lower contact angles.

UO_2: 300°C

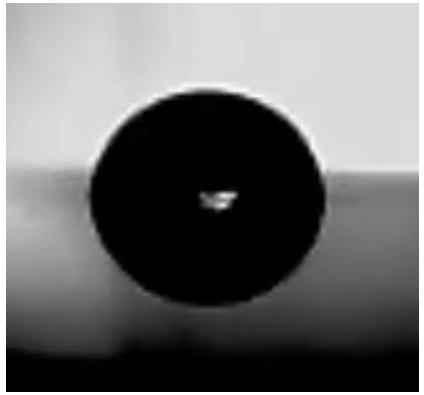

UO_2: 400°C

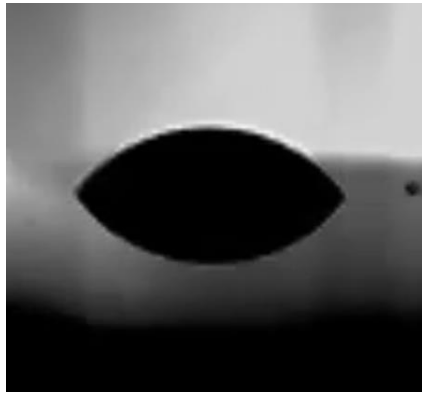

UO_2: 500°C

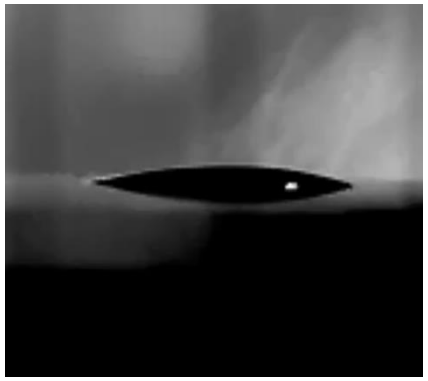

ThO_2: 300°C

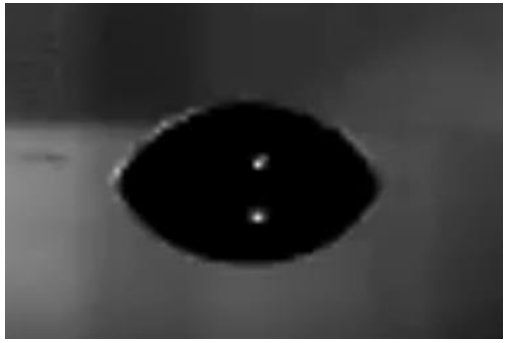

ThO_2: 400°C

ThO_2: 500°C

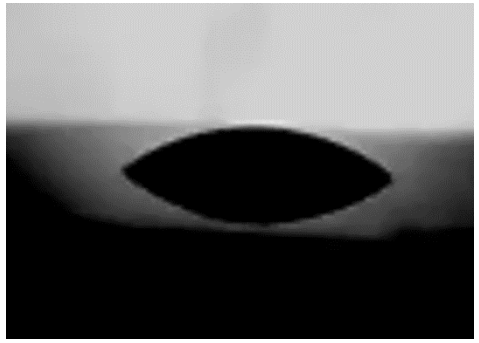

Macroscopic water absorption: contact angle measurements

- metal oxide layer on glass substrate (~ 10 ug metal / cm^2), calcined at 300˚C
- water droplet (1 uL) deposited at initial 40% humidity

ThO_2

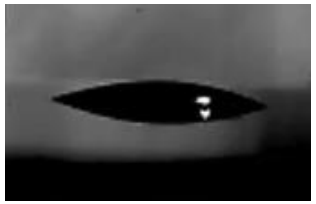

Init. contact angle = 27°

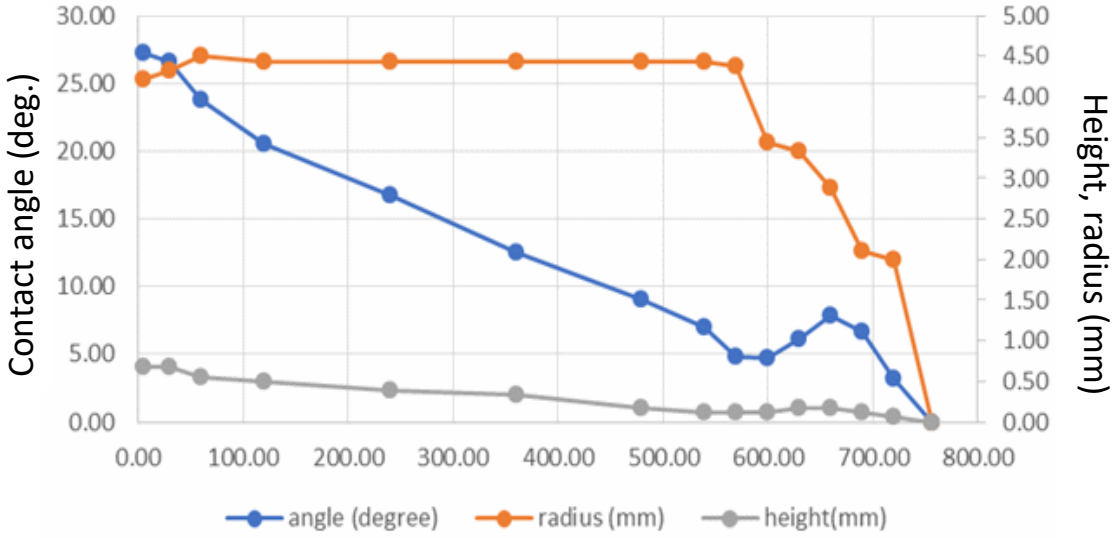

CeO_2

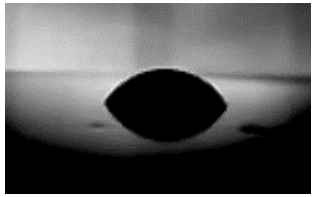

Init. contact angle = 58°

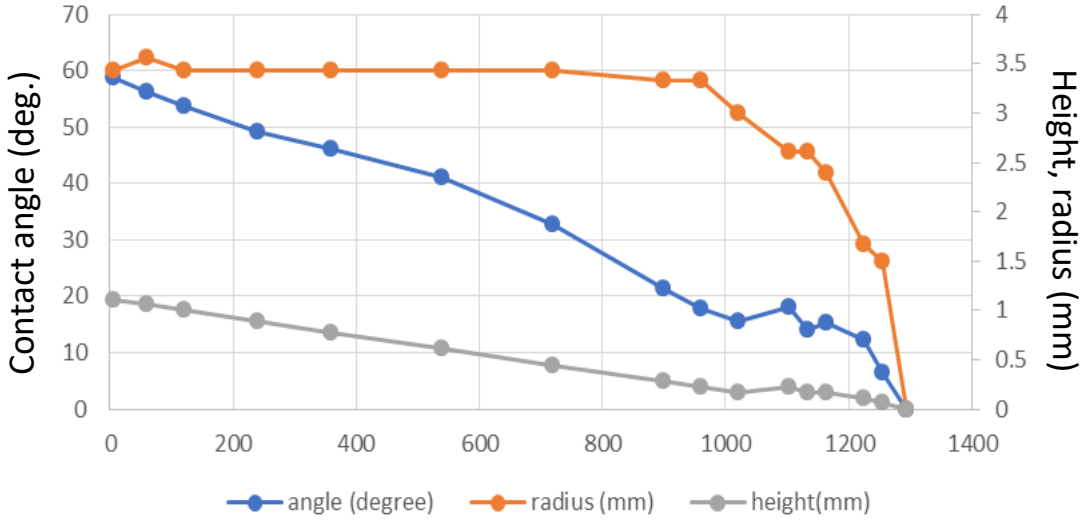

Macroscopic water absorption: contact angle measurements

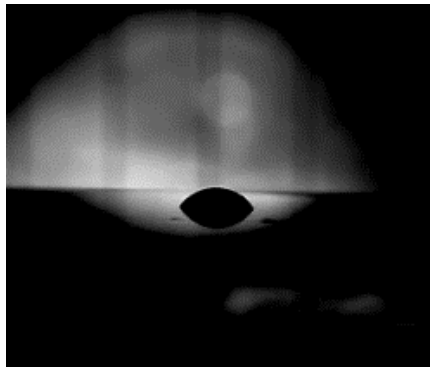

1. Greyscale
2. Blur
3. Edge detect
4. Dilate
5. Erode

Image contour

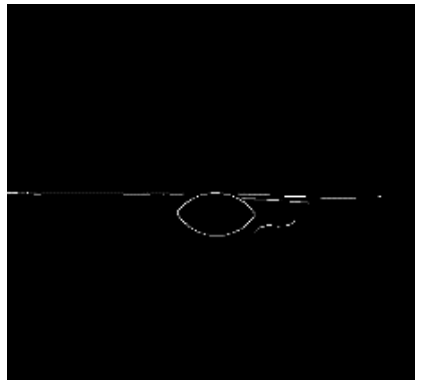

6. Adjust to horizontal
7. Select largest contour
8. Crop, bisect

droplet contour

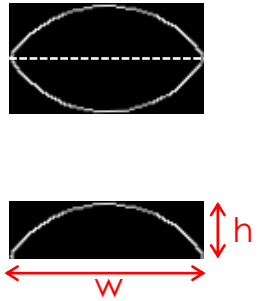

$r = (h / 2) + (w / (8 * h))$

$CA = 90 – \sin^{-1}(r-h / r)$

As the drop evaporates and flattens, the modelled circle gets bigger (w increases, h decreases) and the CA decreases

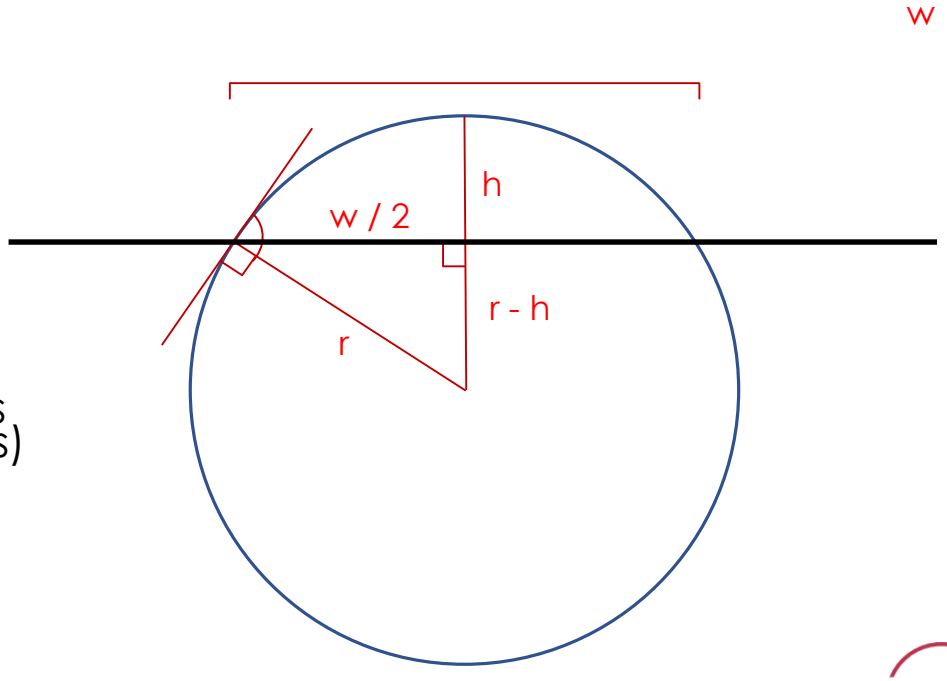

Macroscopic water absorption: contact angle measurements

UO_2 calcined at 300°C, 40% hum.

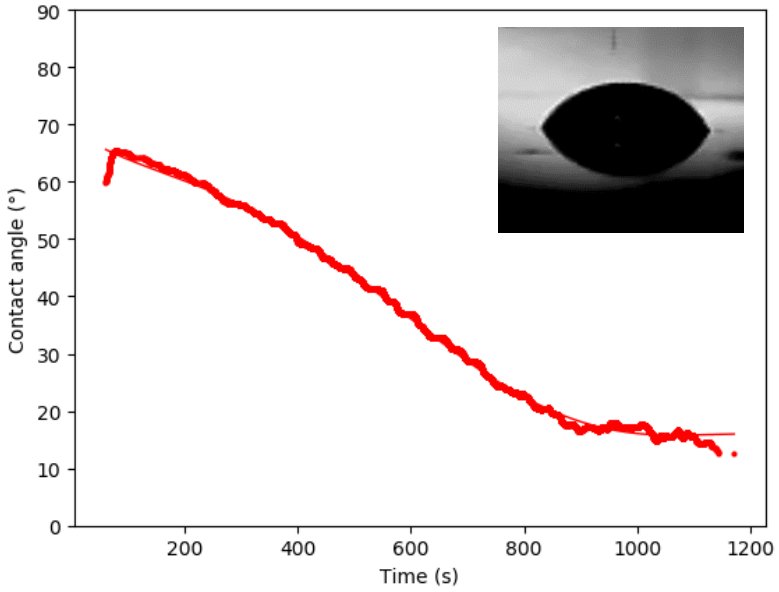

UO_2 calcined at 400°C, 40% hum.

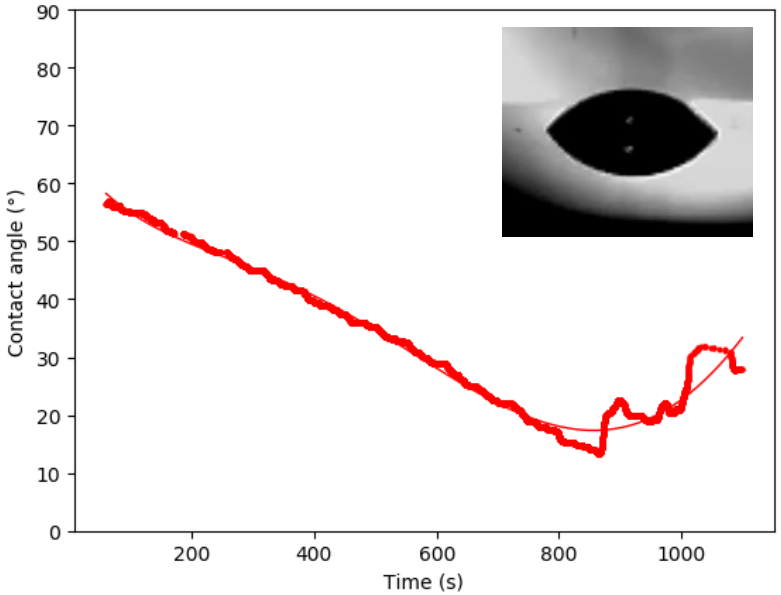

- Calcination at higher temperature gives a lower initial contact angle.
- Rate of evaporation remains approx. the same.
- More contraction events seen for more hydrophilic surface.

Contact angle measurements: Further work

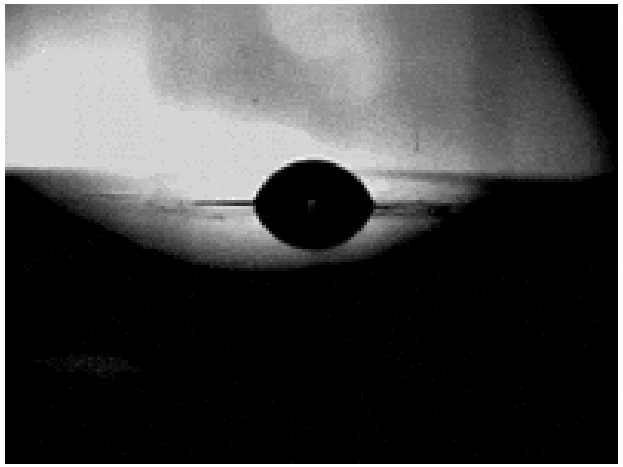

- Reduce size of equipment to fit through glove-box port.
- Improve camera / lighting to give better illumination and resolution.
- Improve automated image recognition.

- Collect more data at different humidities and calcination temperatures, of CeO_2, ThO_2, UO_2.
- Change pH and ionic strength (e.g. salt content) of droplets.
- Measure repeatability of on dry versus pre-wetted surfaces.

Conclusions

- Thin-layers of ceria and thoria (and Urania and plutonia) produced through drop-coating process onto glass and metal surfaces.
- Oxide-coated piezoelectric crystal electrodes used to measure the extent of water absorption onto the oxide surface via changes in frequency.
- Temperature and humidity of the system altered to produce isotherms and the energy of water binding determined.
- Contact angle measurement of water droplets on the oxide layers indicate the wettability and hydrophilicity of the surfaces. Pilot studies indicate significant differences between ceria and thoria, and effects due to calcination temperature and humidity.

Acknowledgments

Lancaster University

Pat Murphy

Richard Wilbraham

ITU

Detlef Wegen

NNL

Robin Taylor

Robin Orr

Dave Woodhead

Thanks for your attention

TRANSCEND

Transformative Science and Engineering for Nuclear Decommissioning

Atomistic Simulation of Helium Incorporation in PuO_2

Elanor Murray, University of Birmingham

TRANSCEND/NDA/NWDRF Virtual Conference

3/12/2020
Zoom

Energy
For a Low Carbon Future

TRANSCEND

Transformative Science and Engineering for Nuclear Decommissioning

Is it pressurised?

Has its structure changed?

What's it like inside?

Is it still edible?

Does it need throwing away?

Can it stay in the storage?

Do I really want to open this?

NATIONAL NUCLEAR LABORATORY

NDA

TRANSCEND

Transformative Science and Engineering for Nuclear Decommissioning

Is it pressurised?
Helium generation

Has its structure changed?

What's it like inside?

Is it still edible?
Can it be used in future reactors?

Does it need throwing away?
Need to go in GDF eventually?

Can it stay in the storage?
Is it safe to remain in interim storage?

Do I really want to open this?
Use computational chemistry methods

NATIONAL NUCLEAR LABORATORY

NDA

Helium Incorporation

- *Static loading – how much helium can the lattice accommodate?*
- *What are the likely trapping sites?*
- *Is helium diffusion vacancy assisted?*
- *How does helium aggregate?*
- *What is the mechanism for bubble formation?*

Modelling procedure

GULP overview

Crystal Structure
'Force Field'

Initial position of ions
Forces acting between them

GULP

Geometry optimise
Final position of ions
Predict properties

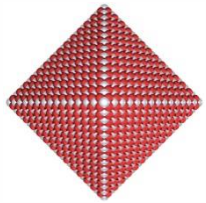

Geometry Optimised Crystal Structure

Physical Properties:
Mechanical
Optical

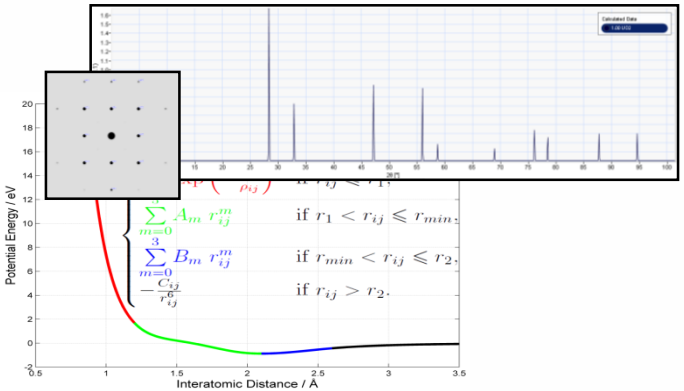

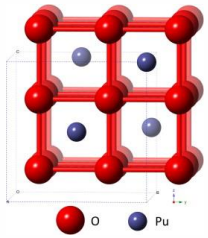

Potential model

Pu ··· Pu ✓
Pu ··· O ✓
O ··· O ✓

O ··· He ✓
Pu ··· He ✗
He ··· He ✗

Atomistic simulations of helium dynamics in a plutonium lattice
Vladimir Dremov, Philipp Sapozhnikov, Andrey Kutepov, Vladimir Anisimov, Michael Korotin, Alexey Shorikov, Dean L. Preston, and Marvin A. Zocher
Phys. Rev. B **77**, 224306 – Published 30 June 2008

$$\Phi(r) = \epsilon \left\{ \left(\frac{6}{\alpha - 6} \right) \exp\left[\alpha \left(1 - \frac{r}{r^*} \right) \right] - \left(\frac{\alpha}{\alpha - 6} \right) \left(\frac{r^*}{r} \right)^6 \right\}$$

Found potential! But exp-6 not included in GULP so need to fit to standard form…

M. Read, S. Walker, and R. Jackson, vol. 448, no. 1, pp. 20 – 25, 2014.
R. W. Grimes, NASO ASI Series B, vol. 279, 1991.
V. Dremov, et al. Phys. Rev. B,vol. 77, p. 224306, 2008.

Fitting

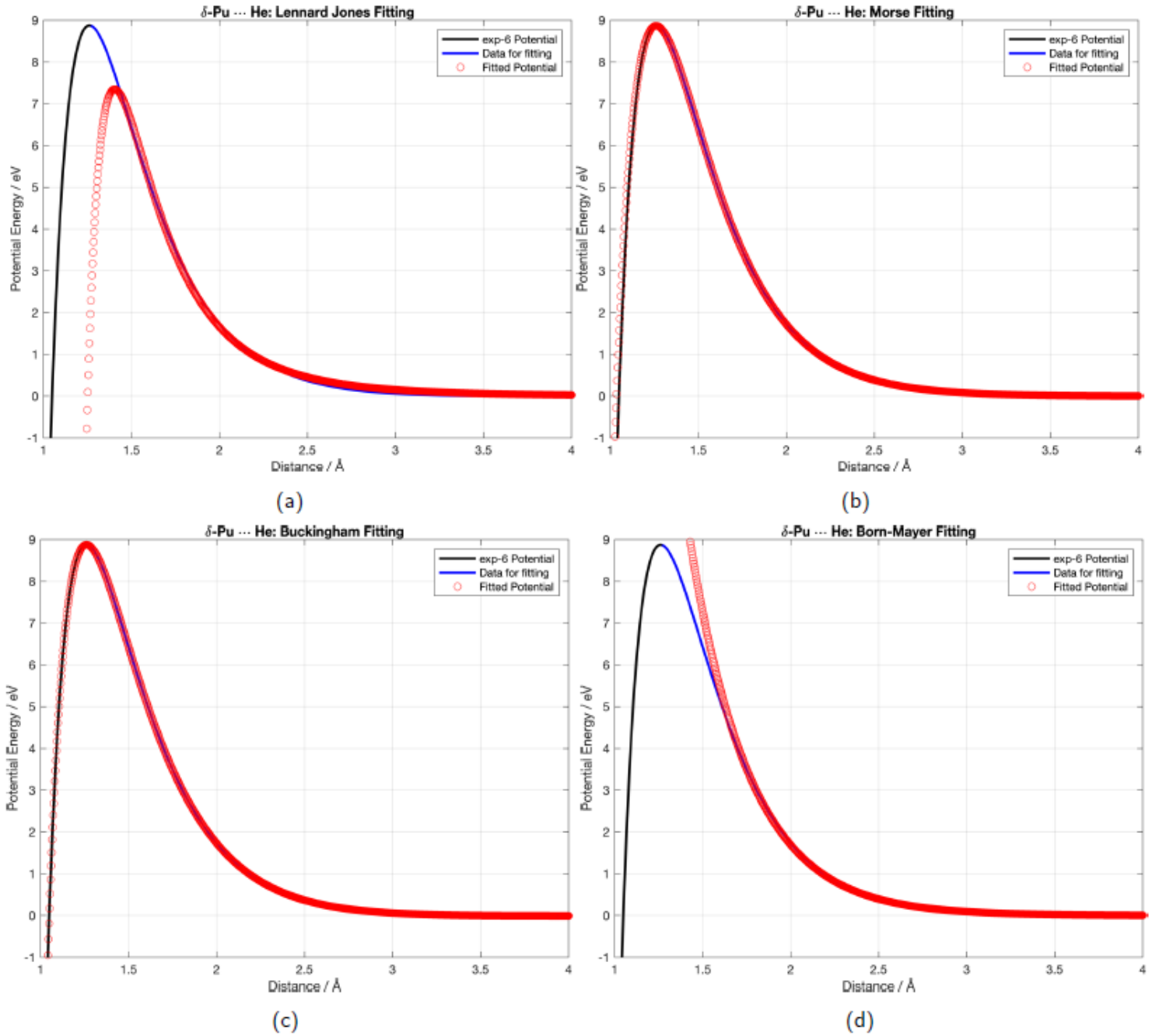
δ-Pu --- He: Lennard Jones Fitting
δ-Pu --- He: Morse Fitting
δ-Pu --- He: Buckingham Fitting
δ-Pu --- He: Born-Mayer Fitting
exp-6 Potential
Data for fitting
Fitted Potential
Potential Energy / eV
Distance / Å
(a)
(b)
(c)
(d)

V_{eq} = 8.9 eV
r_{eq} = 1.26 Å

Pu ··· Pu ✓
Pu ··· O ✓
O ··· O ✓

O ··· He ✓
Pu ··· He ✓
He ··· He ✓

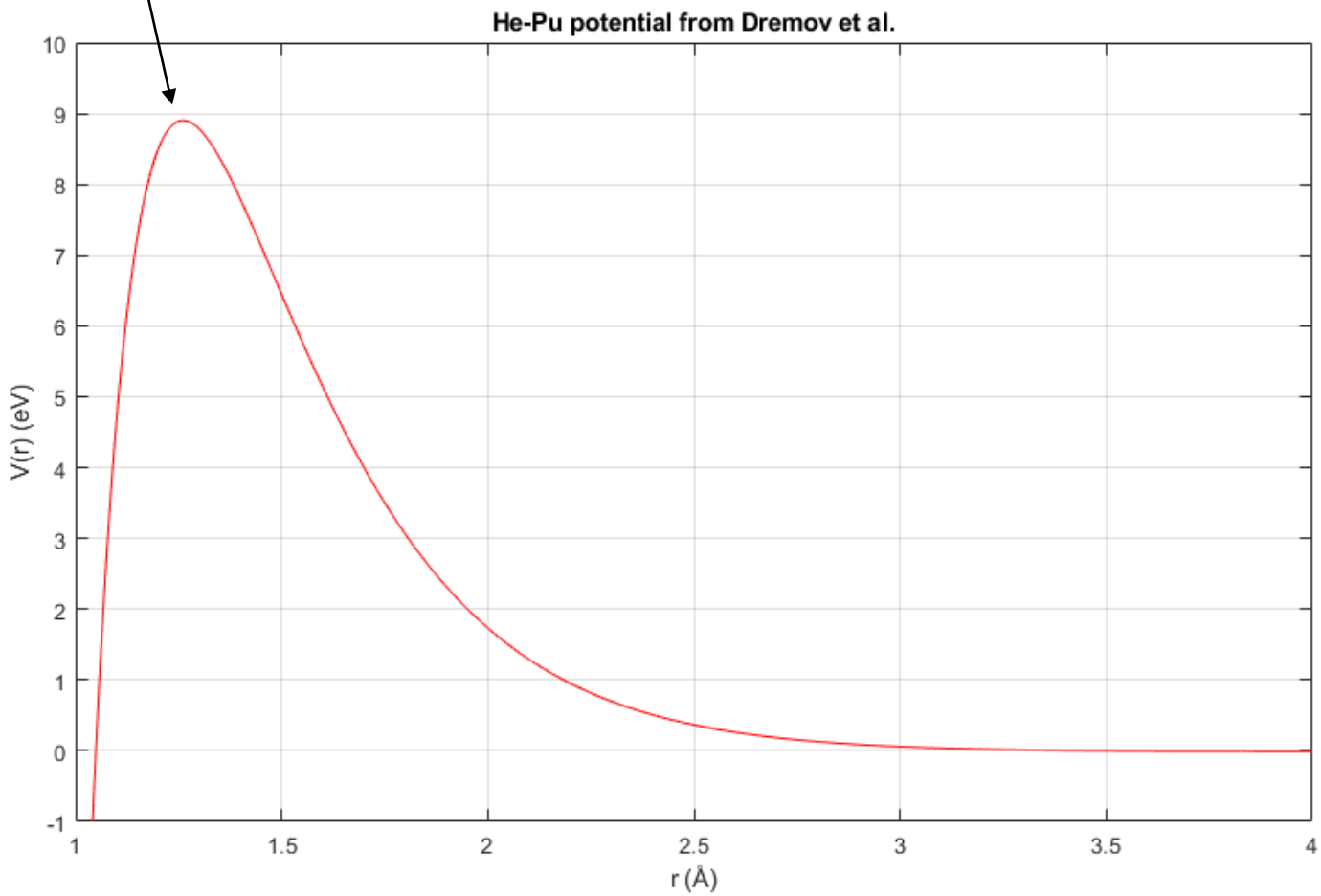

He in Pure PuO_2

Single He Interstitials

Interstitial Sites

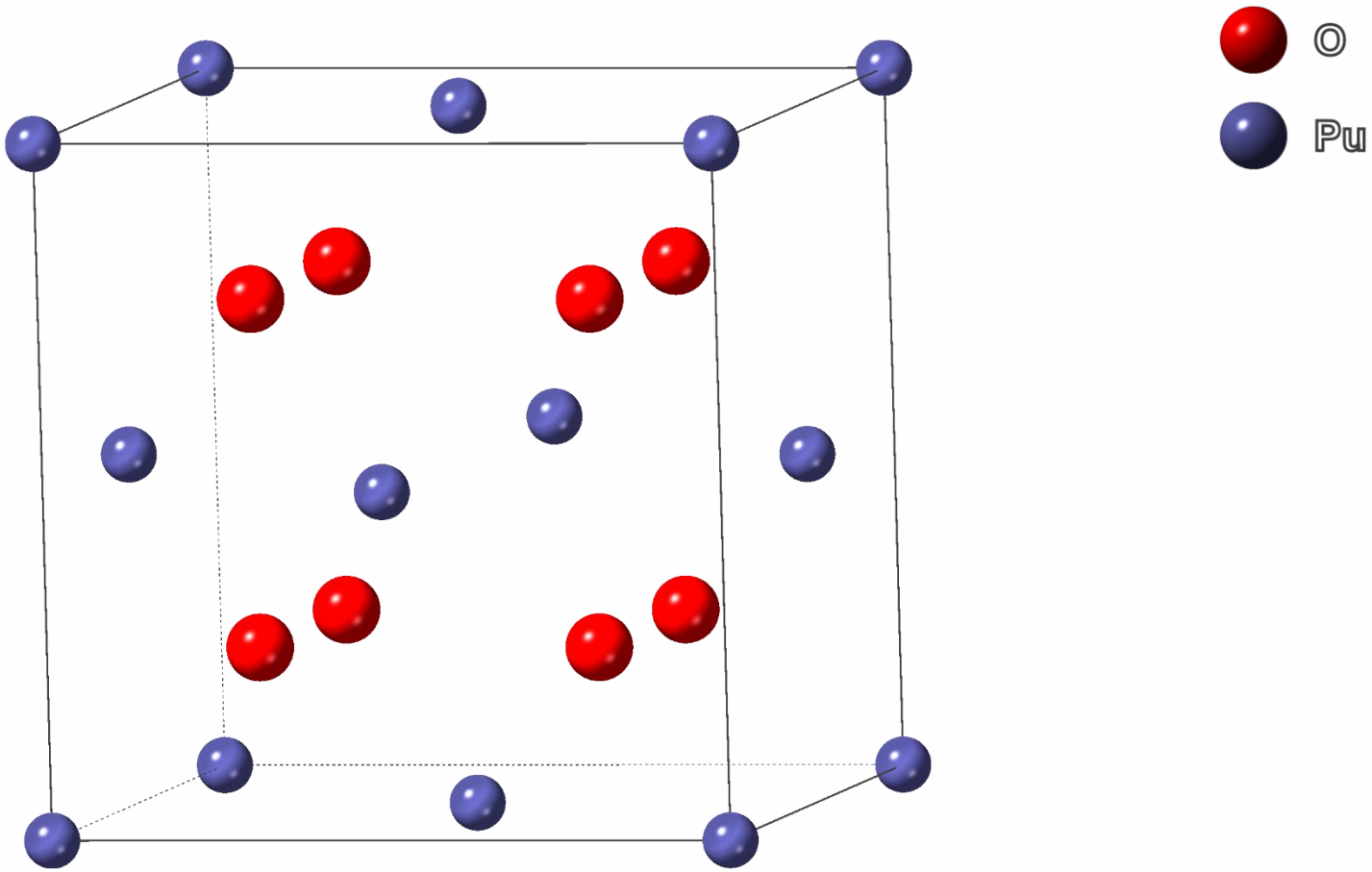

Interstitial Sites

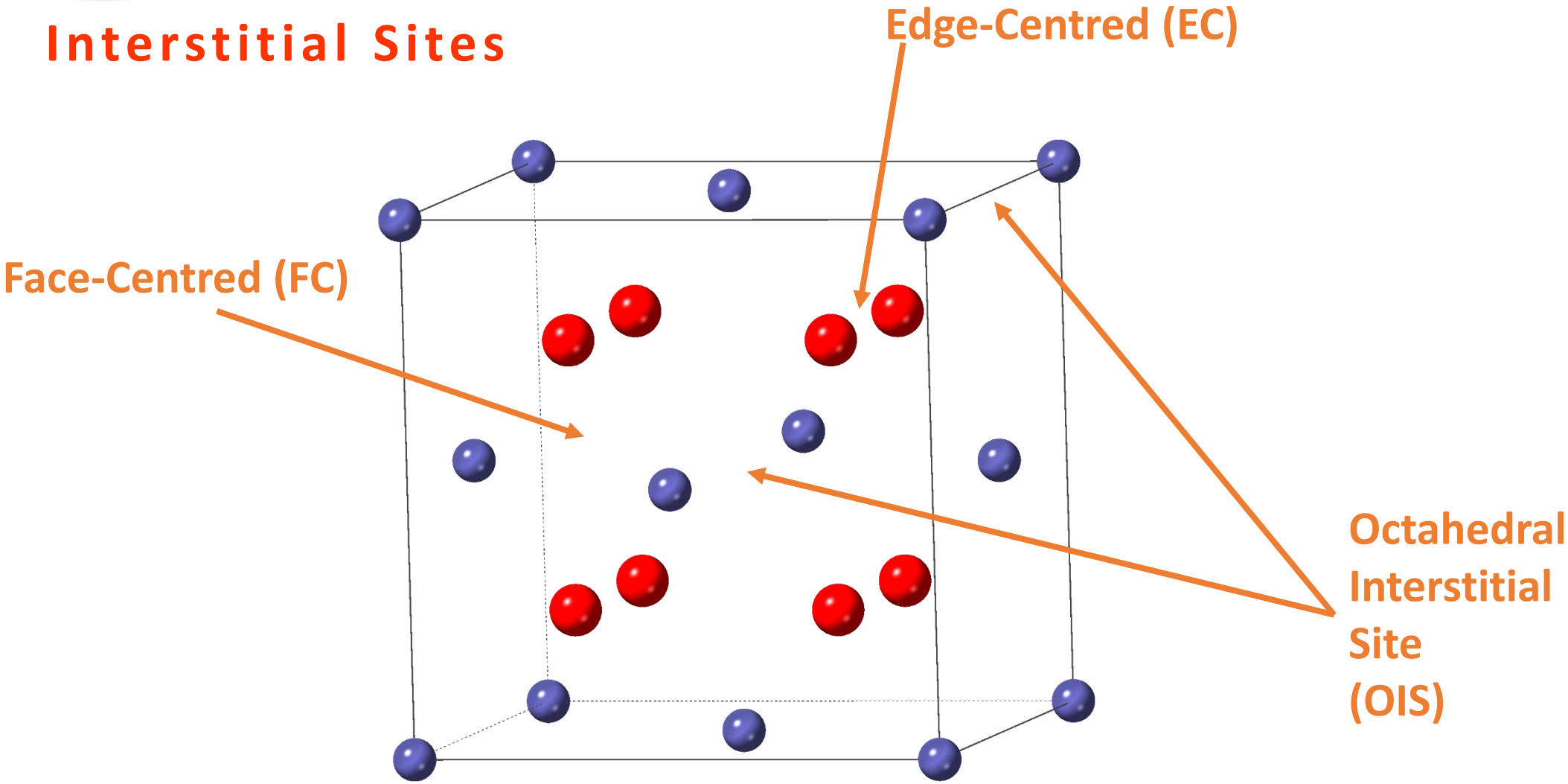

Interstitial Sites

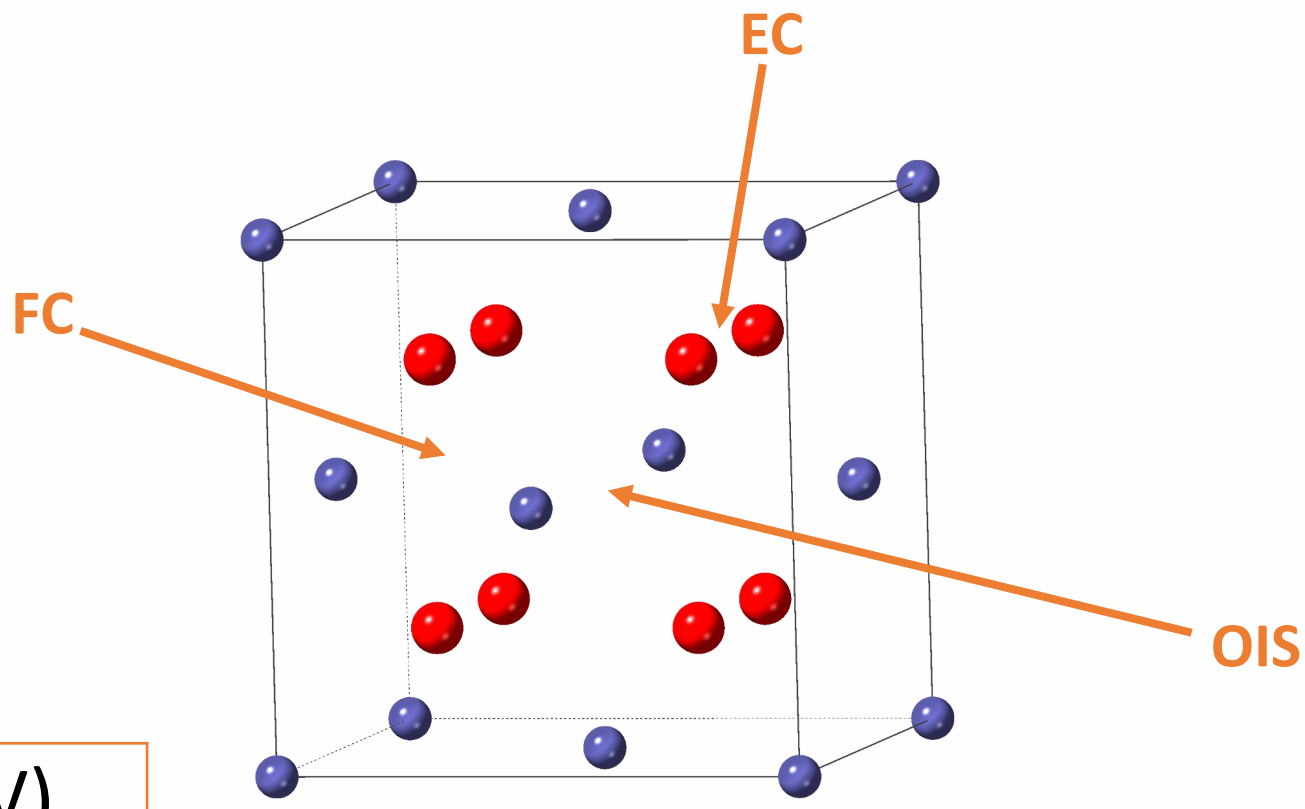

Name	E_d (eV)
OIS	1.06
FC	7.07
EC	5.60

Energy Profile

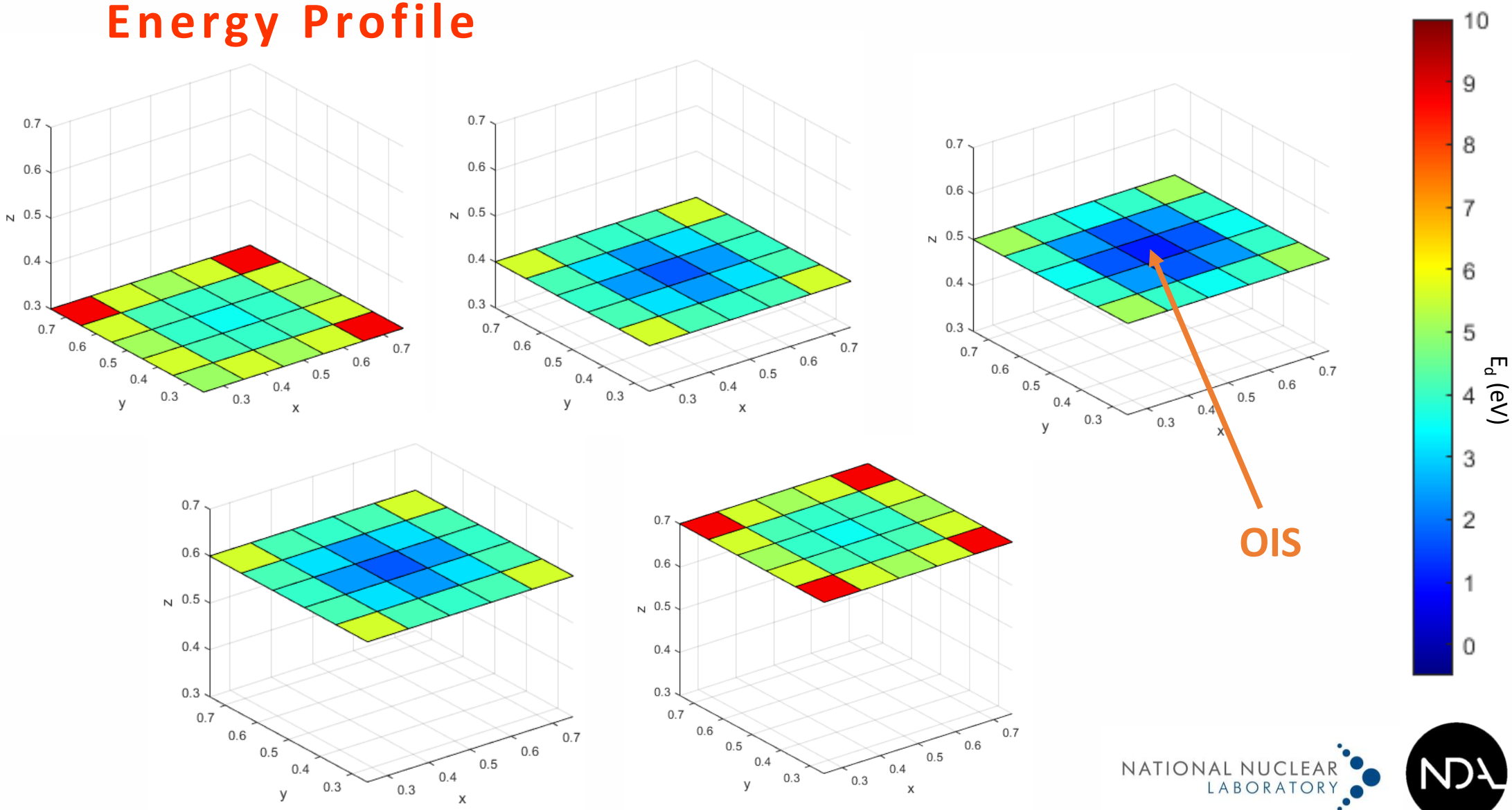

He in Pure PuO_2

Build up of Helium

Two Helium Interstitials

Name	E_d (eV)
OIS_OIS	2.13
EC_OIS	2.11
FC_OIS	8.15
EC_EC	5.25
FC_FC	14.28
EC_FC	6.40
110	2.11
100	2.13
DB	5.25

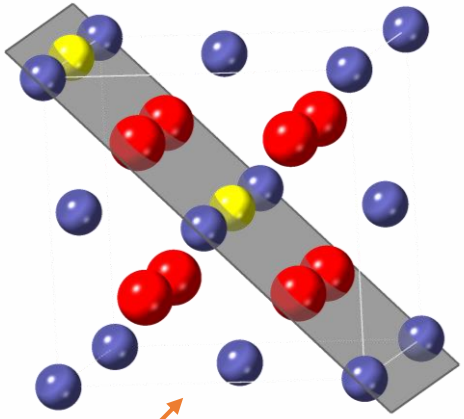

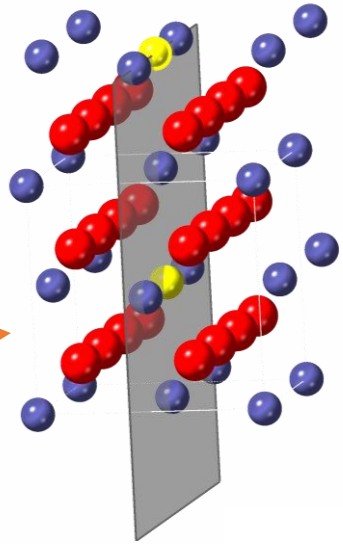

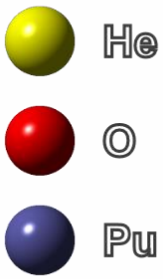

Two Helium Interstitials

Input

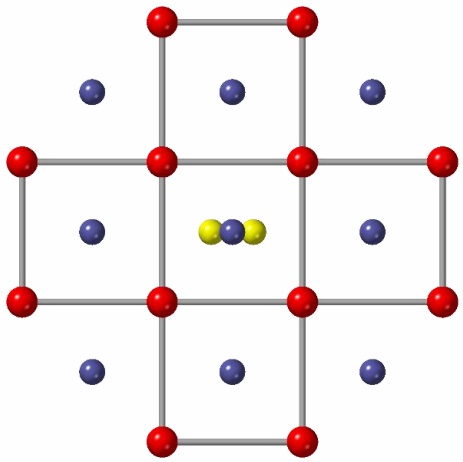

0.81 Å

Atomic relaxation

Relaxed

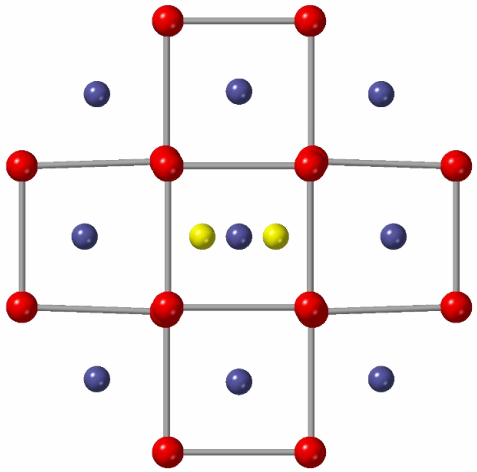

1.39 Å

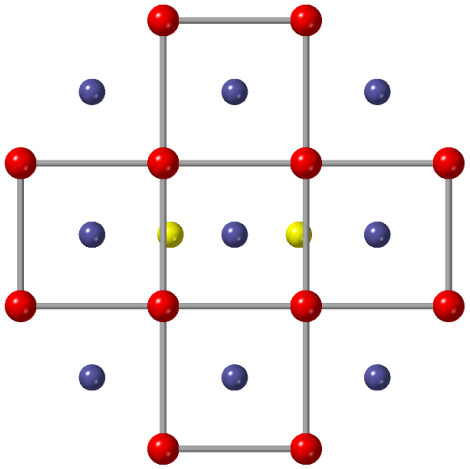

2.43 Å

Atomic relaxation

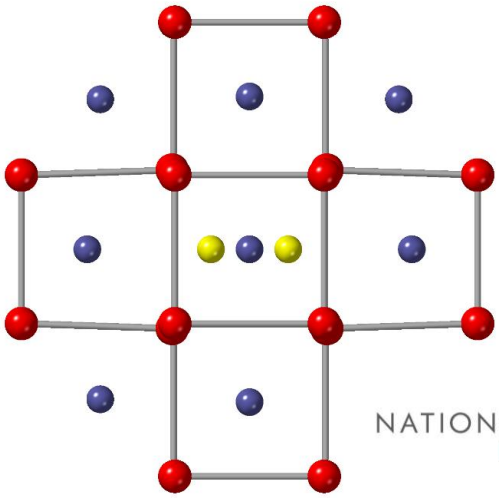

1.39 Å

Dumbbell Configuration

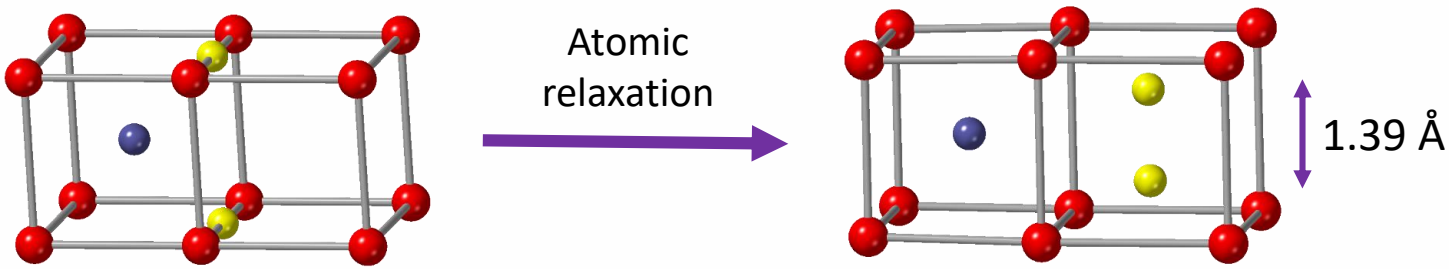

First-principles study of helium behavior in nuclear fuel materials

Younsuk Yun[1], Olle Eriksson[2], and Peter M. Oppeneer[2]
[1]Laboratory for Reactor Physics and Systems Behaviour, Paul Scherrer Institut, CH-5232 Villigen PSI, Switzerland
[2]Department of Physics and Astronomy, Uppsala University, Box 516, SE-751 20 Uppsala, Sweden

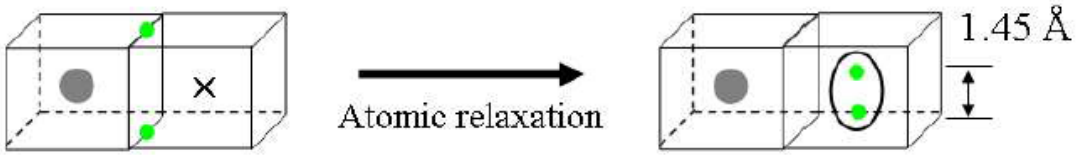

Y. Yun, O. Eriksson, and P. M. Oppeneer, Journal of Nuclear Materials, vol. 385, no. 3, pp. 510 – 516, 2009.
N. Kuganathan, P. Ghosh, A. Arya, and R. Grimes, Journalof Nuclear Materials, vol. 507, pp. 288 – 296, 2018.

Helium Loading

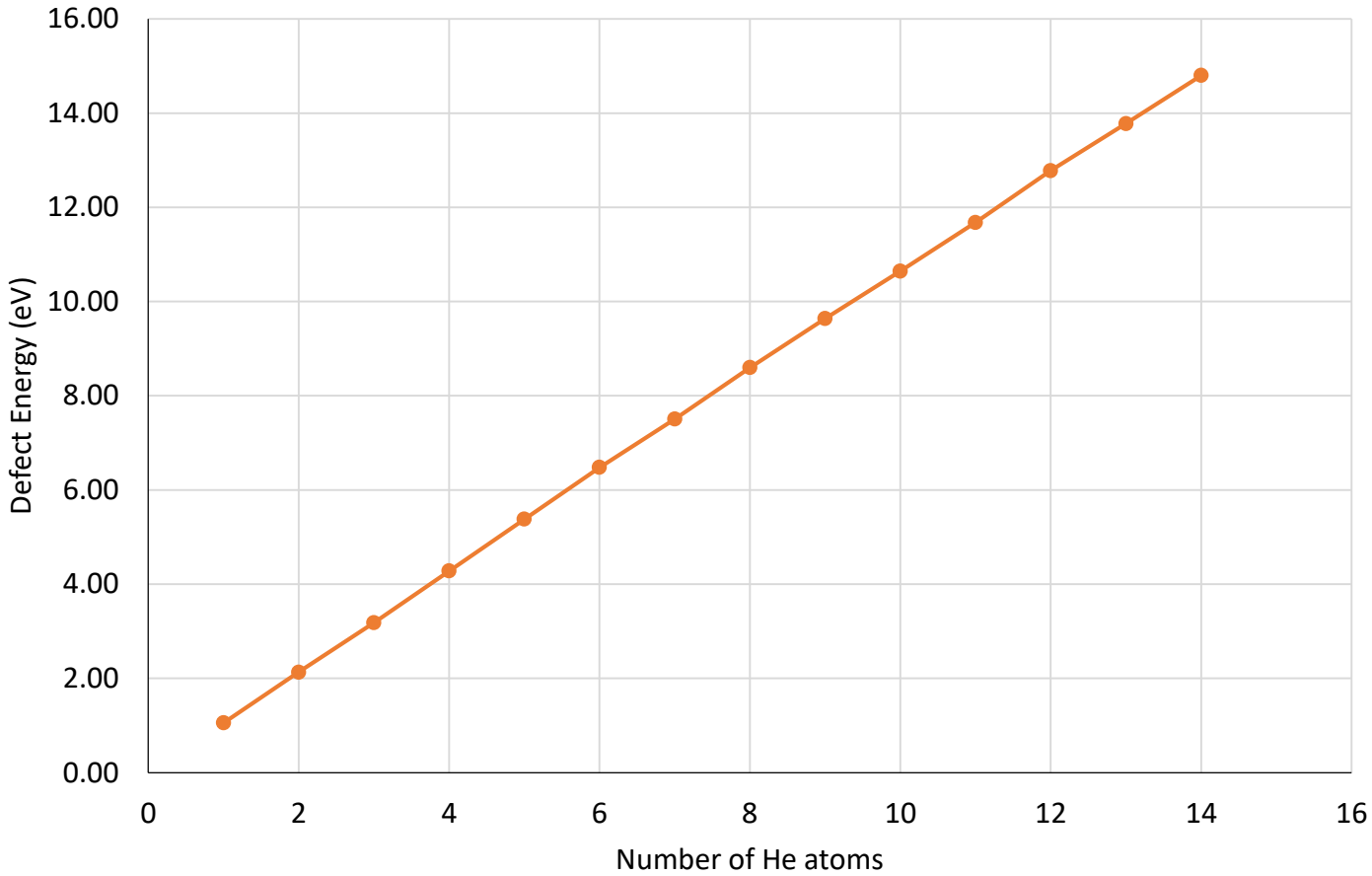

Defective PuO_2

Single Helium Atoms Incorporation

Defect Sites

Frenkel pair:
- Vacancy
- Self-interstitial

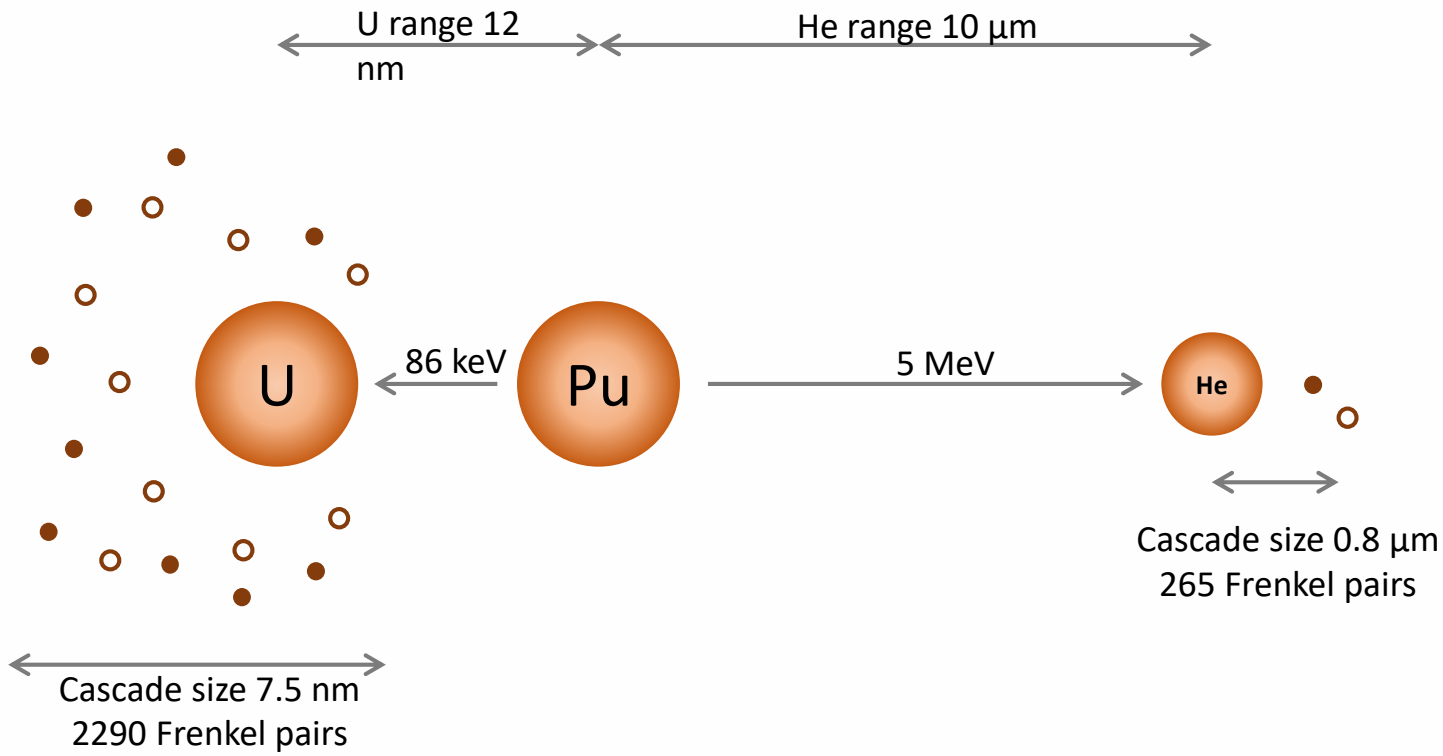

Pu vacancy, O vacancy, Pu Frenkel pair, O Frenkel pair, Divacancy, Schottky Trio

$$E_{inc} = E_d - E_T$$

Helium Incorporation at Vacancies

Oxygen vacancy

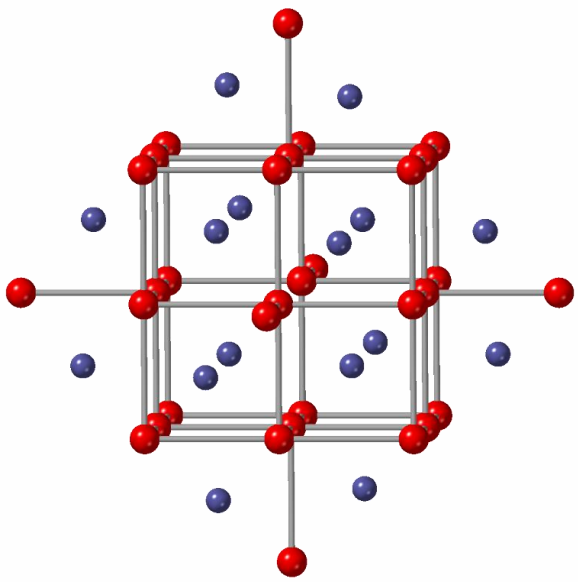

Plutonium vacancy

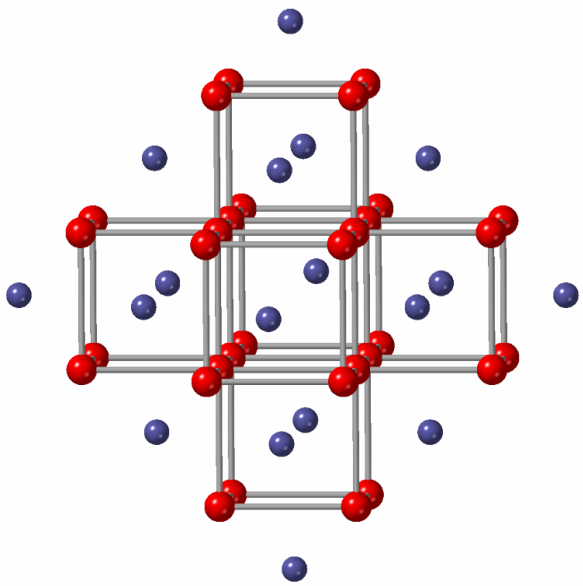

Helium Incorporation at Vacancies

Oxygen vacancy

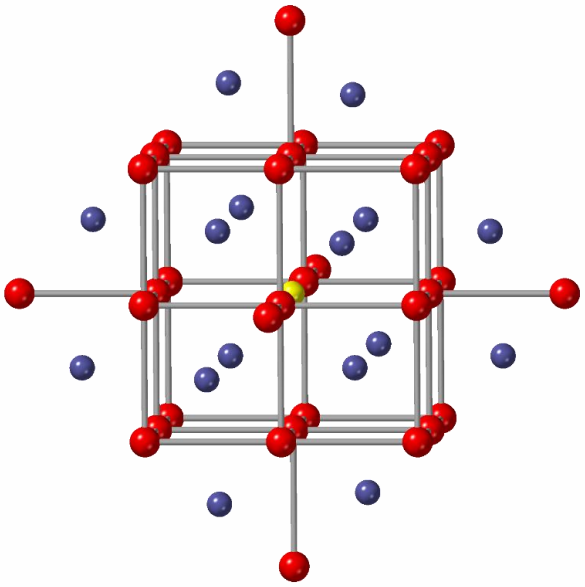

Plutonium vacancy

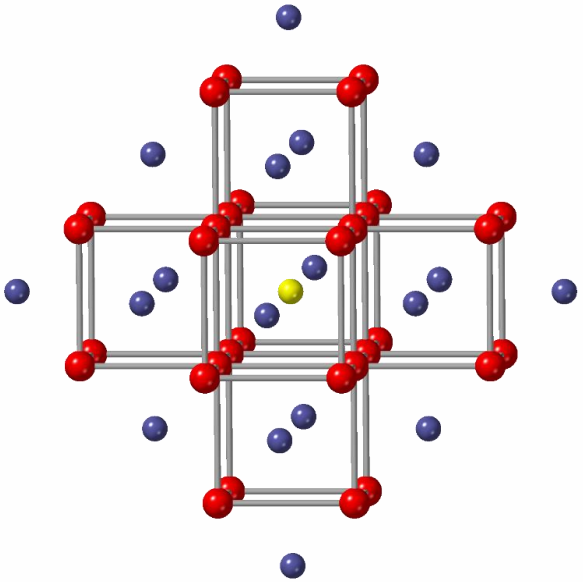

Helium Incorporation at Vacancies

Oxygen vacancy

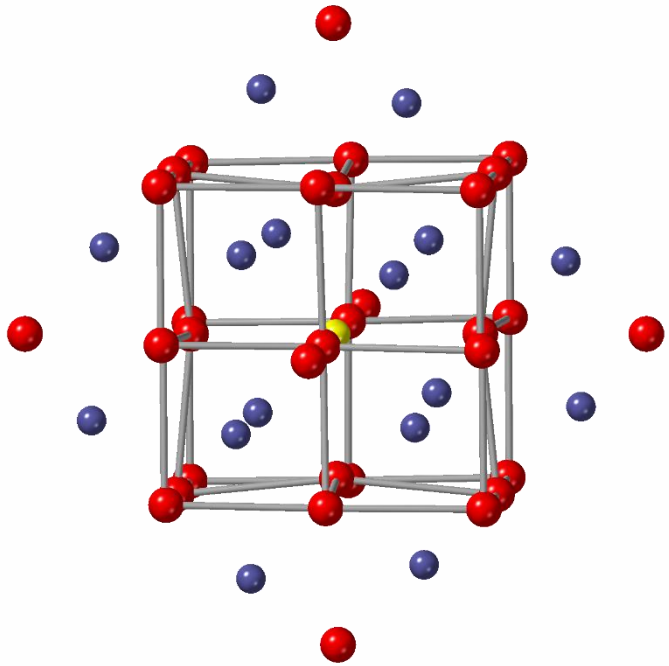

Site	E_d (eV)	E_{inc} (eV)
O_vac	18.37	1.28
OIS	18.12	1.03

Plutonium vacancy

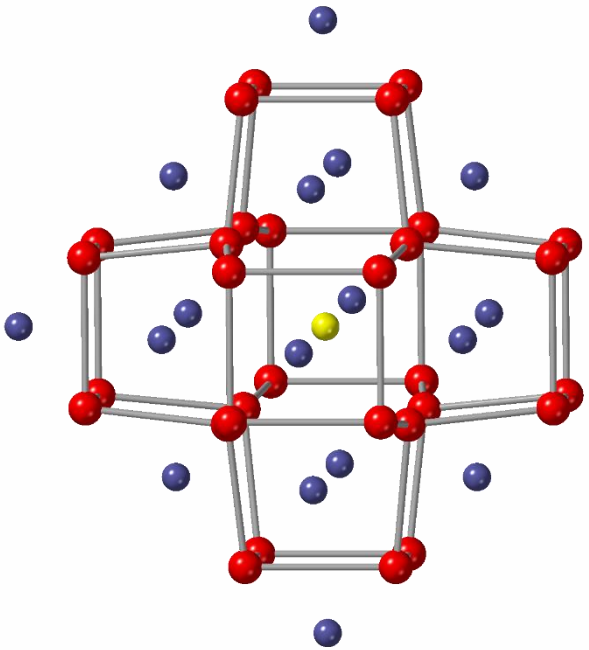

Site	E_d (eV)	E_{inc} (eV)
Pu_vac	94.26	-0.23
OIS	95.54	1.05

Oxygen Vacancy

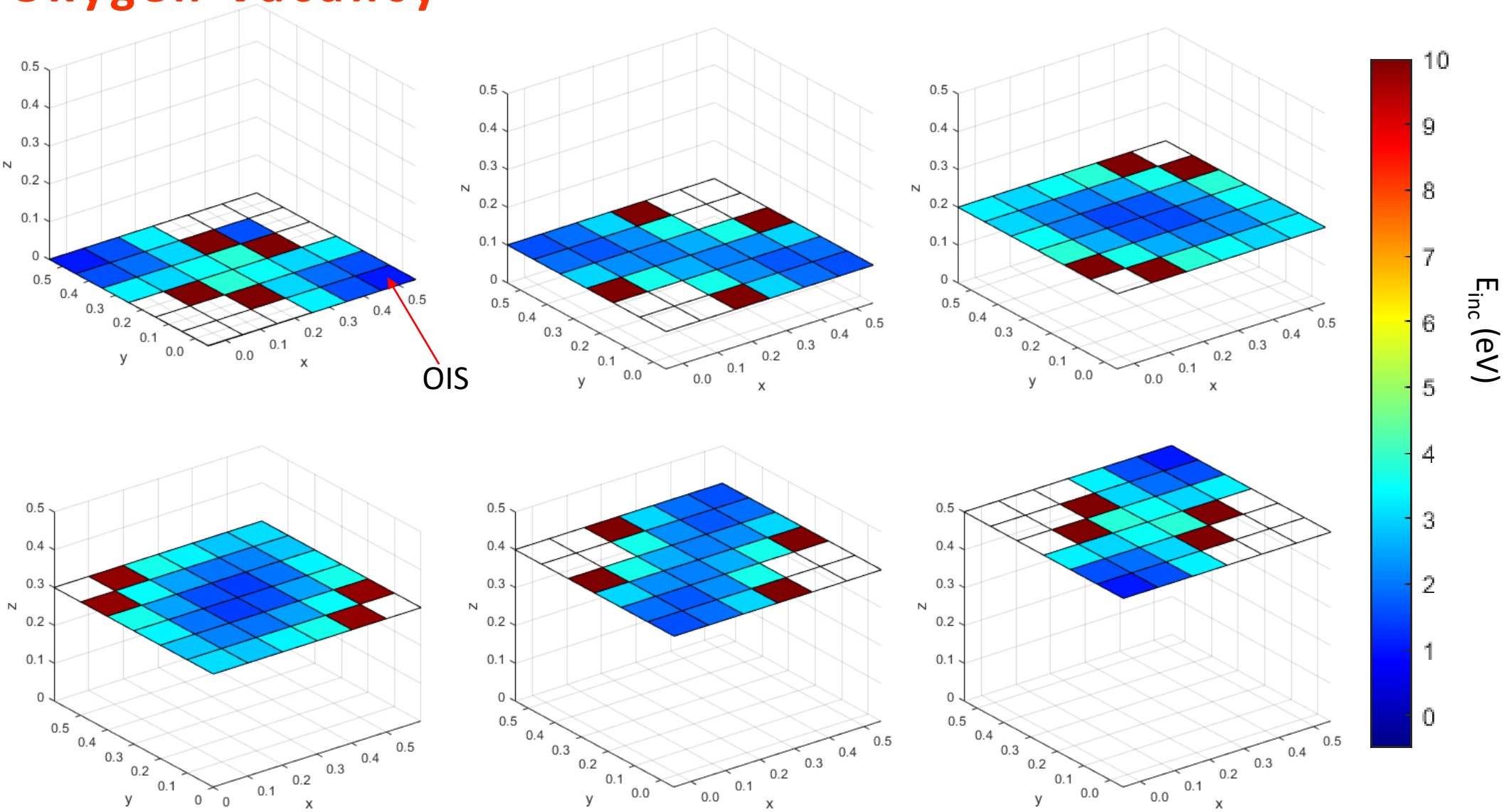

Plutonium Vacancy

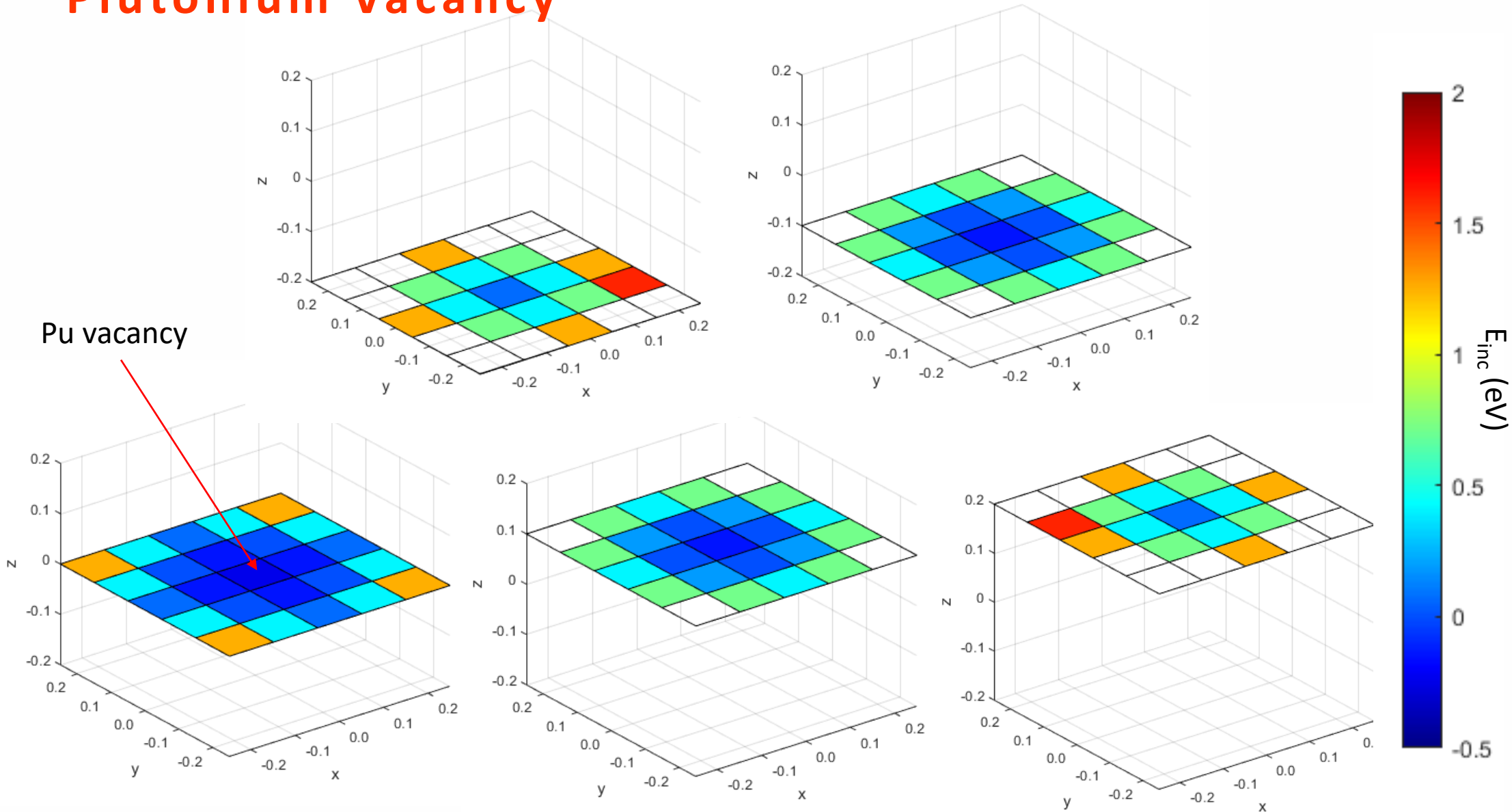

Defective PuO_2

Helium build up

Six He surrounding an O vacancy

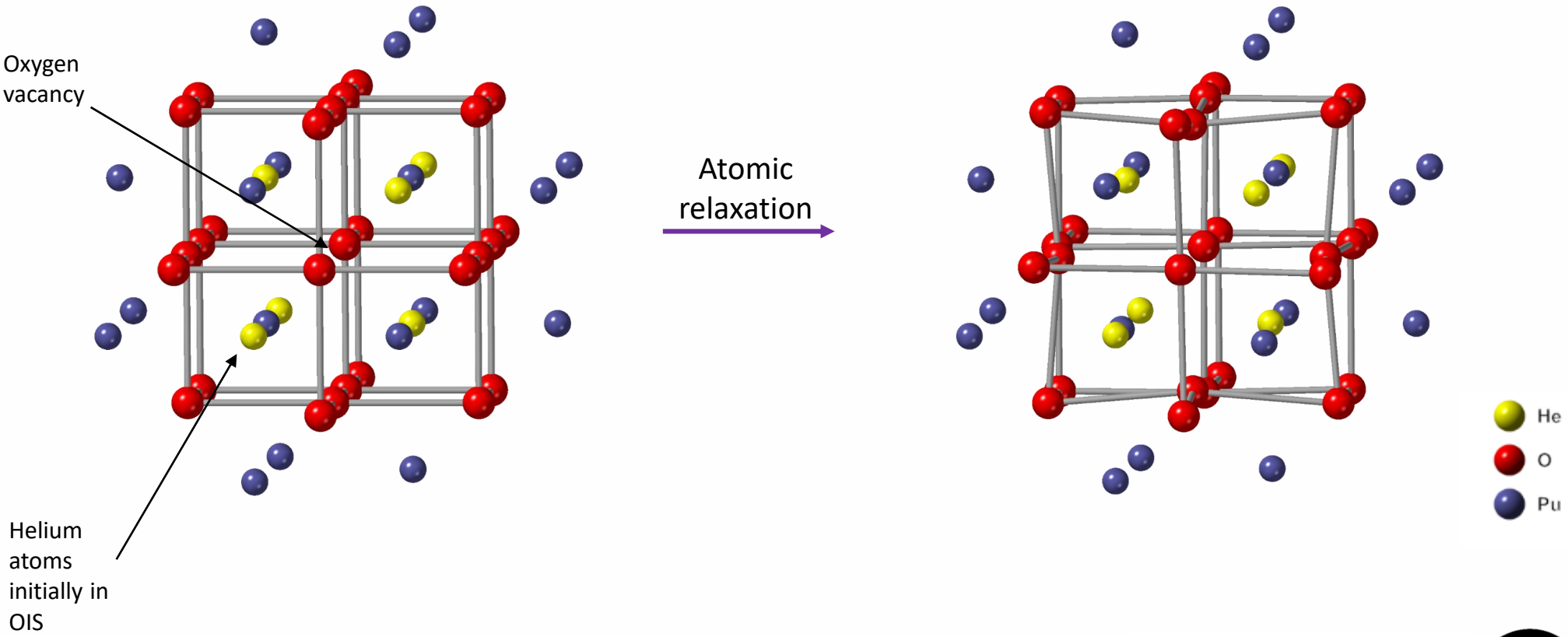

Six He surrounding a Pu vacancy

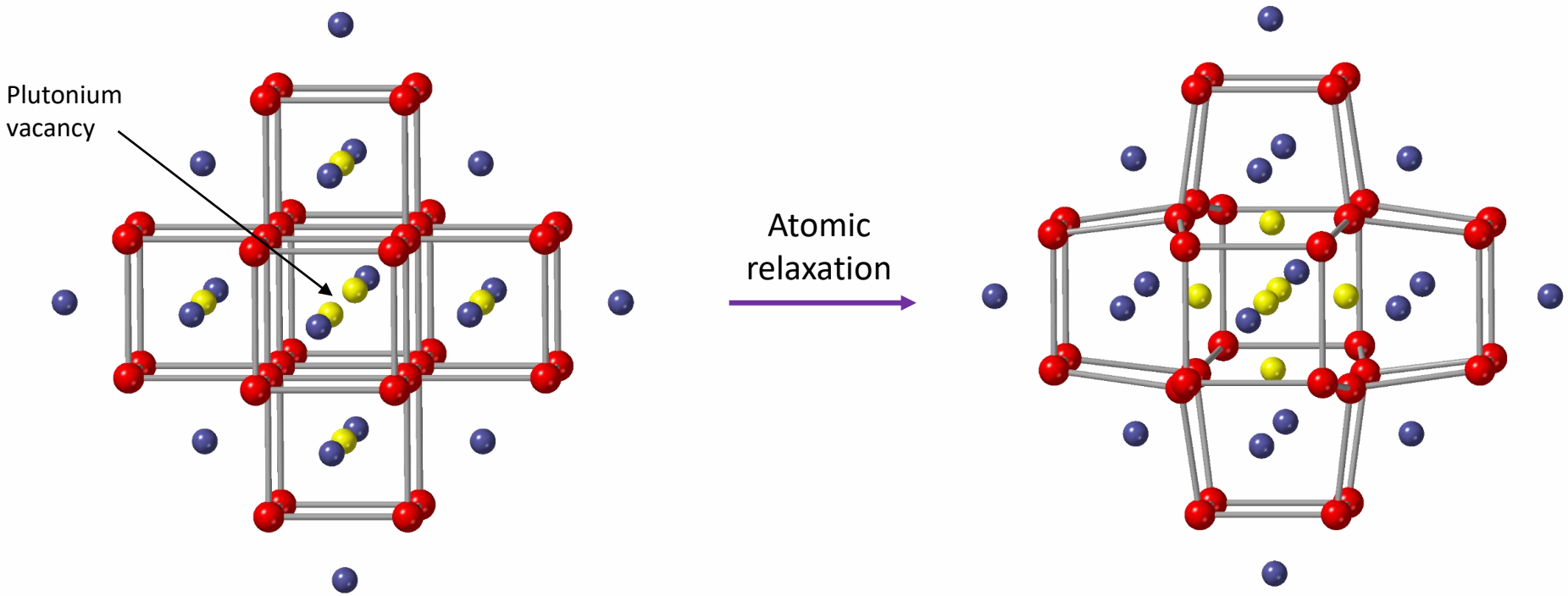

Six He surrounding a Divacancy

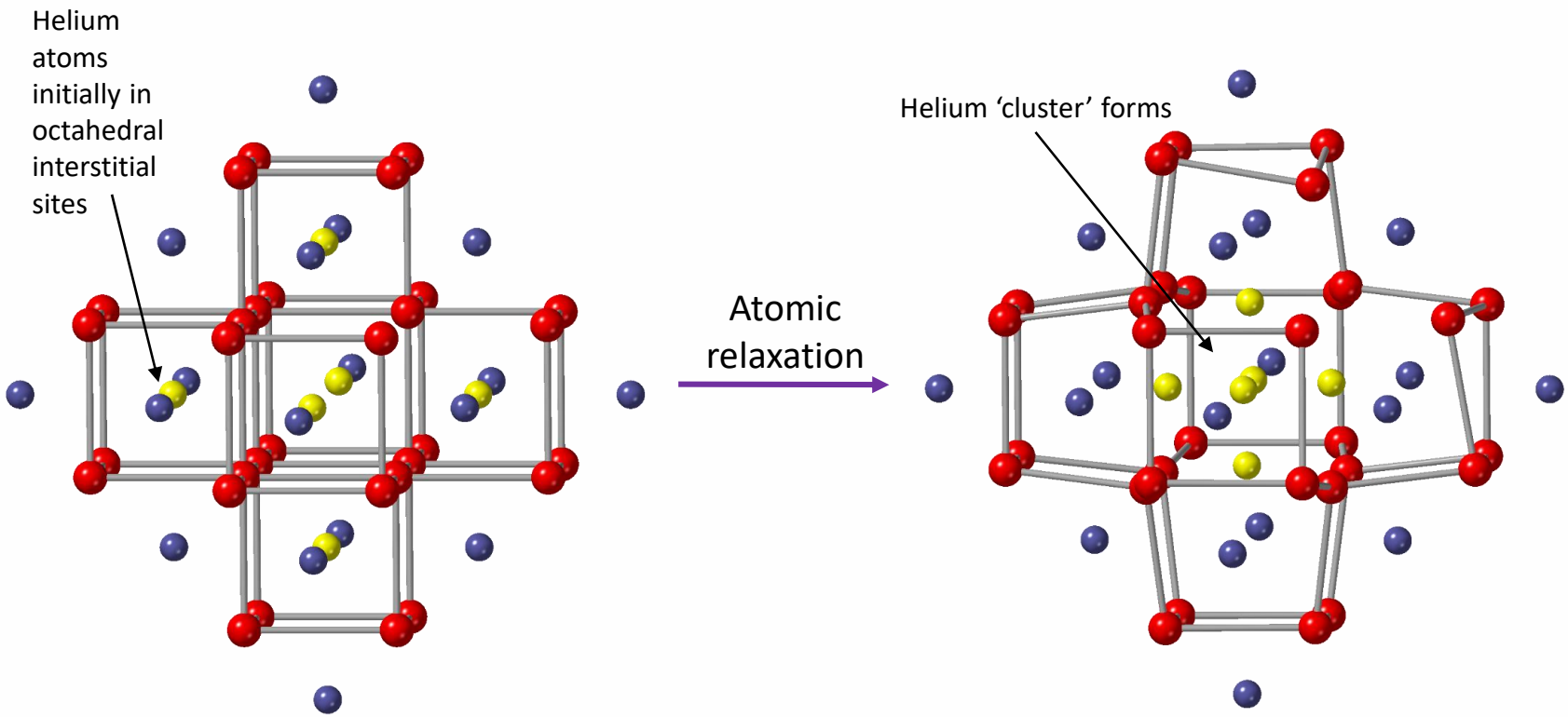

Normalised Incorporation Energies

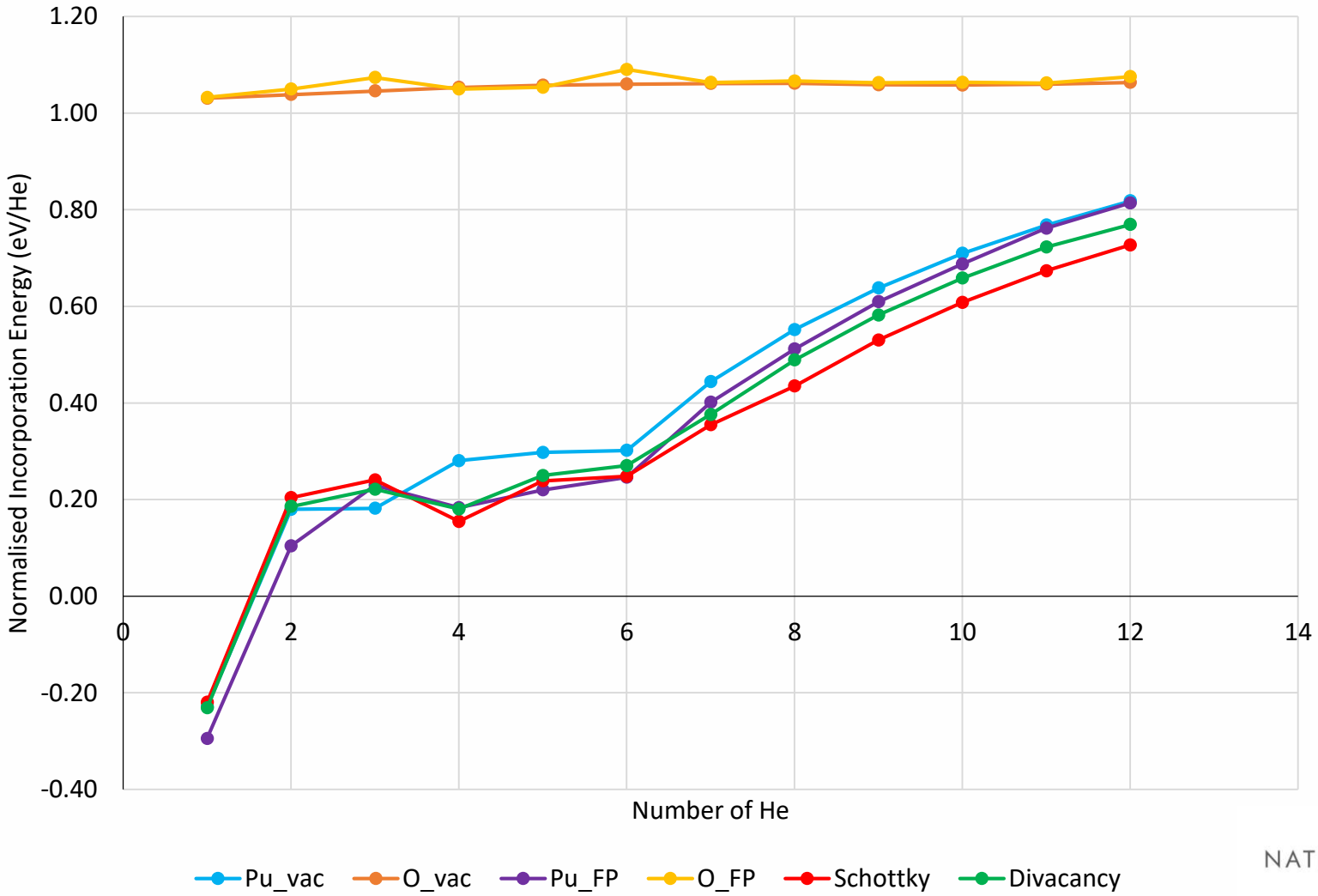

Oxygen Frenkel Pair Results

Oxygen Frenkel Pair Configurations

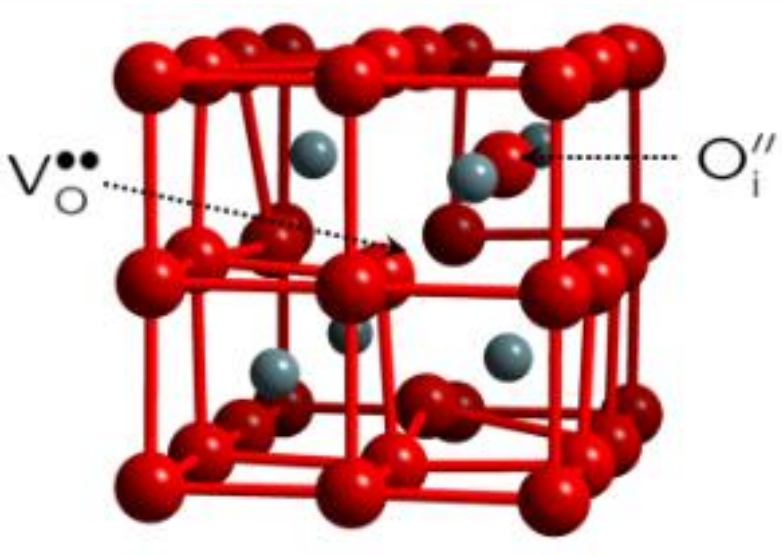

Type of defect	$V^{\cdot\cdot}_O$ position	O_i'' position	Formation energy (eV)	Formation energy (eV/Defect)	Binding energy (eV/Defect)
OFP 1	(-1/4, -1/4, -1/4)	(1/2, 1/2, 1/2)	4.14	2.07	-0.60
OFP 2	(-1/4, -1/4, 1/4)	(1/2, 1/2, 1/2)	4.23	2.12	-0.55

Oxygen Frenkel Pair Configurations

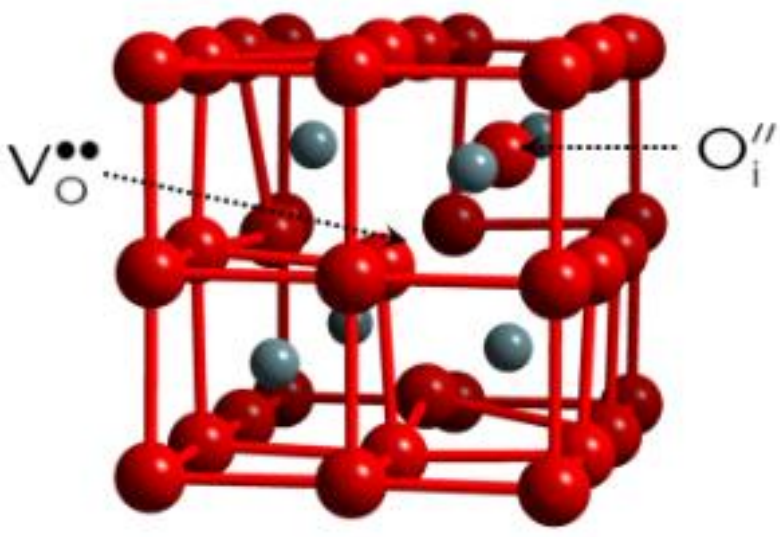

Type of defect	$V^{\cdot}_O$ position	O_i'' position	Formation energy (eV)	Formation energy (eV/Defect)	Binding energy (eV/Defect)
OFP 1	(-1/4, -1/4, -1/4)	(1/2, 1/2, 1/2)	4.14	2.07	-0.60
OFP 2	(-1/4, -1/4, 1/4)	(1/2, 1/2, 1/2)	4.23	2.12	-0.55
OFP 3	(1/4, 1/4, 1/4)	(1/2, 1/2, 1/2)	0.00	-	-

He in OFP 3

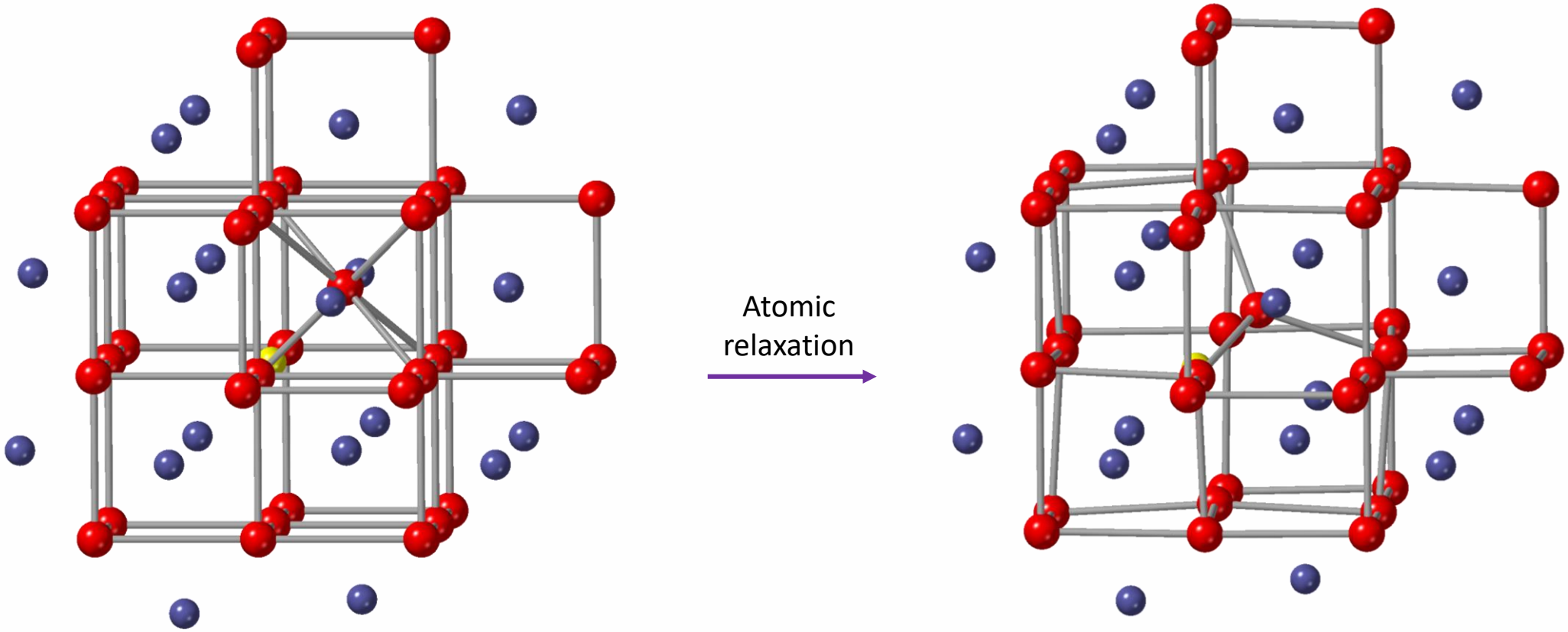

Oxygen doesn't recombine! He interstitial makes more Frenkel pairs possible

DB in OFP

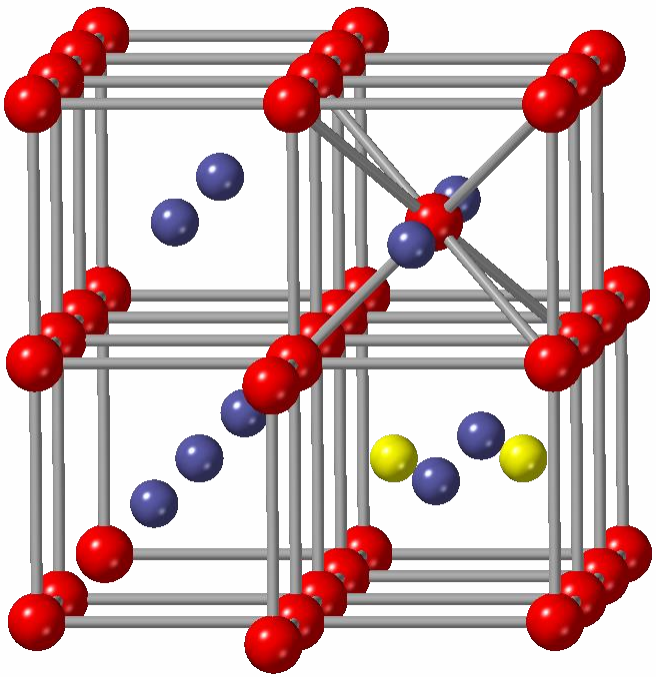

Atomic relaxation

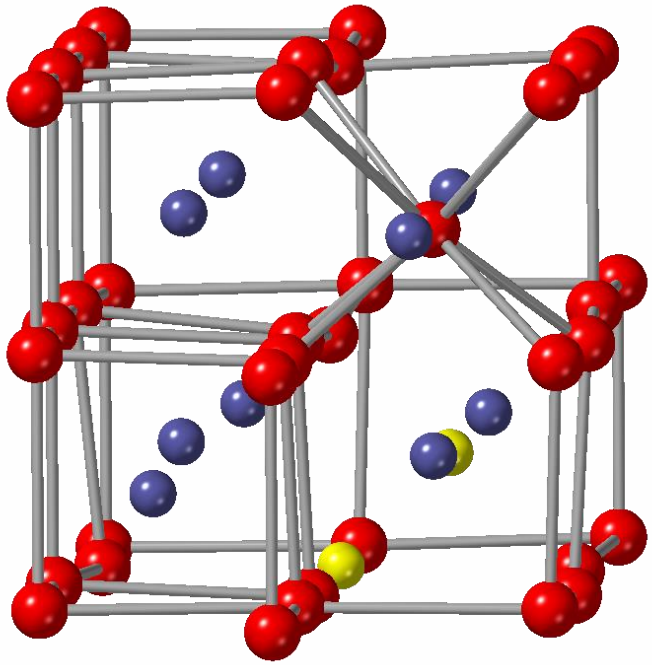

DB in OFP

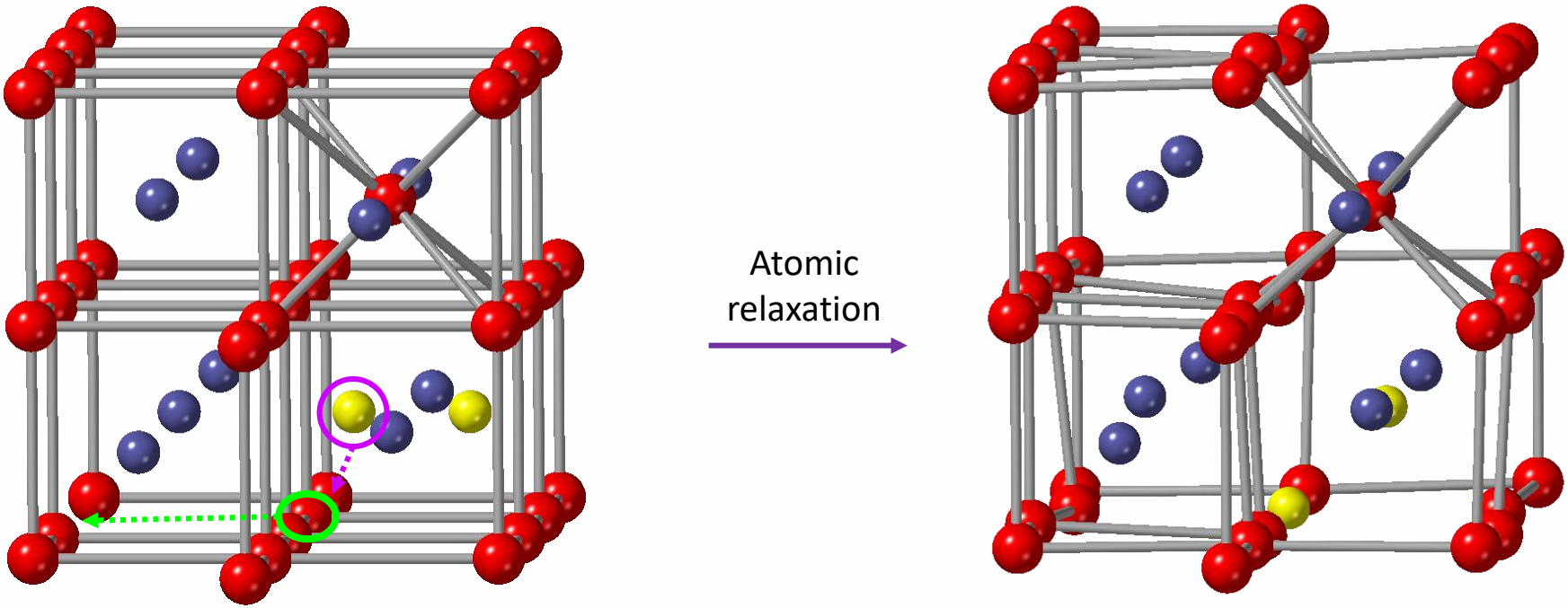

Lots of new questions!

- Does the helium push the oxygen?
- Which moves first?
- How close does the helium have to be for this rearrangement?
- What if there is more helium atoms in the OIS – do more oxygen atoms move?

Great place to start a Molecular Dynamics simulation from…

What's Next?

What's next?

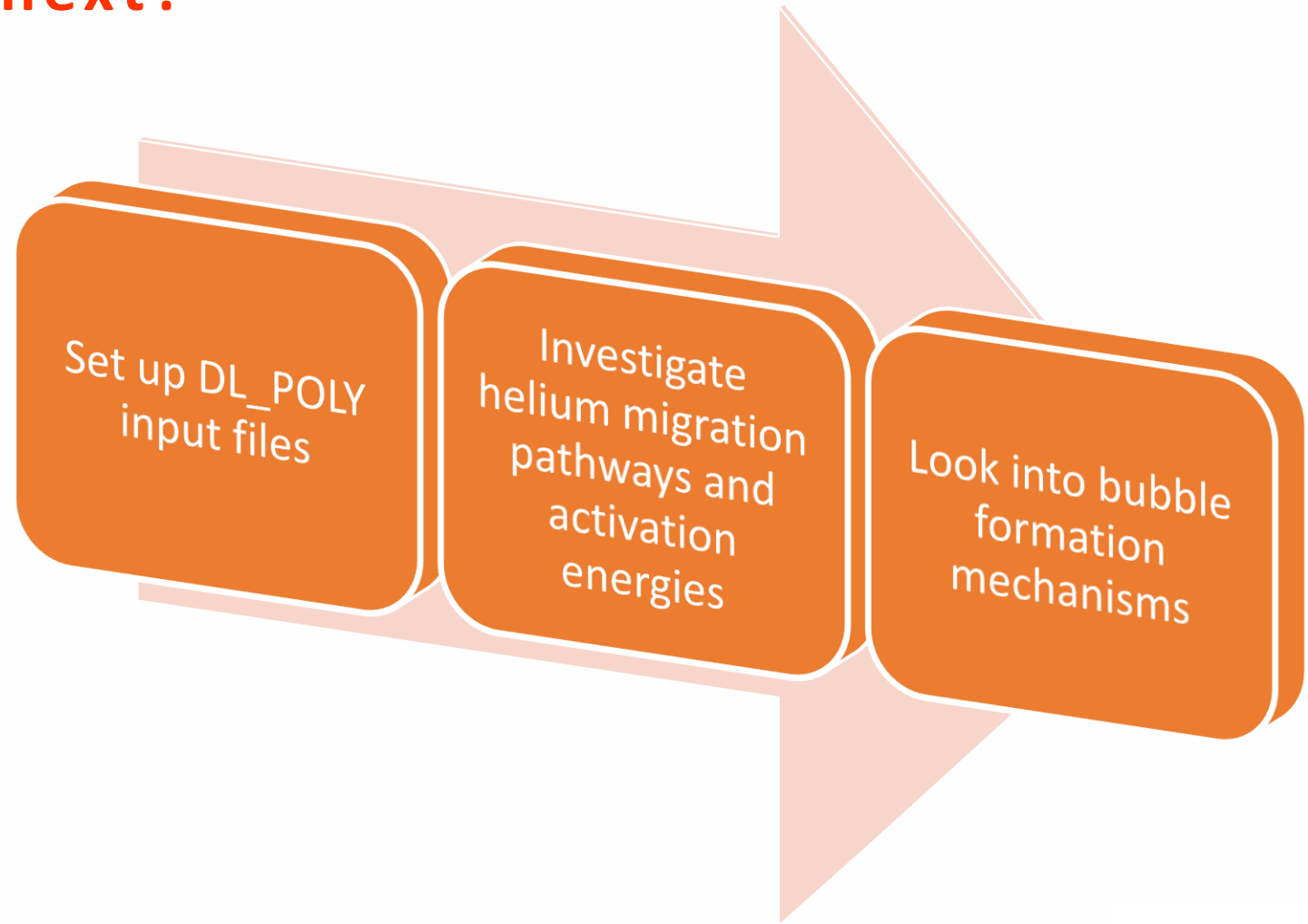
Set up DL_POLY input files
Investigate helium migration pathways and activation energies
Look into bubble formation mechanisms

Thanks to

Dr Mark Read - University of Birmingham

Dr Rob Jackson – University of Keele

Dr Helen Steele - Sellafield Ltd.

Dr Robin Orr - NNL

NDA

UNIVERSITY OF BIRMINGHAM

NATIONAL NUCLEAR LABORATORY

Sellafield Ltd

TRANSCEND

Transformative Science and Engineering for Nuclear Decommissioning

Thank you

exm350@student.bham.ac.uk

References

- J. D. Gale, J. Chem.Soc., Faraday Trans., vol. 93, pp. 629–637, 1997.
- M. Read, S. Walker, and R. Jackson, vol. 448, no. 1, pp. 20 – 25, 2014
- N. A. Palmer. PhD thesis, 2019.
- R. W. Grimes, NASO ASI Series B, vol. 279, 1991.
- V. Dremov, P. Sapozhnikov, A. Kutepov, V. Anisimov, M. Korotin, A. Shorikov, D. L. Preston,and M. A. Zocher, Phys. Rev. B,vol. 77, p. 224306, Jun 2008.
- N. Kuganathan, P. Ghosh, A. Arya, and R. Grimes, Journal of Nuclear Materials, vol. 507, pp. 288 – 296, 2018.
- C. L. J. S. H. X. X. Tian, T. Gao, Eur. Phys. J. B, vol. 86, no. 179, 2013.
- M. Freyss, N. Vergnet, and T. Petit, Journal of Nuclear Materials, vol. 352, no. 1, pp. 144 – 150, 2006.Proceedings of the E-MRS 2005 Spring Meeting Symposium N on Nuclear Materials (including the10th Inert Matrix Fuel Workshop).
- X.-Y. Liu and D. Andersson, Journal of Nuclear Materials, vol. 498, pp. 373 – 377, 2018.
- Y. Yun, O. Eriksson, and P. M. Oppeneer, Journal of Nuclear Materials, vol. 385, no. 3, pp. 510 – 516, 2009.
- T. Petit, M. Freyss, P. Garcia, P. Martin, M. Ripert, J.-P. Crocombette, and F. Jollet, Journal of Nuclear Materials, vol. 320, no. 1, pp. 133– 137, 2003. Proceedings of the 2nd Seminar on European Research on Materials for Transmutation

TRANSCEND

Transformative Science and Engineering for Nuclear Decommissioning

Impact of Am on the defect chemistry of PuO_2

William Neilson, Lancaster University

w.neilson@lancaster.ac.uk

Supervisor: Dr Samuel T. Murphy

TRANSCEND Thematic Meeting

3rd Dec 2019

Energy

For a Low Carbon Future

INTRODUCTION

This project has used atomistic simulations to understand the defect chemistry of PuO_2, followed by investigating how Am is accommodated into PuO_2 and what impact Am has on the defect chemistry.

Defect chemistry:

- The formation of defects (the addition or removal of atoms from the perfect lattice) can describe deviations from stoichiometry in PuO_2, resulting in $PuO_{2\pm x}$
- Can examine the defect concentrations as a function of temperature and oxygen partial pressure.
- Describes how impurities, such as Am, are incorporated into the lattice .
- Help in understanding of how PuO_2 continues to evolve when kept in storage.
- May help identify hazards, such as the potential pressurisation of canisters used for storage.

Modelling the PuO_2 ground state

Create PuO_2 unit cell

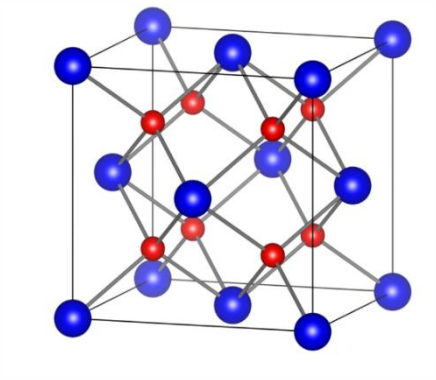

$Fm\bar{3}m$ crystal symmetry
12 atoms
Pu (blue)
O (red)

Apply magnetic properties

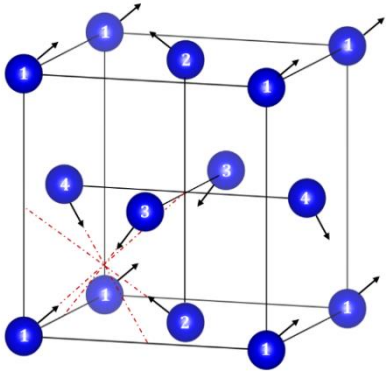

Atom	Magnetic moment
1	(1, 1, 1)
2	(-1, -1, 1)
3	(-1, 1, -1)
4	(1, -1, -1)

Longitudinal 3k anti-ferromagentic ground-state found and adopted

J.T. Pegg *et al.*, *Phys. Chem. Chem. Phys.*, **20**, 20943-20951, 2018.
J.T. Pegg *et al.*, *J. Nucl. Mater*, **492**, 269-278, 2017.

Computational details

Simulate with DFT.

Computational method: VASP, PBEsol + *U*
Noncolinear with spin orbit coupling.

Choose *U* value such that bandgap is reproduced. However large discrepancy exists in the reported bandgap:
McNeilly *et al*. reports a bandgap of 1.8 eV
McCleskey *et al*. reports a bandgap of 2.8 eV

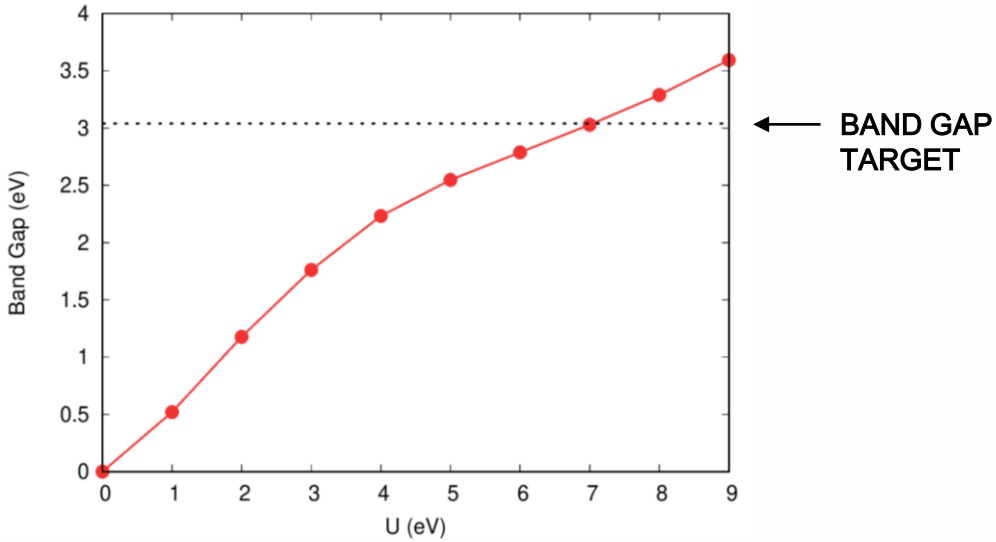

U = 7.0 eV, reproducing hybrid functional (HSE06) band gap (3.04 eV).

Adding intrinsic defects

Create supercell

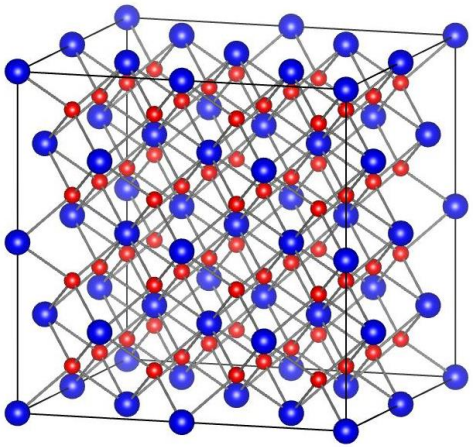

2 x 2 x 2, 96 atoms

Add defects to supercell

ADD OXYGEN ATOMS

Oxygen interstitials: $O_i^{\times}$,$O_i^{1-}$and O_i^{2-}

REMOVE OXYGEN ATOMS

Oxygen vacancies: $V_O^{\times}$, $V_O^{1+}$and V_O^{2+}

ADD PLUTONIUM ATOMS

Plutonium interstitials: $Pu_i^{\times}$, Pu_i^{1+}, Pu_i^{2+}, $Pu_i^{3+}$and Pu_i^{4+}

REMOVE PLUTONIUM ATOMS

Plutonium vacancies: $V_{Pu}^{\times}$, V_{Pu}^{1-},V_{Pu}^{2-},V_{Pu}^{3-} and V_{Pu}^{4-}

Defect formation: methodology

$$\Delta G_f^i = E_{\text{def}} - E_{\text{per}} - T\Delta S_{\text{vib}} + \sum_\alpha n_\alpha \mu_\alpha + q_i \mu_e + E_{\text{corr}}$$

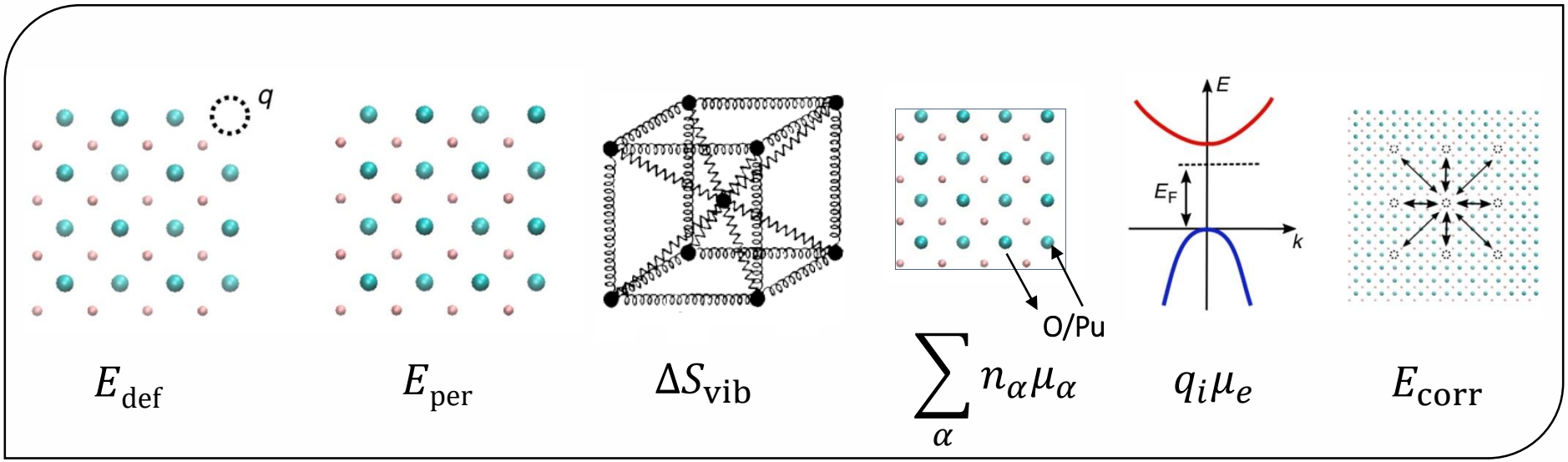

Defect formation: methodology

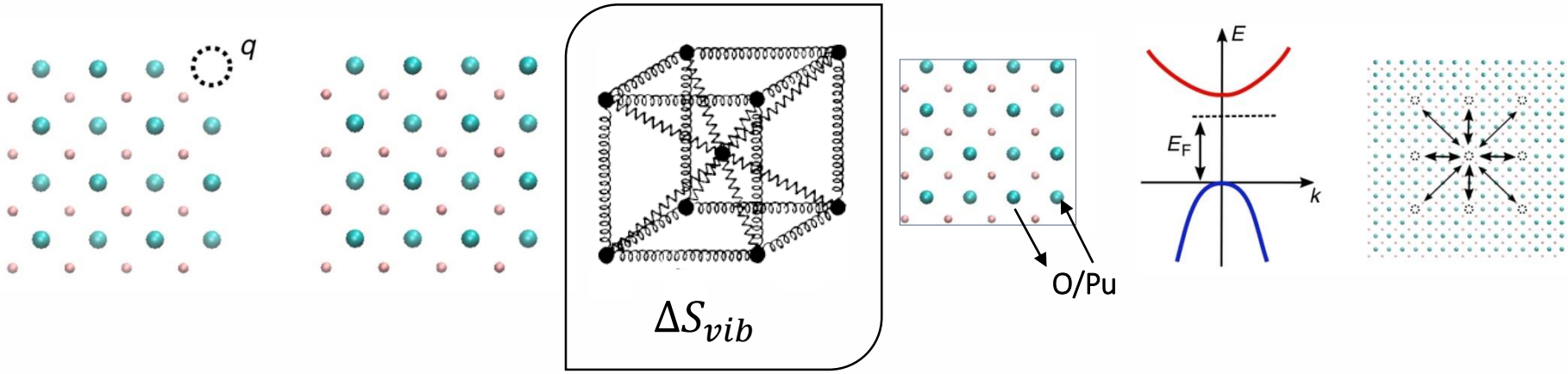

- Vibrational entropies are obtained using empirical potentials due to limitations in computational resources; the force calculations required become very large when defects are introduced, due to the removal of symmetry.
- The General Utility Lattice Program (GULP) together with the Cooper, Rushton and Grimes (CRG) potential is adopted.
- The CRG potential is a many-body potential model used to describe actinide oxide systems which achieves good reproduction of thermodynamic and mechanical properties.

Defect formation: methodology

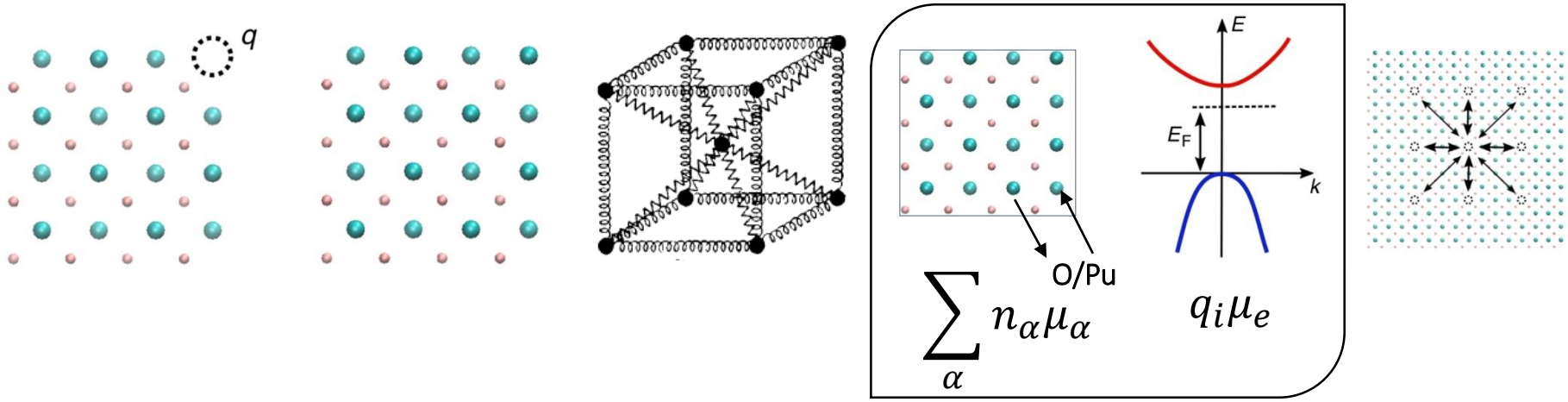

$\mu_{Pu(s)}$: Obtained in DFT

$\mu_{O_2}(P_{O_2}, T)$: Calculated as a function of pressure and temperature using real gas relations.

$\mu_e = E_{VBM} + \varepsilon_F$: Fermi level computed such that the whole system is charge neutral Fermi-Dirac statistics applied to the electronic density of states to obtain the concentrations of electrons (e^-) in the conduction band and concentration of holes (p^-) in the valance band

μ_{Am} : Found in DefAP: Linear bisection finds values that achieve desired concentration of Am

Defect formation: methodology

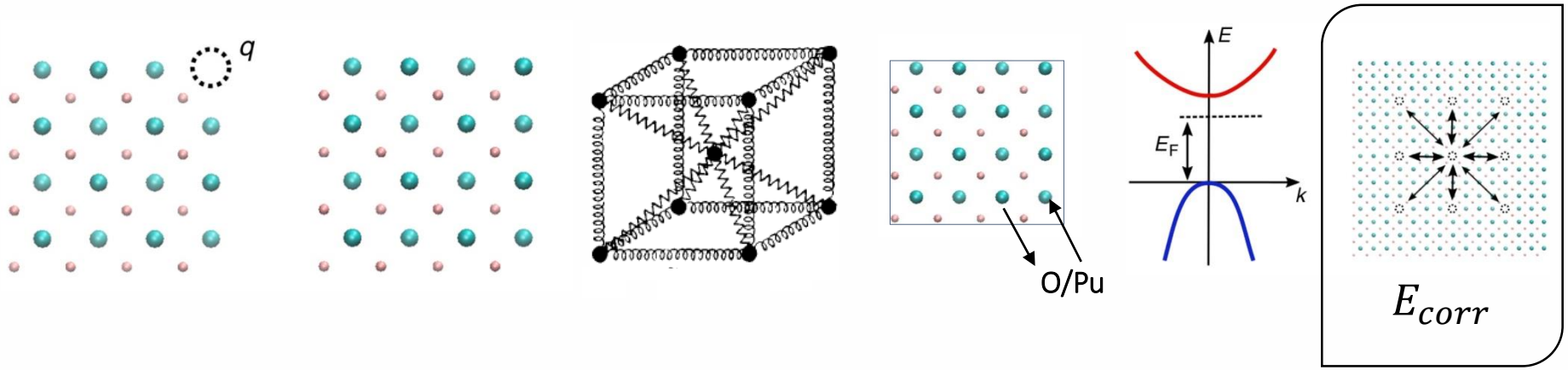

- The introduction of charge defects into the small simulation supercells accessible using DFT introduces a number of finite size effects, including coulombic interactions between the defect and its periodic image as well as with the background charge.

- Use scheme of Kumagai and Oba which uses atomic site electronic potentials to compare perfect and defective supercell.

Difference in DFT energy (eV) between perfect supercell and V_{Pu}^{4-} containing supercell

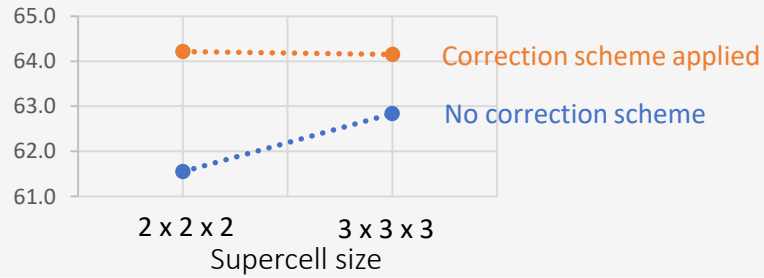

Y. Kumagai and F. Oba, *Phys. Rev. B,* **89**, 195205, 2014.

Defect formation: methodology

$$\Delta G_f^i = E_{\text{def}} - E_{\text{per}} - T\Delta S_{\text{vib}} + \sum_\alpha n_\alpha \mu_\alpha + q_i \mu_e + E_{\text{corr}}$$

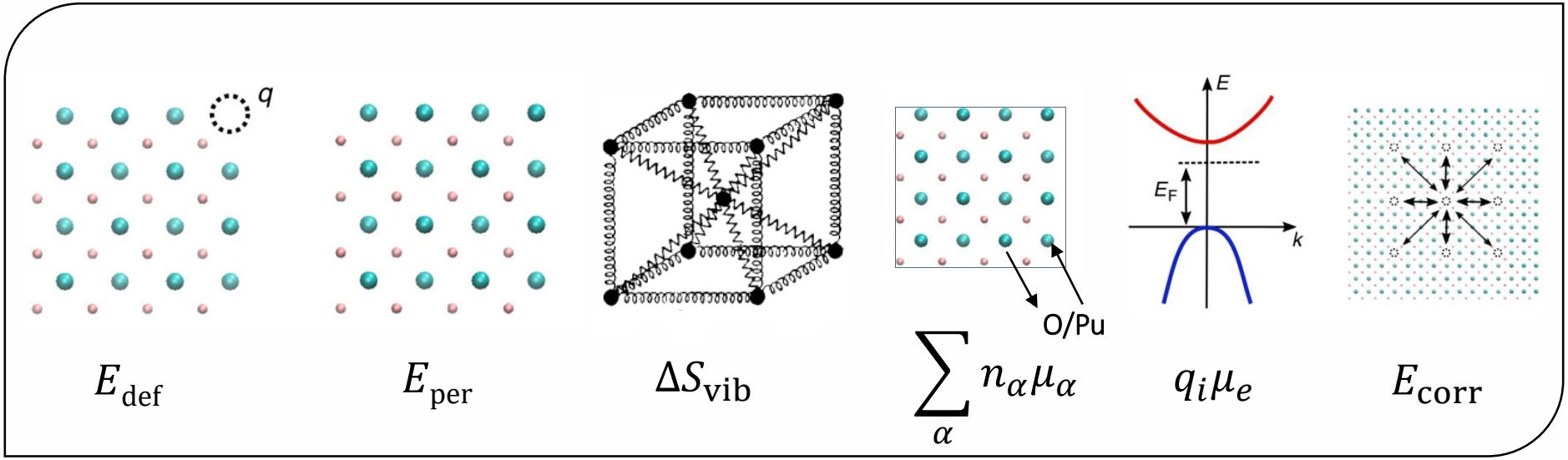

$$c_i = m_i \exp\left(\frac{-\Delta G_f^i}{k_B T}\right)$$

Brouwer diagram - Defect concentrations in PuO_2 as a function of oxygen partial pressure.
Temperature: 1000 K

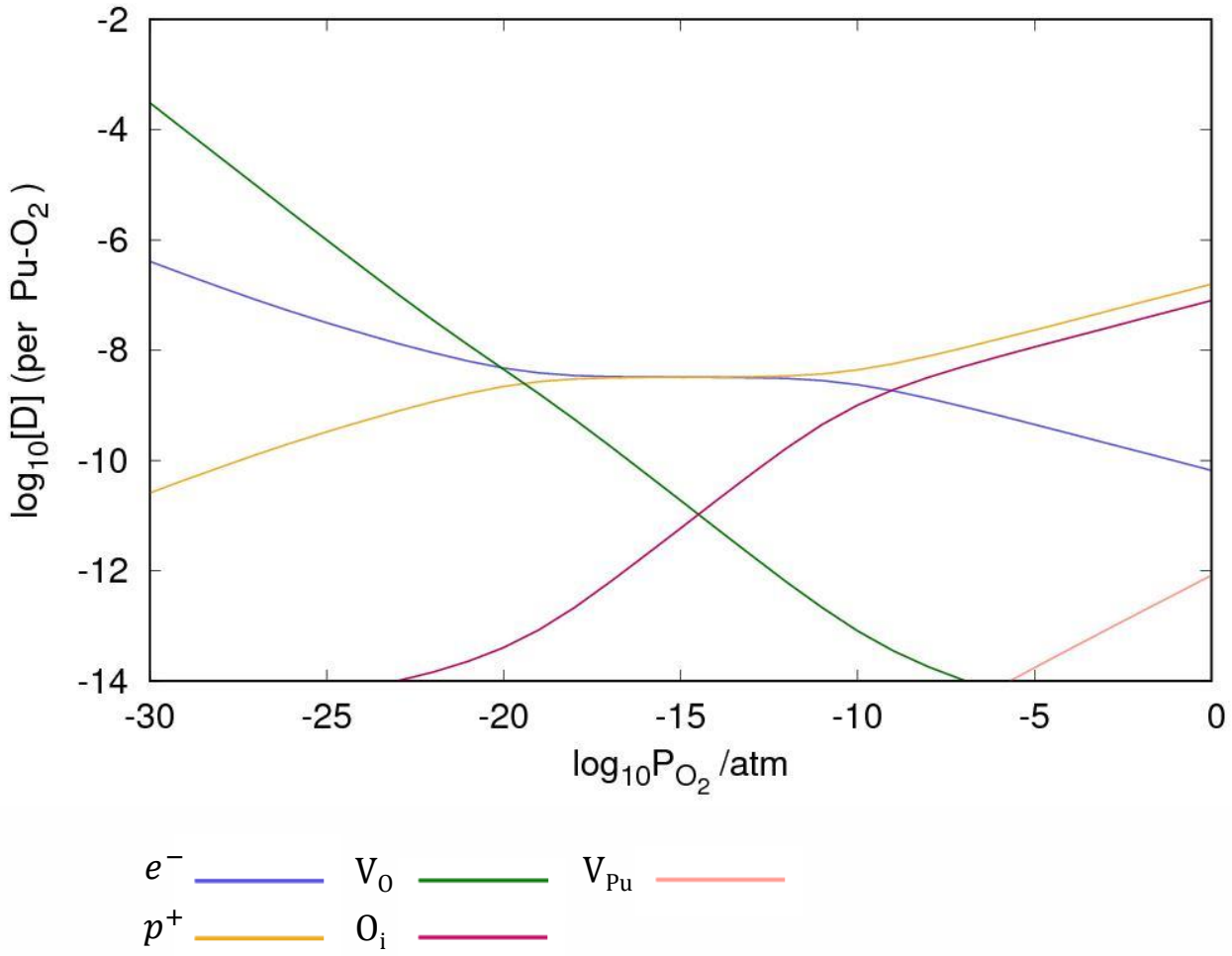

- Oxygen defects dominant

Brouwer diagram - Defect concentrations in PuO_2 as a function of oxygen partial pressure.
Temperature: 1000 K

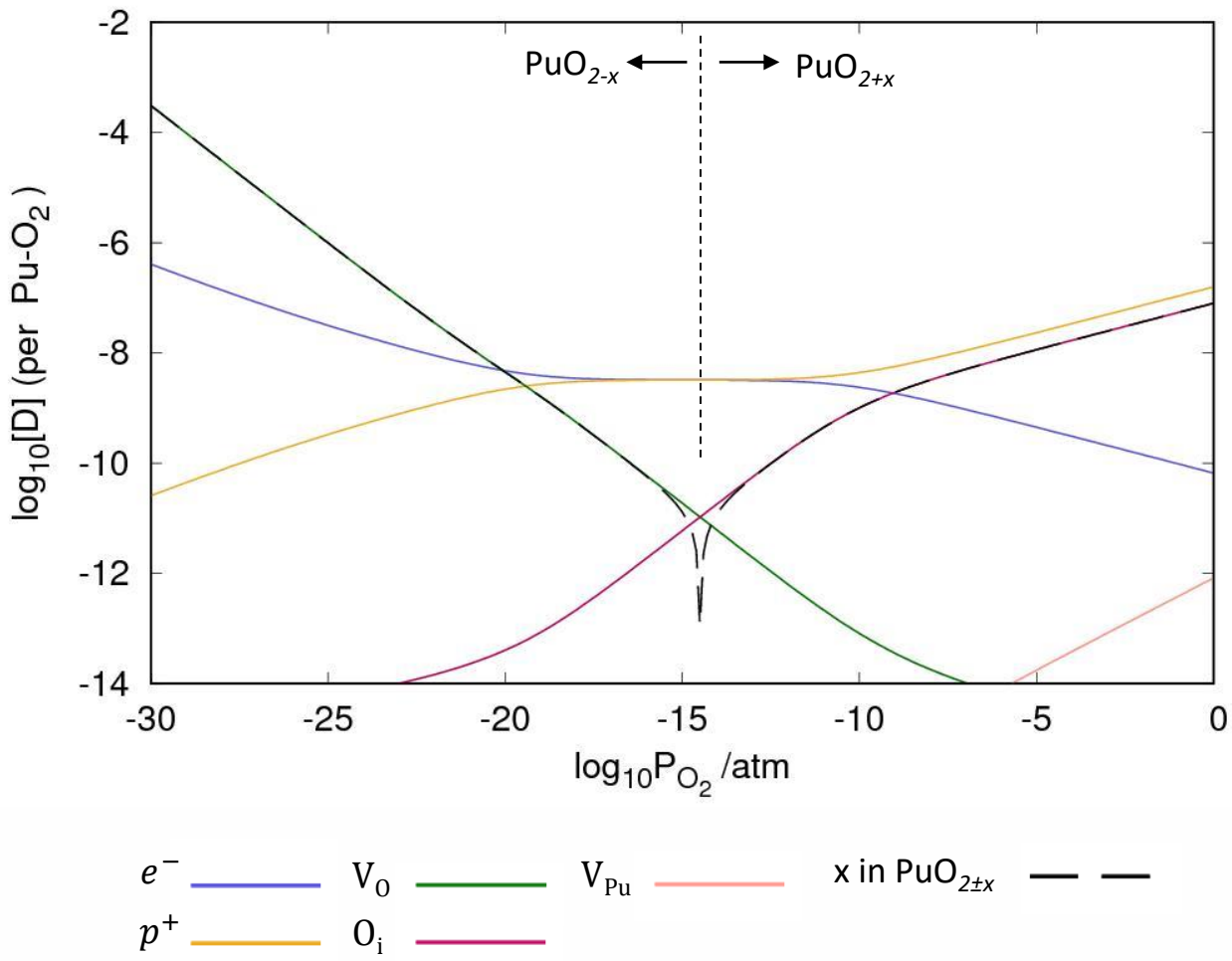

- Oxygen defects dominant
- Hyper-stoichiometry negligible
- Hypo-stoichiometry much more favourable

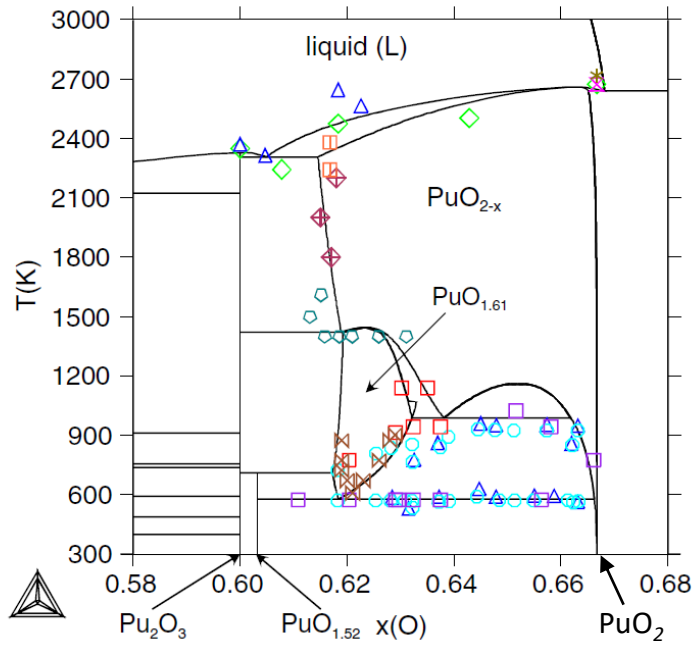

Brouwer diagram - Defect concentrations in PuO_2 as a function of oxygen partial pressure.
Temperature: 1000 K

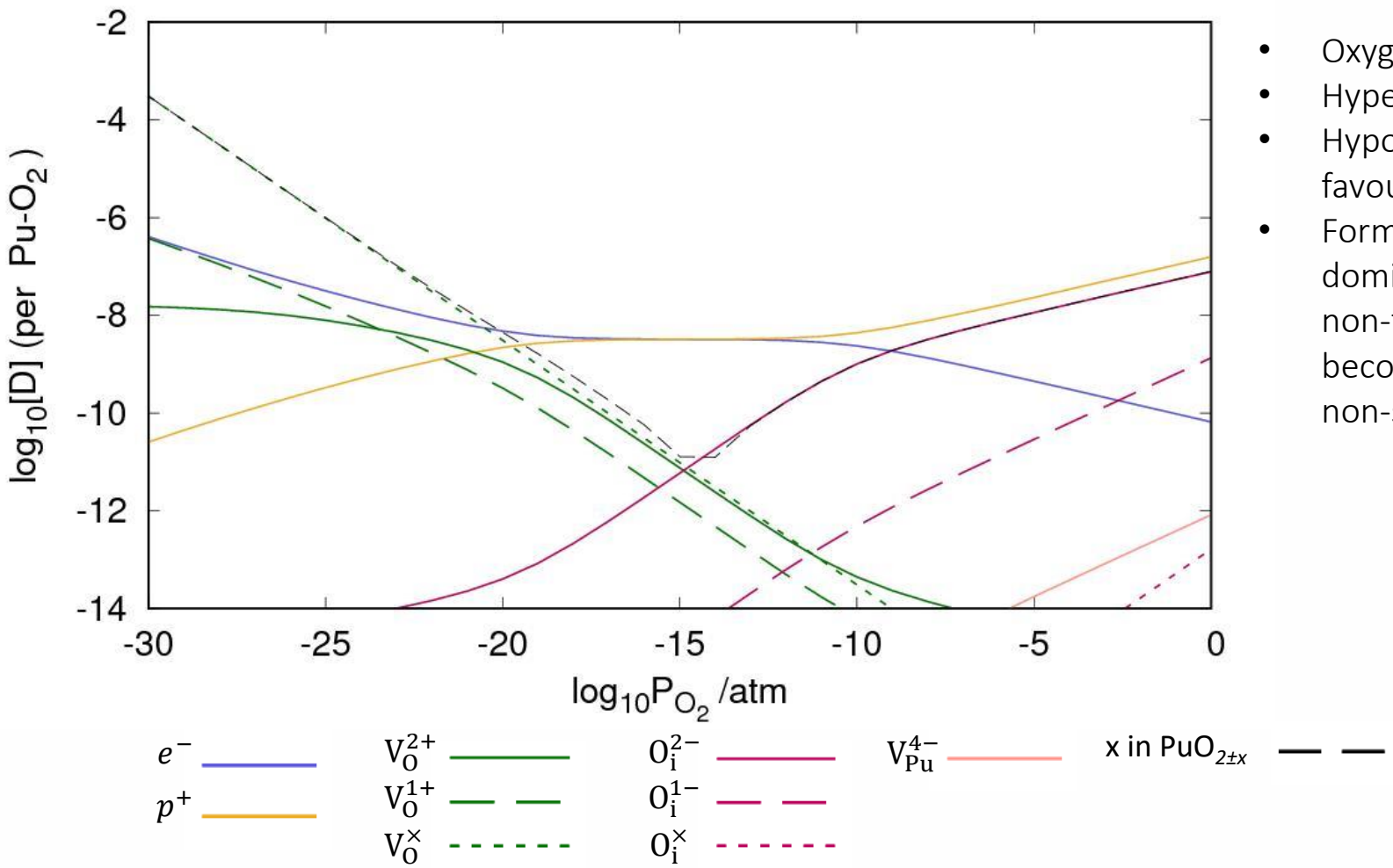

- Oxygen defects dominant
- Hyper-stoichiometry negligible
- Hypo-stoichiometry much more favourable
- Formally charged defects dominate at near-stoichiometry, non-formally charged defects become dominant with increased non-stoichiometry.

Adding americium defects

Create supercell

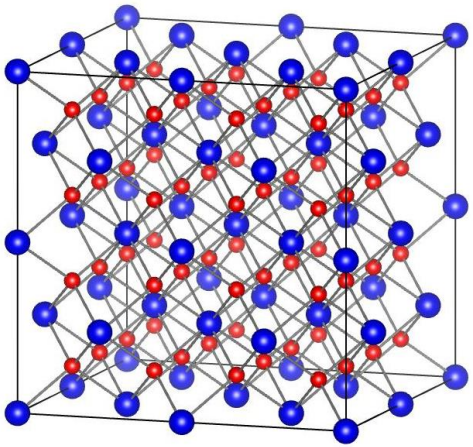

2 x 2 x 2, 96 atoms

Add defects to supercell

ADD AMERICIUM ATOMS

Americium interstitials: $Am_i^{\times}$, Am_i^{1+}, Am_i^{2+}, Am_i^{3+}, Am_i^{4+}

Oxygen substitutions: $Am_O^{\times}$, Am_O^{1+}, Am_O^{2+}, Am_O^{3+}, Am_O^{4+}, Am_O^{5+} and Am_O^{6+}

Plutonium substitutions: Am_{Pu}^{4-}, Am_{Pu}^{3-}, Am_{Pu}^{2-}, Am_{Pu}^{1-}, $Am_{Pu}^{\times}$, Am_{Pu}^{1+}, Am_{Pu}^{2+}, Am_{Pu}^{3+}, Am_{Pu}^{4+} and Am_{Pu}^{5+}

Accommodation of americium

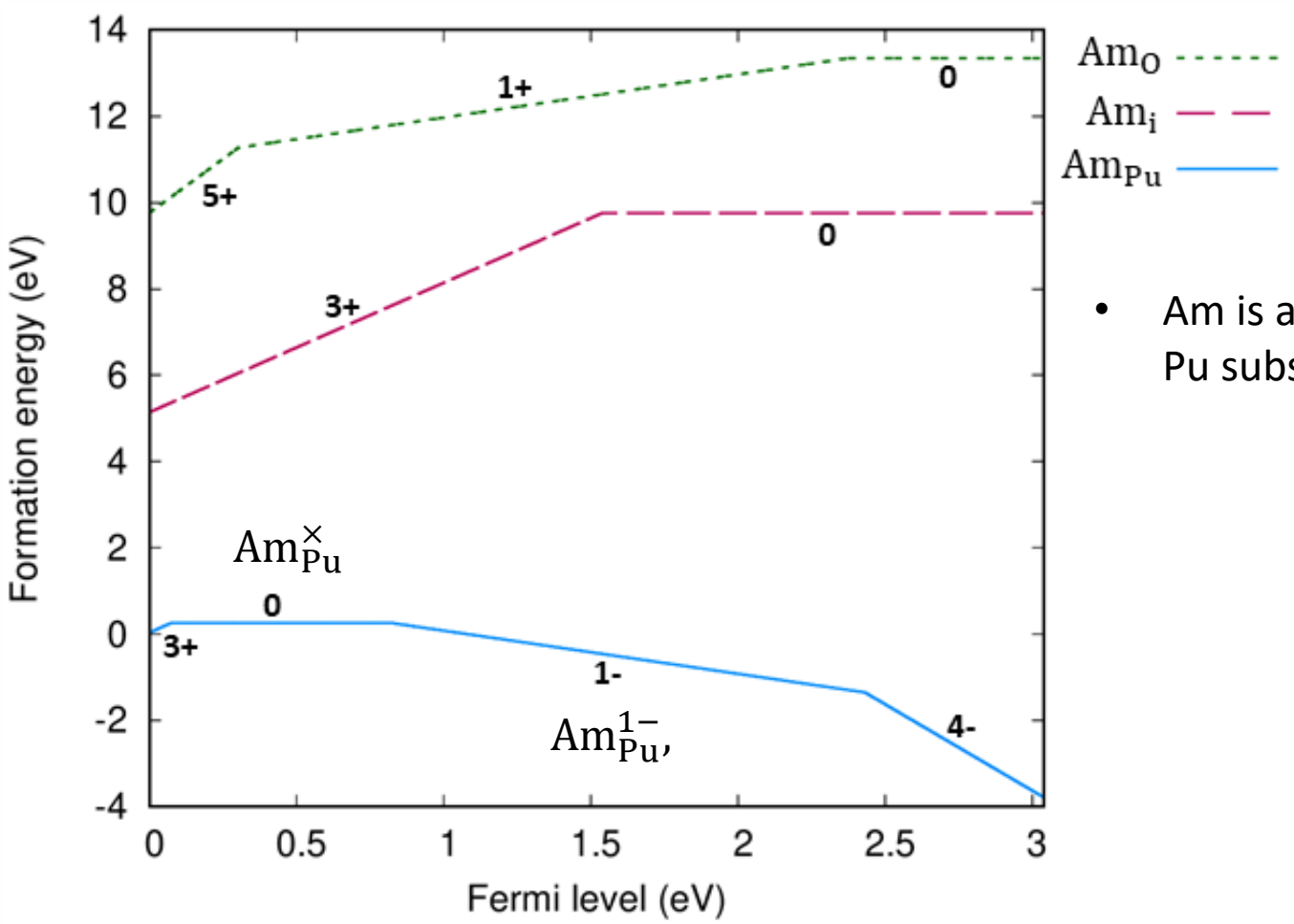

- Am is accommodated in Pu substitutions.

Brouwer diagram - Defect concentrations in $Pu_{0.999}Am_{0.001}O_{2\pm x}$ as a function of oxygen partial pressure. Temperature: 1000 K

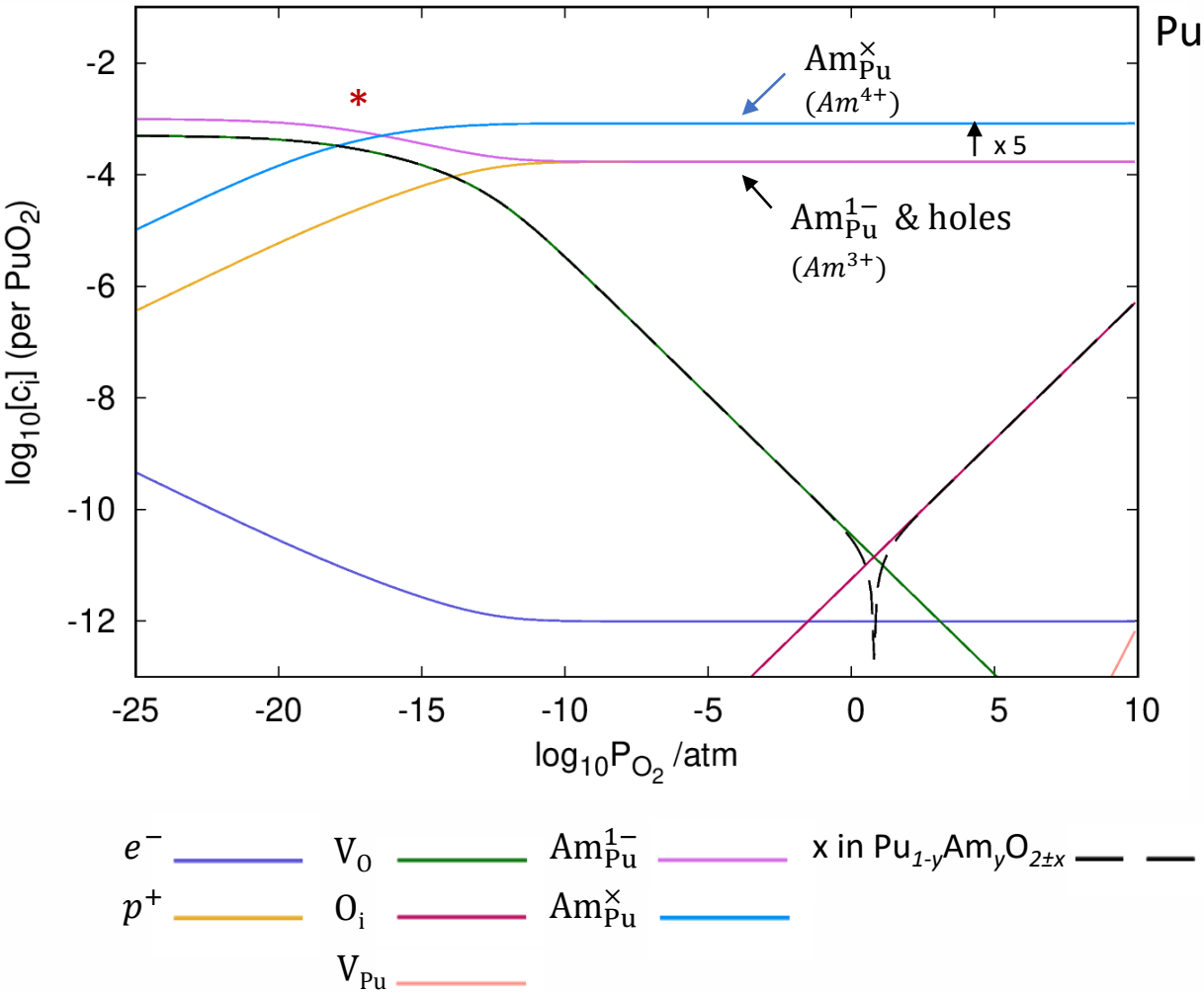

$Pu_{0.999}Am_{0.001}O_{2\pm x}$

- Oxygen defects are the dominant intrinsic defect and control the stoichiometry in $Pu_{1-y}Am_yO_{2\pm x}$. Hyper-stoichiometry always found negligible.
- Am is accommodated in Pu substitutions under all conditions.
- At * Am reduced from +IV to +III as partial pressure decreases, in agreement with experimental observation.

Comparison with experiment

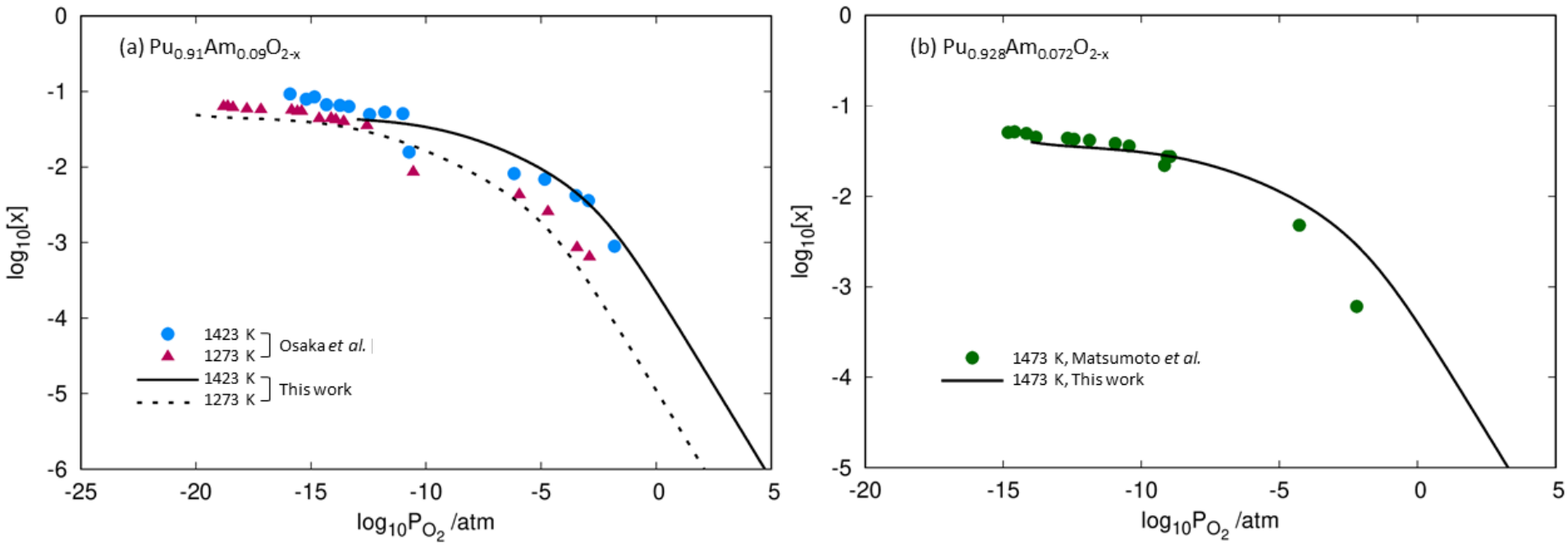

Values of x in $Pu_{1-y}Am_yO_{2\pm x}$ as a function of oxygen partial pressure at y values of a) 0.09 and b) 0.072, with comparison to experimental results

M. Osaka, K. Kurosaki, S. Yamanaka, Oxygen potential of $(Pu_{0:91}Am_{0:09})O_{2-x}$, J. Nucl. Mater. 357 (2006) 69–76. doi:10.1016/j.jnucmat.2006.05.044.
T. Matsumoto, T. Arima, Y. Inagaki, K. Idemitsu, M. Kato, K. Morimoto, T. Sunaoshi, Oxygen potential measurement of $(Pu_{0:928}Am_{0:072})O_{2-x}$ at high temperatures, J. Nucl. Sci. Technol. 52 (2015) 1296–1302. doi:10.1080/00223131.2014.986243.

Defect concentrations in $Pu_{1-y}Am_yO_{2\pm x}$ as a function of temperature.
Oxygen partial pressure: 0.01 atm.

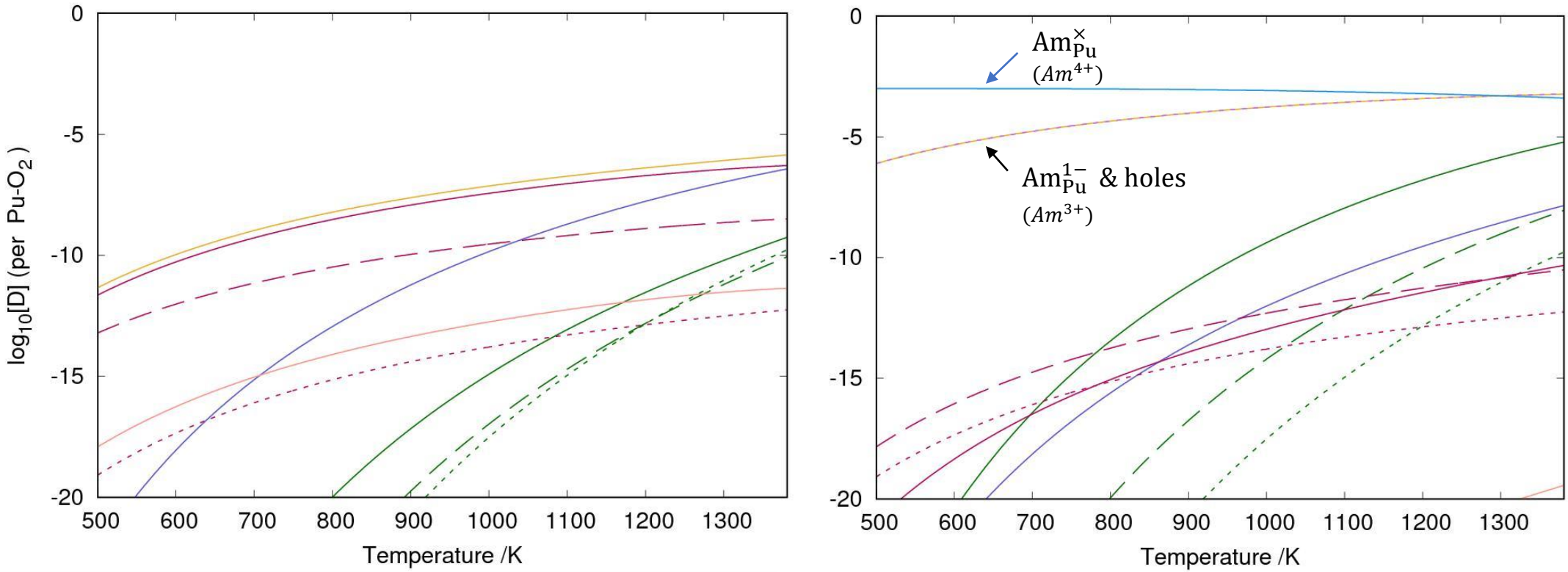

$PuO_{2\pm x}$ **$Pu_{0.999}Am_{0.001}O_{2\pm x}$**

e^- p^+ V_O^{2+} V_O^{1+} $V_O^{\times}$ O_i^{2-} O_i^{1-} $O_i^{\times}$ V_{Pu}^{4-} Am_{Pu}^{1-} $Am_{Pu}^{\times}$

Defect concentrations in $Pu_{1-y}Am_yO_{2\pm x}$ as a function of Am concentration.
Oxygen partial pressure: 0.01 atm. Temperature: 800 K.

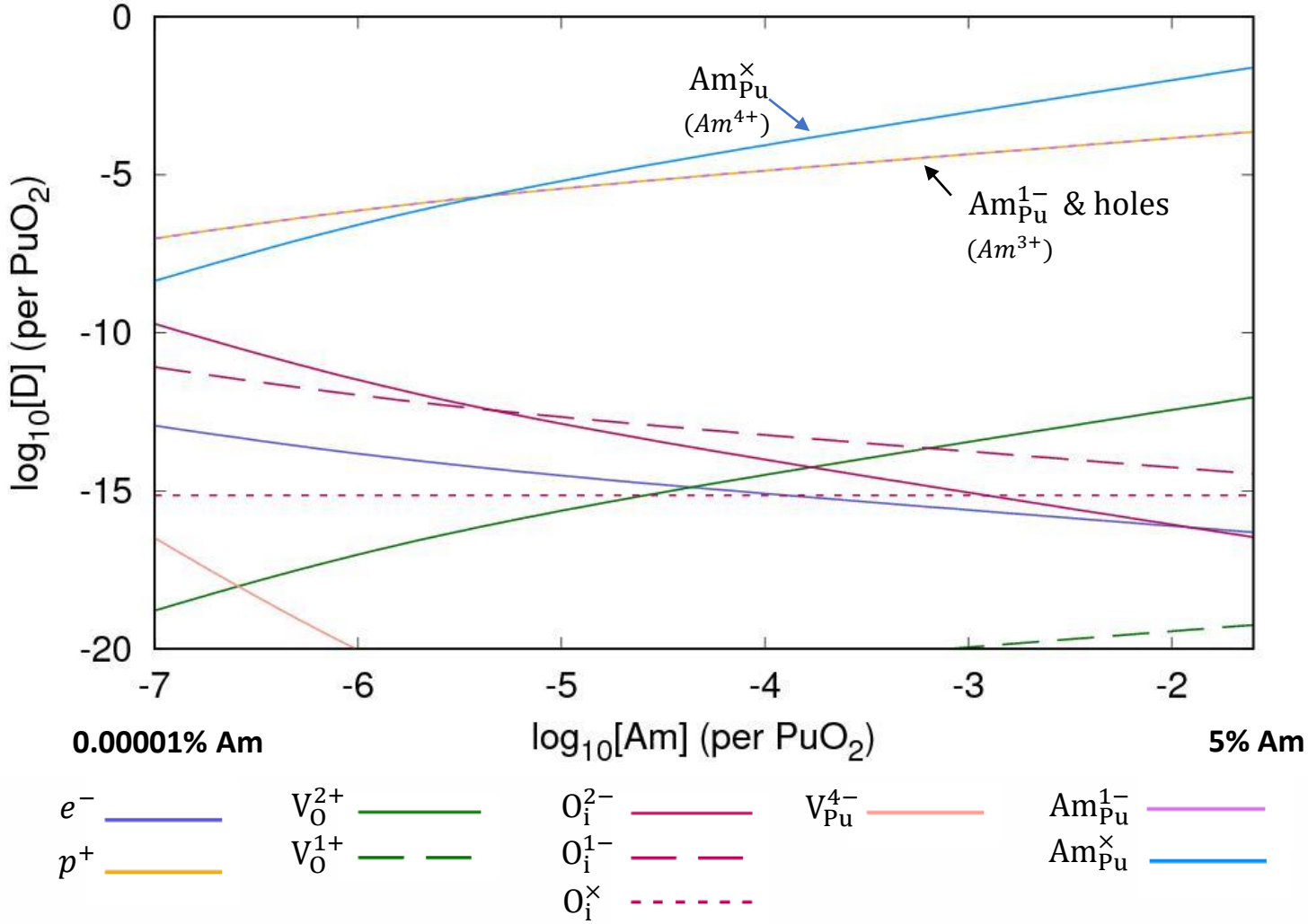

Acknowledgements

- Dr. James T. Pegg
- Dr. Helen Steele
- The High End Computing facility at Lancaster University

Thank you

w.neilson@lancaster.ac.uk

TRANSCEND

Transformative Science and Engineering for Nuclear Decommissioning

Water Adsorption on ThO_2(111) surface

Xiaoyu Han, University of Manchester

Nuclear Materials

2-3 December, 2020

Energy

For a Low Carbon Future

The Sellafield nuclear reprocessing site in Cumbria © Redharc Images/Alamy

UK has the world's largest stockpile of the PuO_2.

- Sellafield in Cumbria
- 2 "Magnox" research sites and 10 nuclear power stations

Inside of the PuO_2 storage container, **water** and other small molecules might interact with PuO_2

A major barrier to making progress --- **lack of knowledge** about the retired facilities.

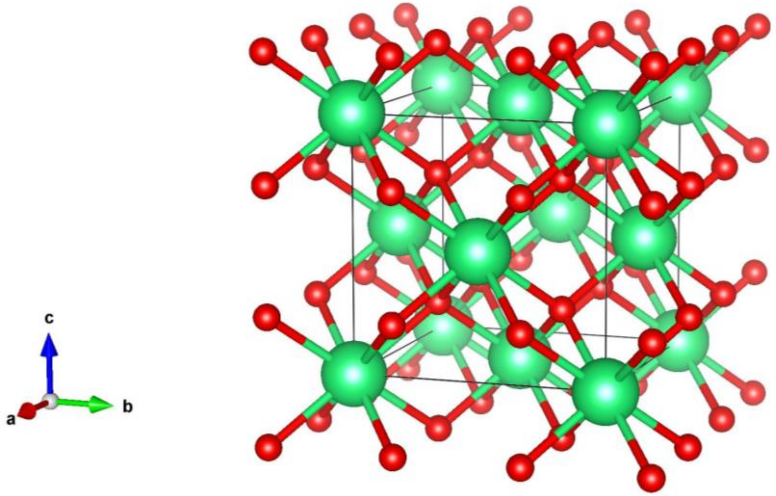

ThO_2 as the surrogate for PuO_2

- Ionic radii
- The fluorite fm-3m structure
- +IV oxidation state
- No open-shell 5f electron as in PuO_2
- Less radioactivity as PuO_2 experimentally

Computational settings

- VASP
- PAW method
- 650 eV cutoff
- $5 \times 5 \times 5$ and $15 \times 15 \times 15$ *k* point mesh for bulk geometry relaxation and pDOS, respective
- For the slab, 2×2 supercell with 5 layers, the bottom 2 layer fixed.
- Dipole correction along the surface direction
- 15 Å vacuum slab
- DFT- D4 correction for the vdW correction
- Ci-NEB method for the dissociation energy calculation
- The elementary reaction free energy were calculated, $\Delta G = \Delta E_{DFT} + \Delta E_{ZPE} - T\Delta S$

OUTLINE

- The computational challenge of the ThO_2;
  - The Dudarev approach vs The Liechtenstein approach;
- The water reaction on the ThO_2 (111) surface;
  - 1st water adsorption and dissociation;
  - 2nd water adsorption and dissociation;

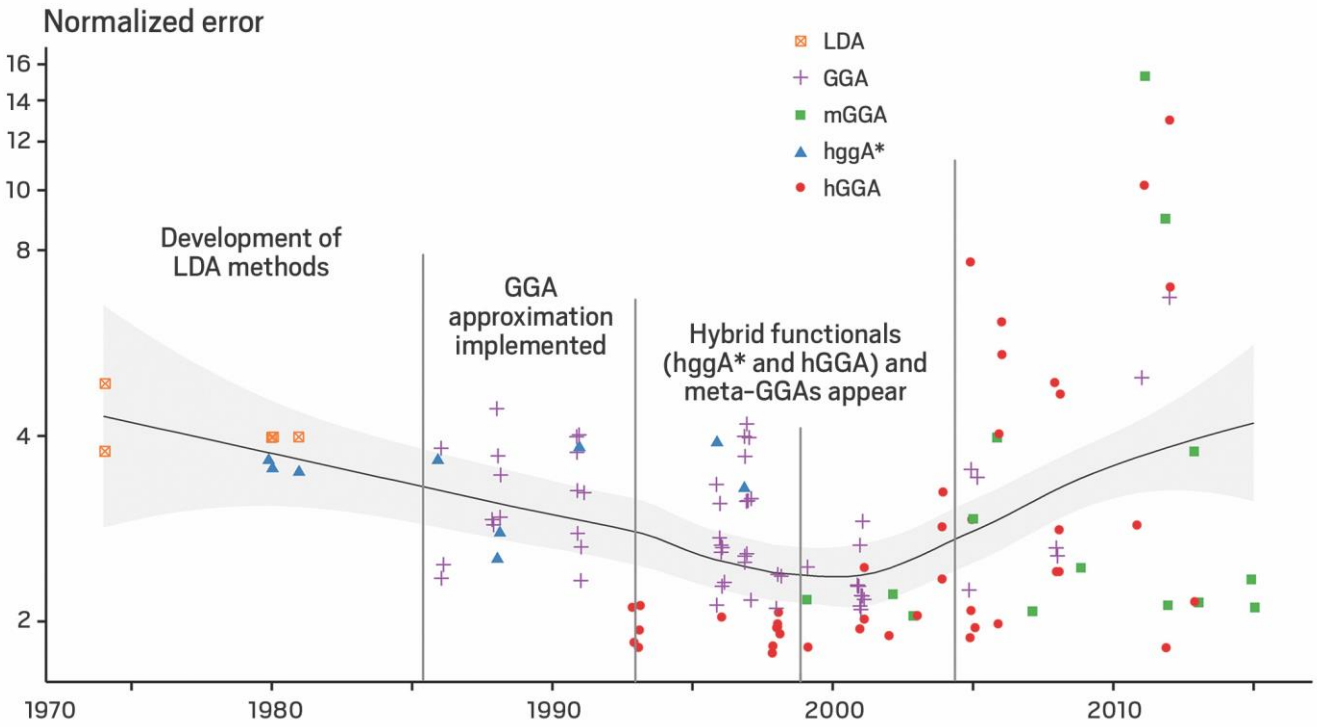

The historical trends in maximal deviation of the density produced by various DFT methods from the exact one. [1]

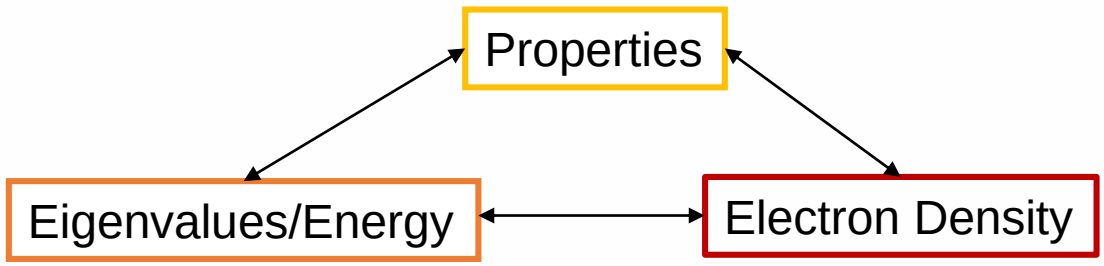

Lattice parameters error

$$\sigma_L = \frac{L - L_{exp}}{L_{exp}}$$

Bandgap errors

$$\sigma_{gap} = \frac{G - G_{exp}}{G_{exp}}$$

the root mean square error **(RMS)**

$$\sigma_{RMS} = \sqrt{\frac{\left(\sigma_L{}^2 + \sigma_{gap}{}^2\right)}{2}}$$

1. *Science* Vol. 355, Issue 6320, pp. 49-52

The Dudarev approach

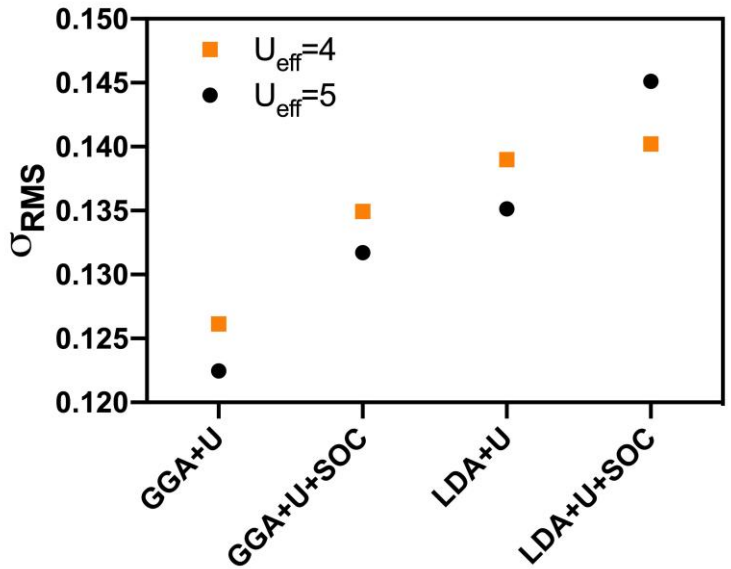

The best setting for Dudarev approach GGA with U_{eff}= 5 eV

Balanced the **mechanical** and **electronic** properties

The Liechtenstein approach

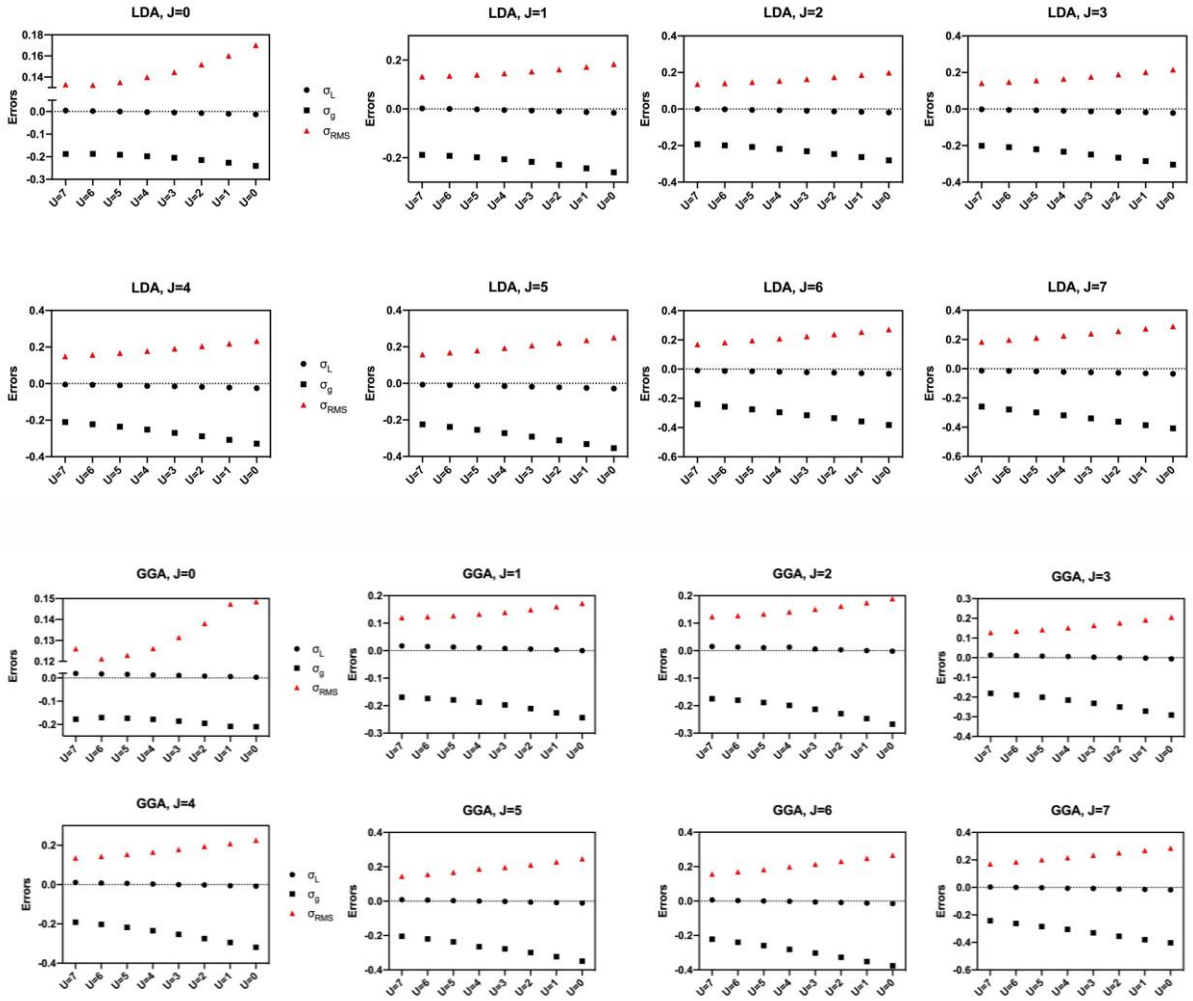

When **U = 6 and J = 0, LDA+U using GGA functional** give the best performance

H_2O adsorption sites

Long pair v.s. H bond

0-leg

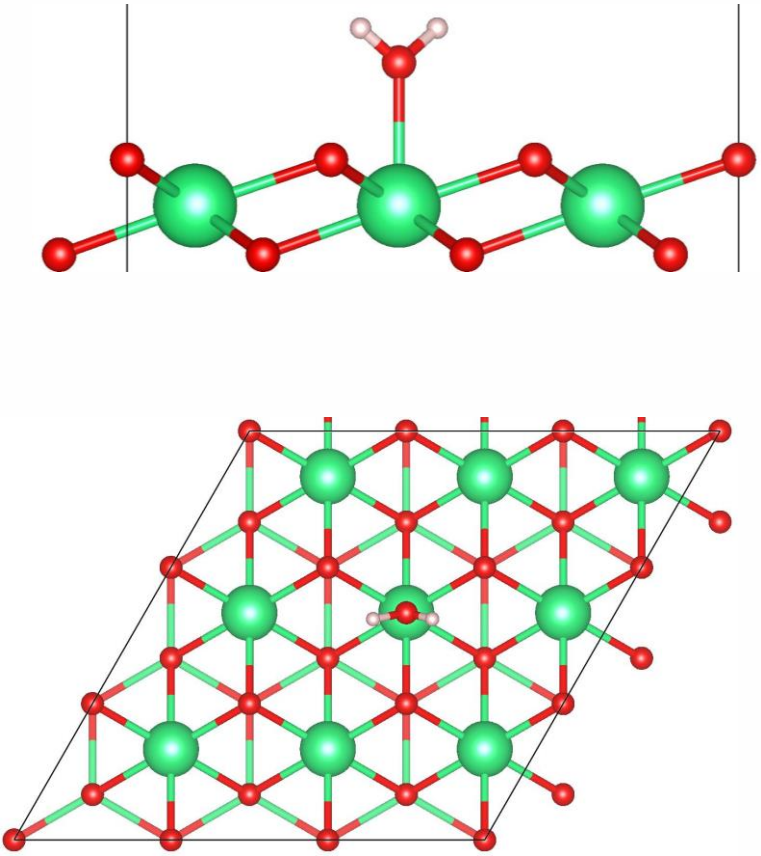

1-leg

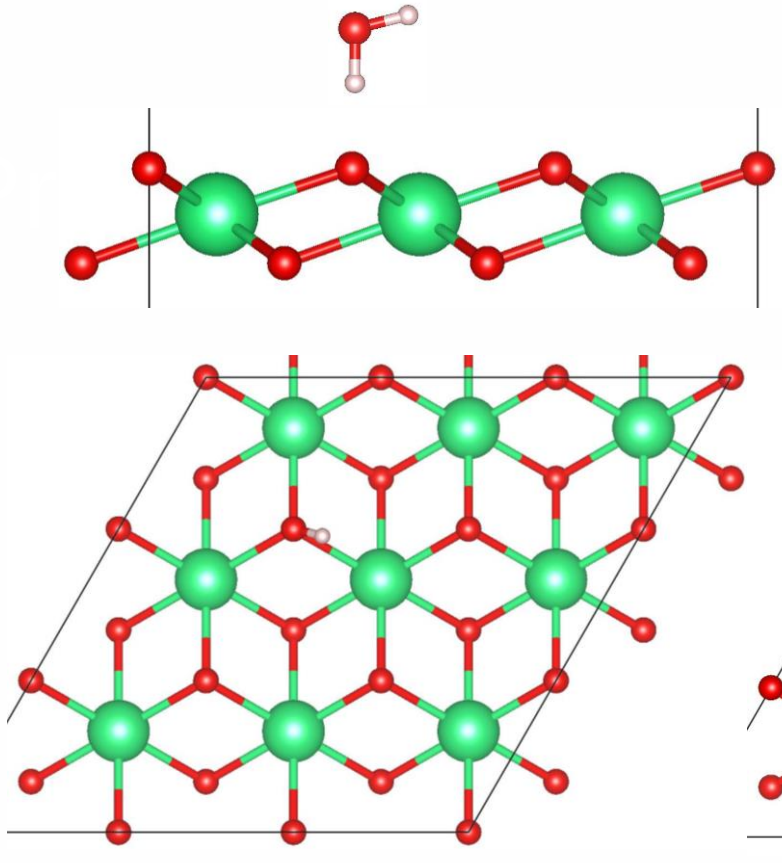

2-leg

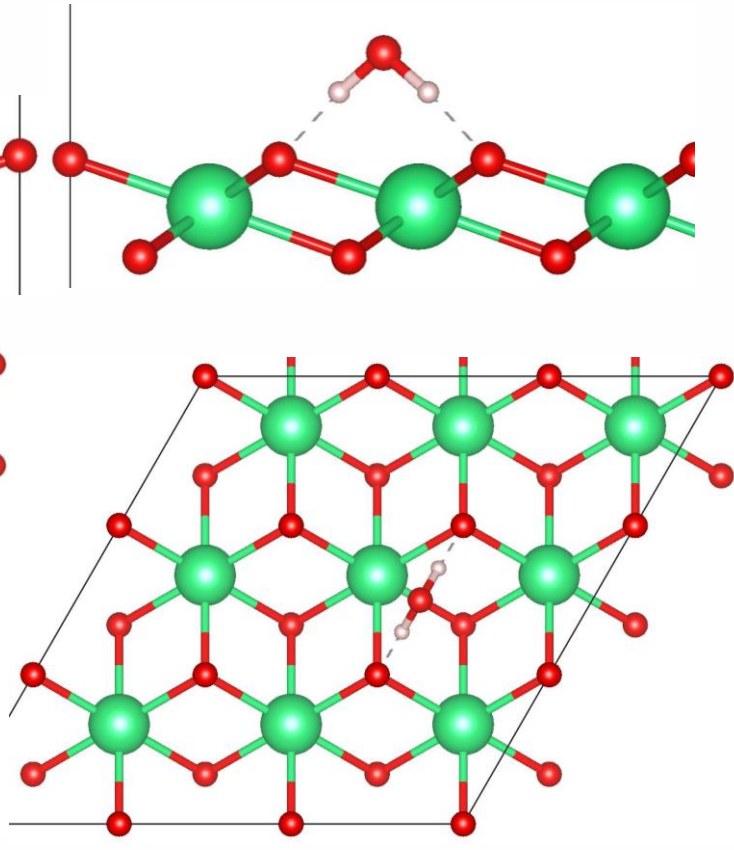

Step 1 $H_2O + * \rightarrow {}^{*}H_2O$

0-leg

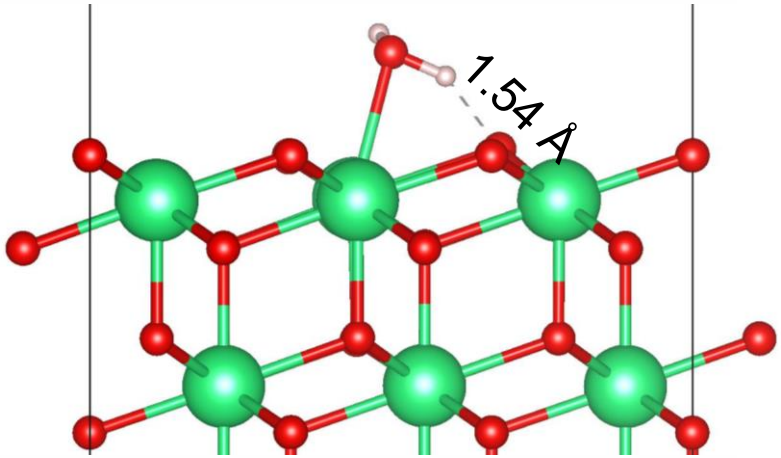

E_{ad}= -0.88 eV

1-leg

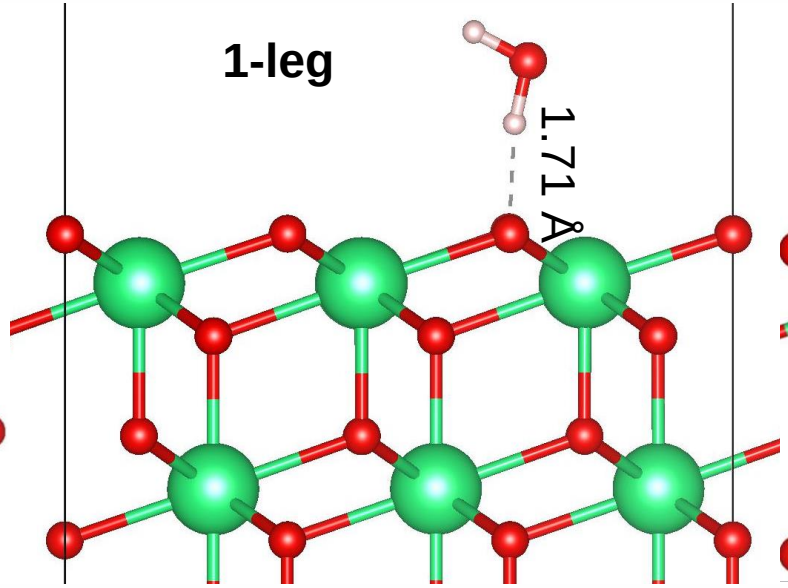

E_{ad}= -0.51 eV

2-leg

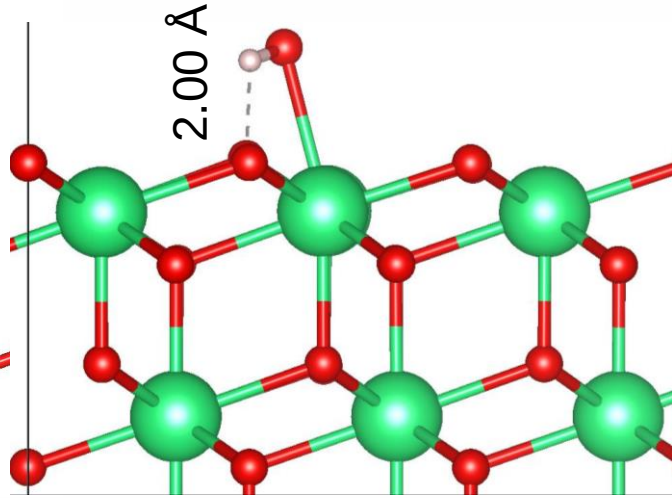

E_{ad}= -0.85 eV

ΔG_0	298K (RT)	500K
0-leg	-0.82 eV	-1.31 eV
1-leg	-0.46 eV	-0.95 eV
2-leg	-0.78 eV	-1.26 eV

- **Exothermic reaction**
- **High T promotes the reaction**

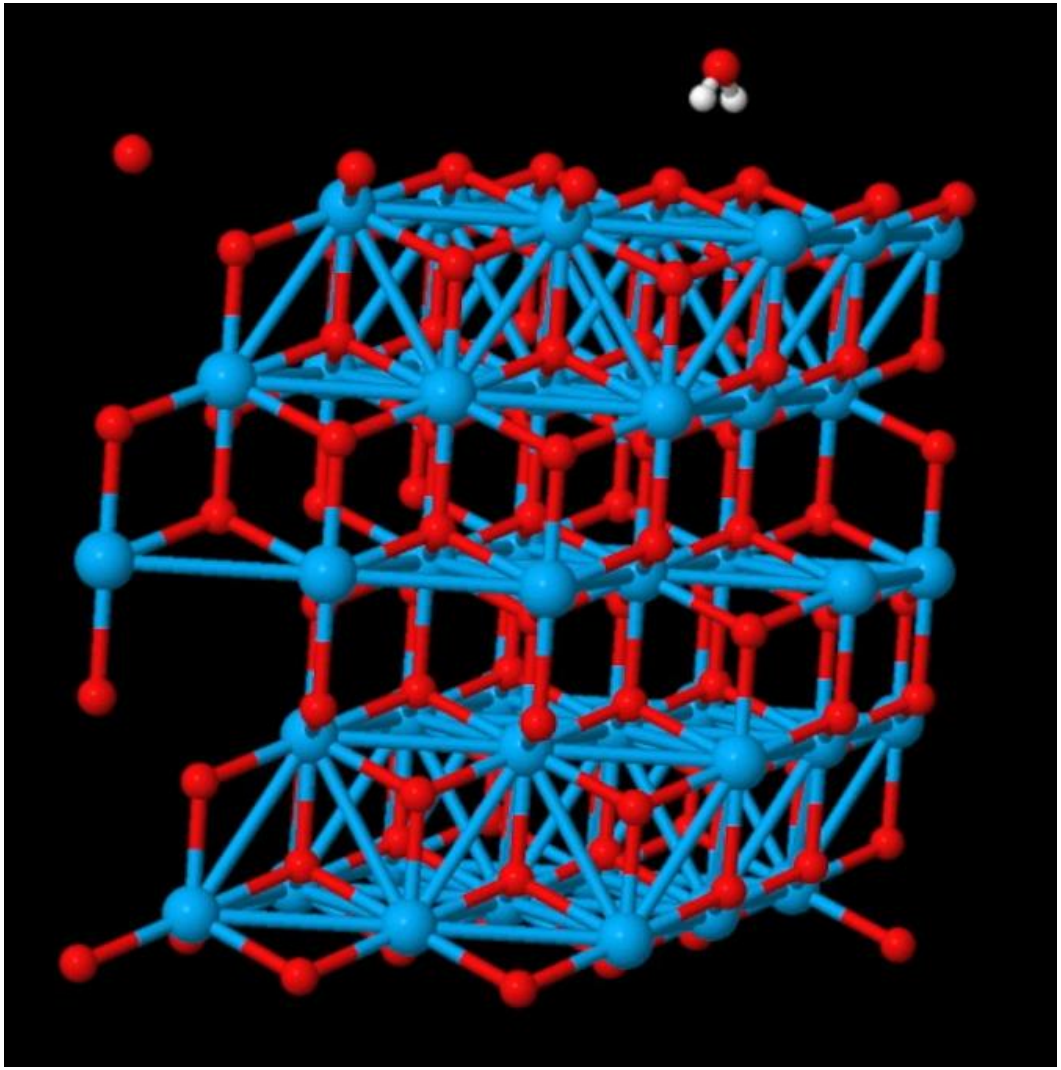

Lone pair > H bond

Charge difference of $H_2O@ThO_2(111)$

The Bader charge analysis* on the (111) ThO_2 vs. bulk

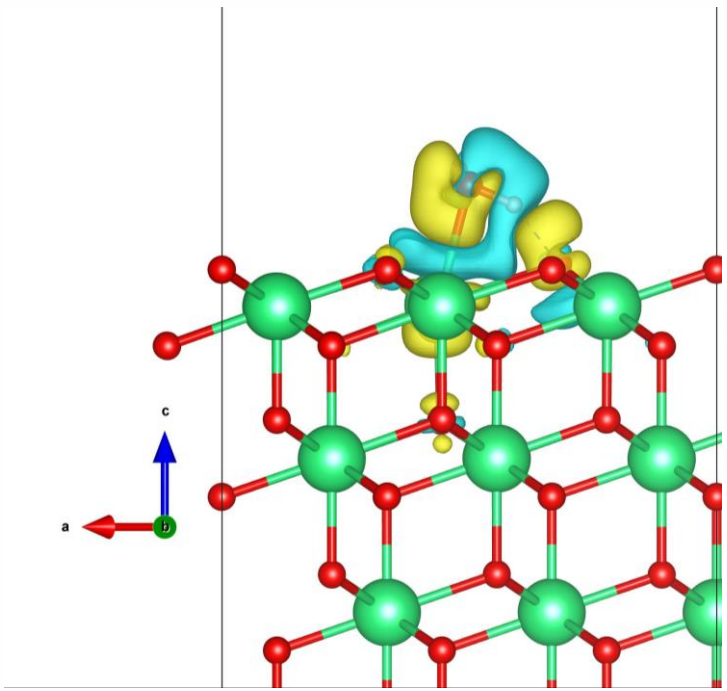

	Before adsorption	After adsorption
Top layer O (6)	7.39	7.39
Top layer Th (12)	9.24	9.19
2nd layer O(6)	7.38	7.41
3rd layer O (6)	7.38	7.41
water	8	8.04

Blue **-** Yellow **+** ($0.001e/r_b^3$)

Summary

1. Water adsorption is an **Exothermic reaction;**
2. Water **lone pair** outplay the H bond
3. The surface back donate electron to water;
4. More polarized hydroxyl group in water for further water splitting.

Step 2 $^{*}H_2O \rightarrow {}^{*}OH + {}^{*}H$

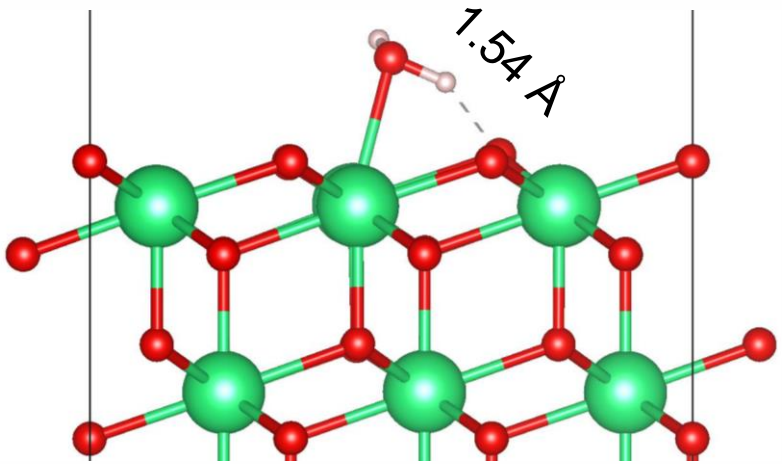

$\Delta G_{1(rt)}$= -0.65 eV

$\Delta G_{1(500)}$= -0.72 eV

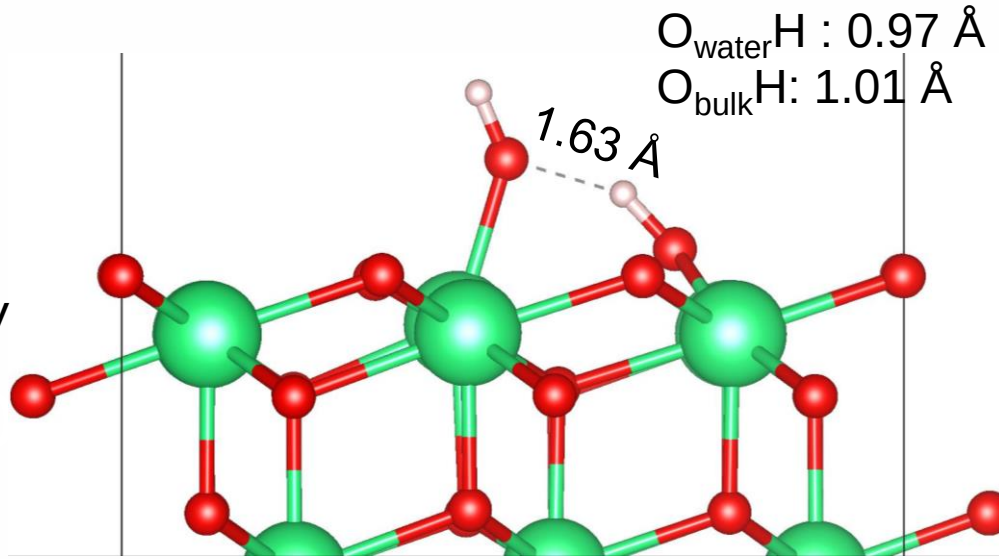

The dissociation energy barrier E_d is only **14.8 meV**

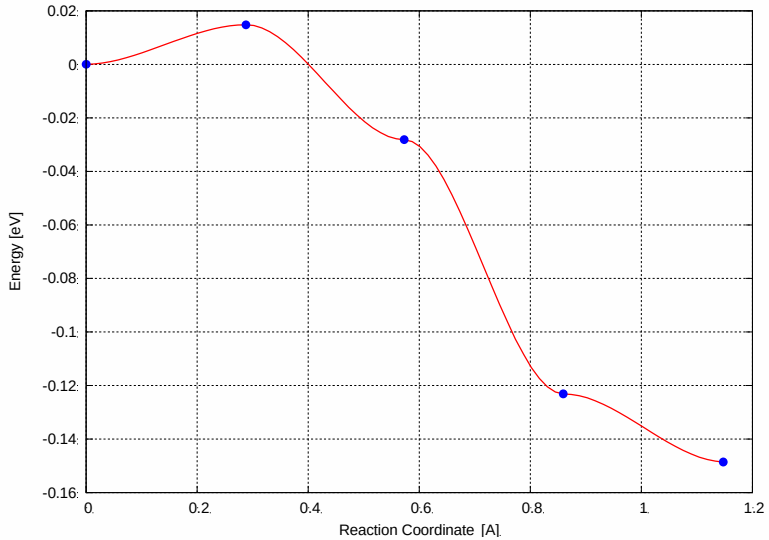

The desorption E (0.88 eV) is more than 55 times larger than E_d ;
K_bT at Room temperature is 25 meV.

The water dissociation is barrierless

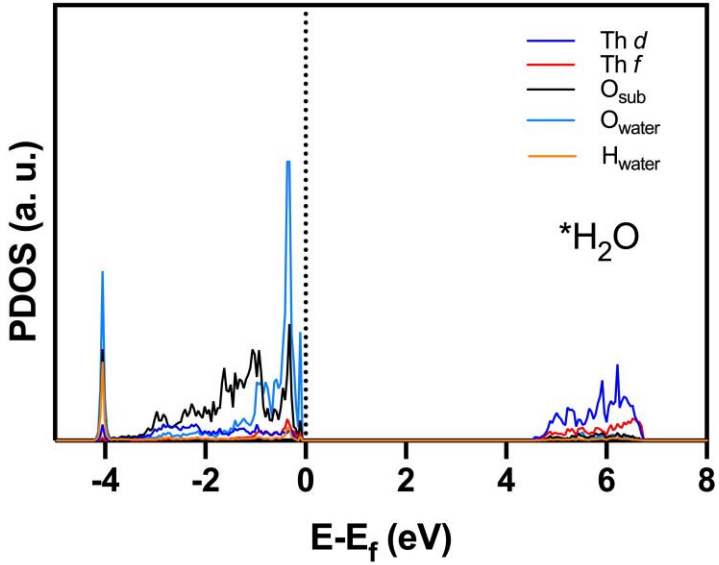

The hybridization of H with O_{water} , the surface O remain unchanged;
Only the O_{water} moved to the lower level.

The splitting of water is driven by itself

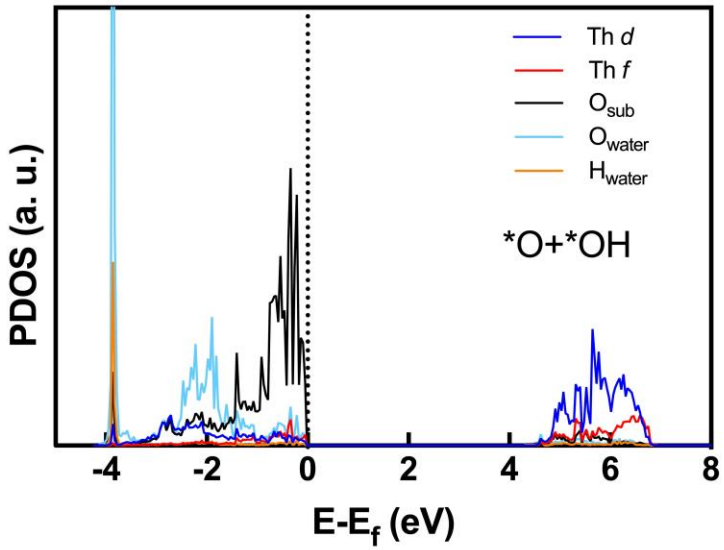

→ The “wetted” surface is ready for further water adsorption

TRANSCEND

Transformative Scien ng

Step 3 $H_2O_{2nd} + {}^{*}H + {}^{*}_{0}OH \rightarrow {}^{*}H_2O_{2nd} + {}^{*}H + {}^{*}OH$

A: the water interact with substrate first
B the water interact with the hydroxyl group

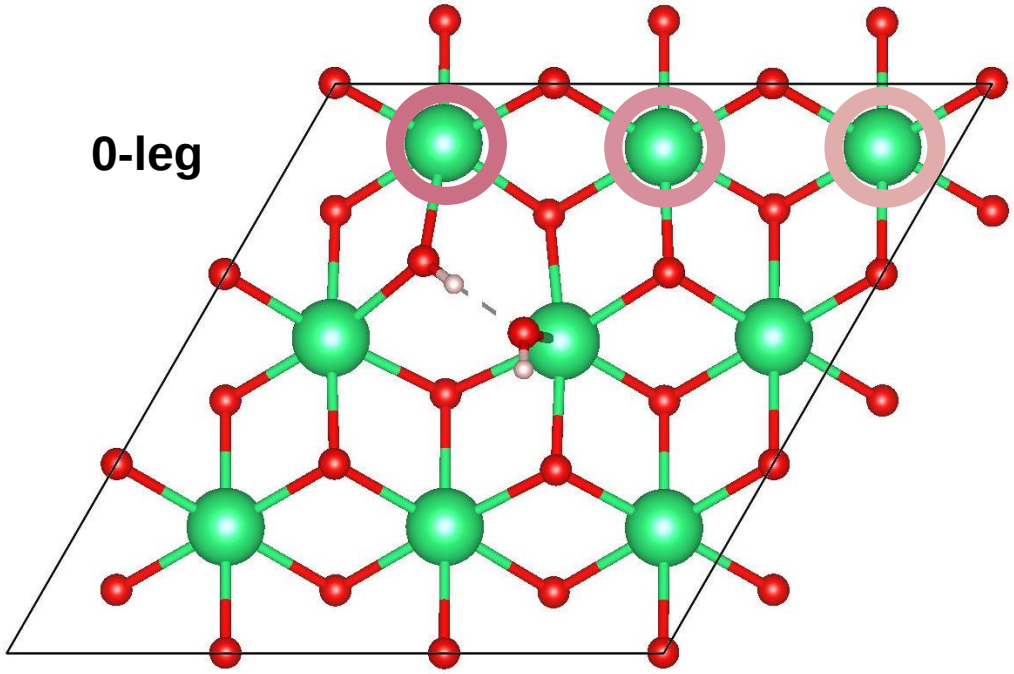

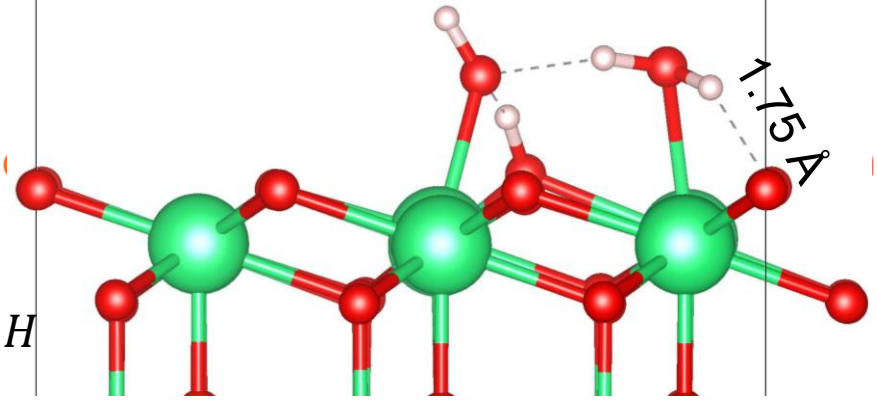

A1

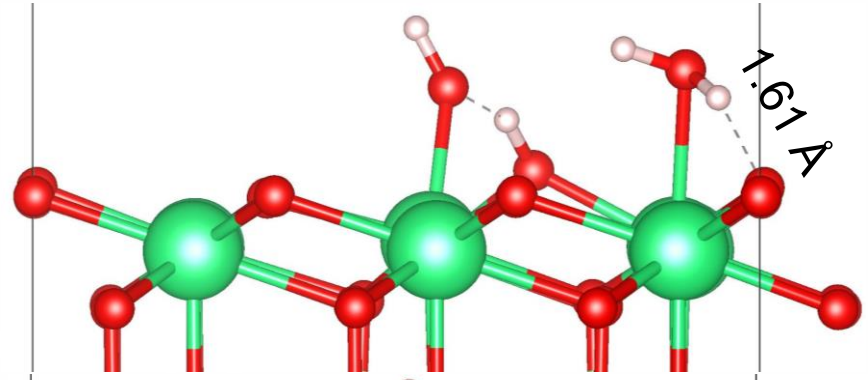

A2

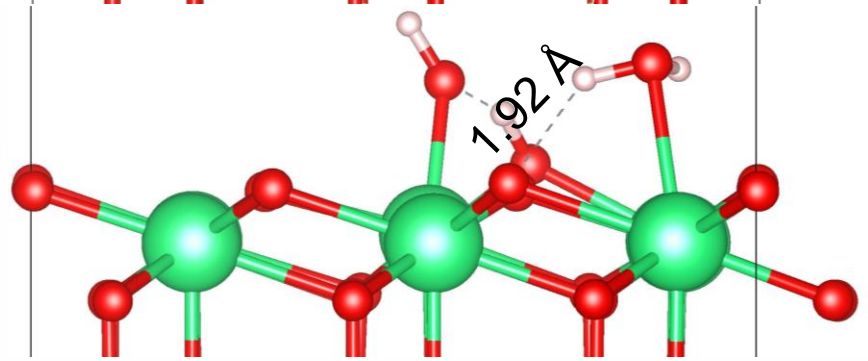

A3

- A1: Th atom nearby –$O_{bulk}H$ group
- A2: Th atom nearby –$O_{water}H$ group
- A3: far away

	A1	A2	A3	0-leg
E_{ad}	-1.06 eV	-0.89 eV	-0.86 eV	-0.88 eV
$\Delta G_{2(rt)}$	-0.89 eV	-0.77eV	-0.72 eV	-0.82 eV
$\Delta G_{2(500)}$	-1.38 eV	-1.26 eV	-1.21 eV	-1.31 eV

TRANSCEND

Transforma

ommissioning

1-leg

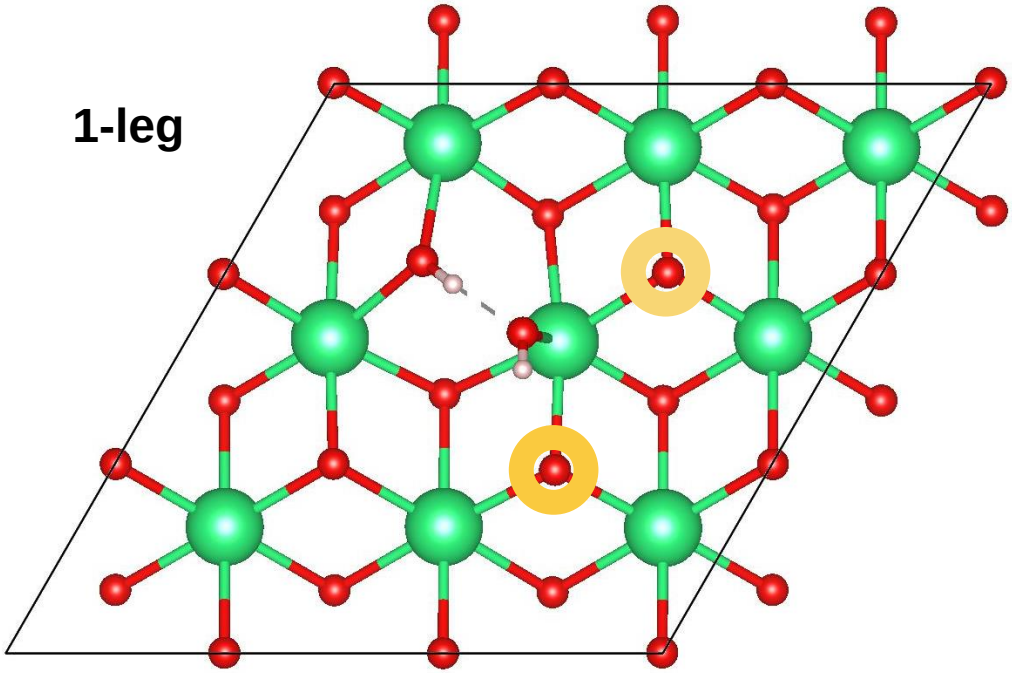

B1

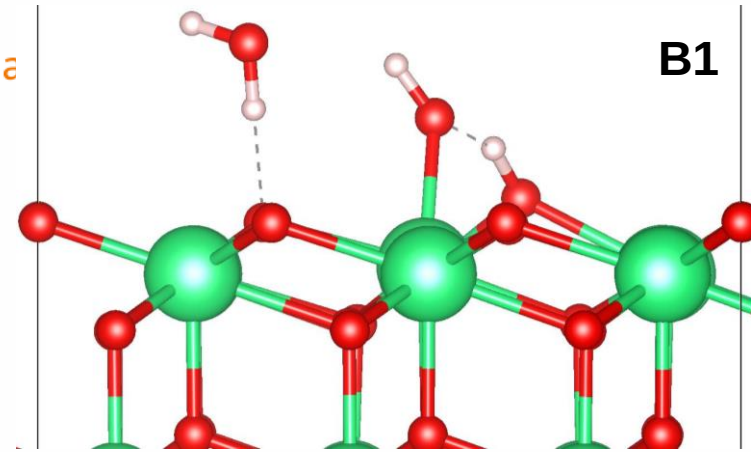

E_{ad} = -0.61 eV
$\Delta G_{2(rt)}$= -0.53 eV
$\Delta G_{2(500)}$= -1.02 eV

B2

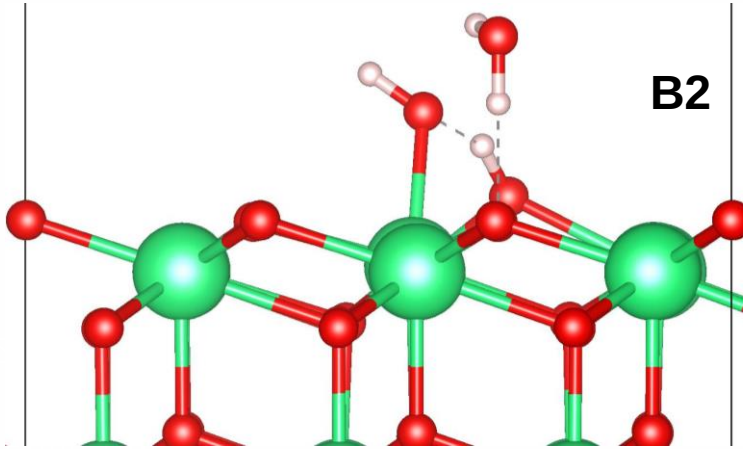

E_{ad} = -0.61 eV
$\Delta G_{2(rt)}$= -0.54 eV
$\Delta G_{2(500)}$= -1.02 eV

B1: water lone pair facing H in $–O_{water}H$, i.e. 2nd water in 1-leg configuration at ●

B2: H_{water} facing O in $–O_{water}H$, i.e. 2nd water in 1-leg configuration at ●

Summary

The ”wetted” surface promote further water adsorption at nearby **$–O_{sub}H$** hydroxyl group

Step 4 $^{*}H_2O_{2nd} + {}^{*}H + {}^{*}OH \rightarrow 2\ {}^{*}H + 2\ {}^{*}OH$

A1

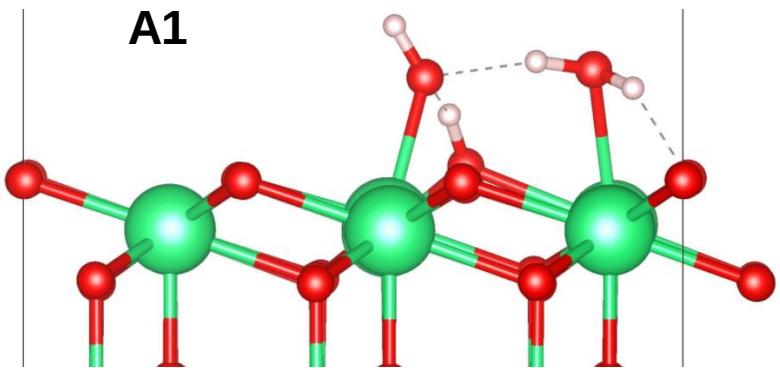

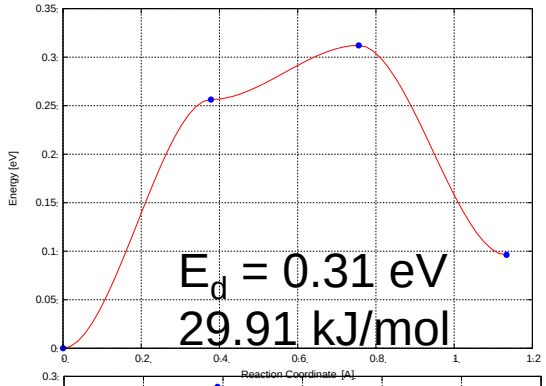

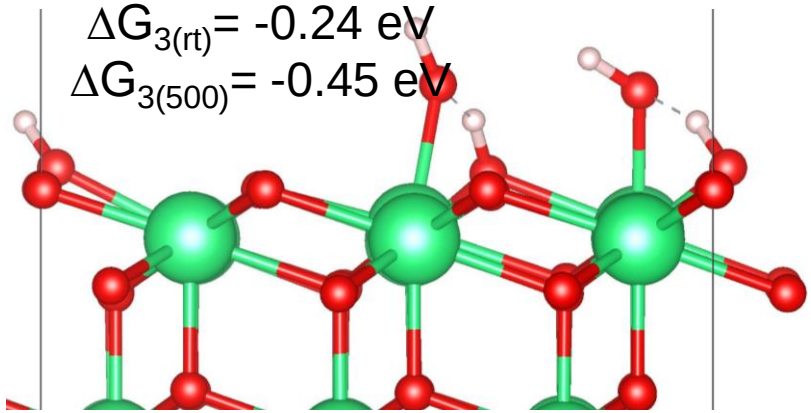

A2

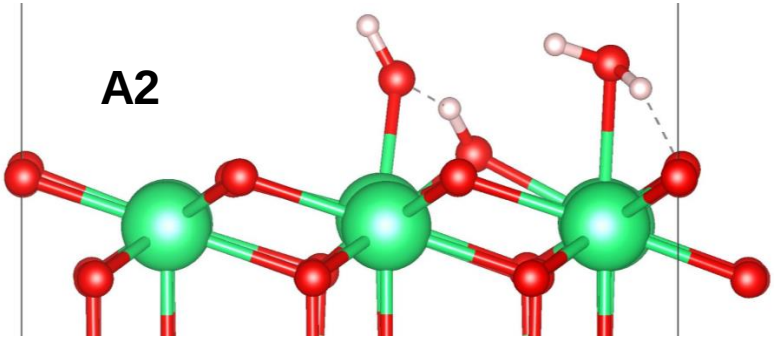

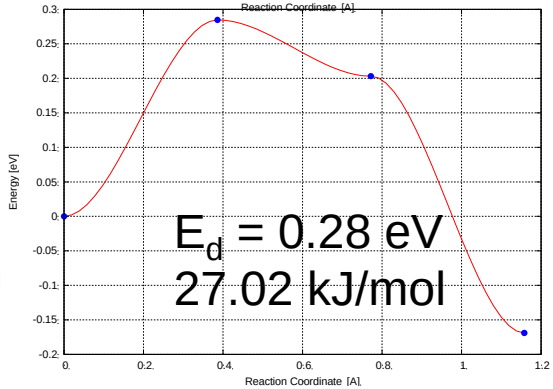

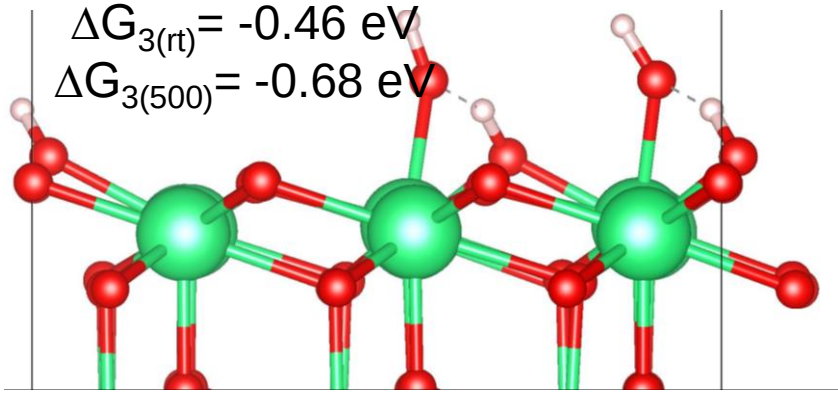

A3

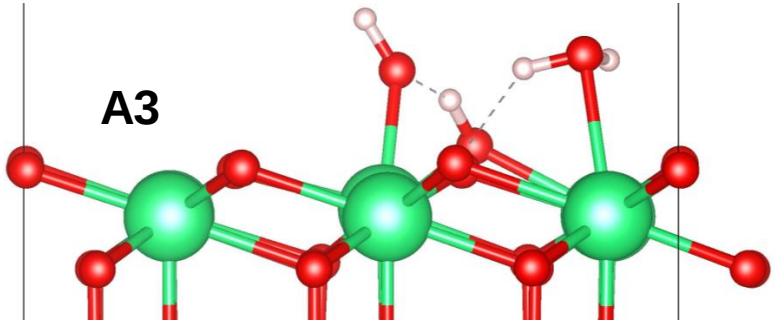

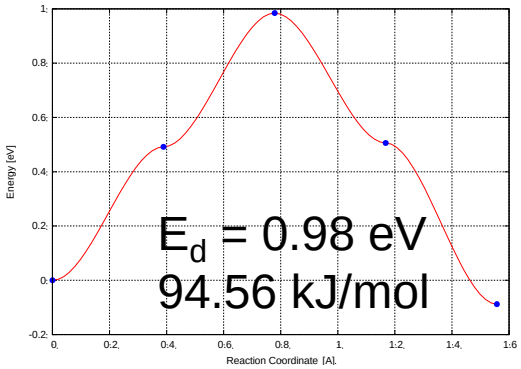

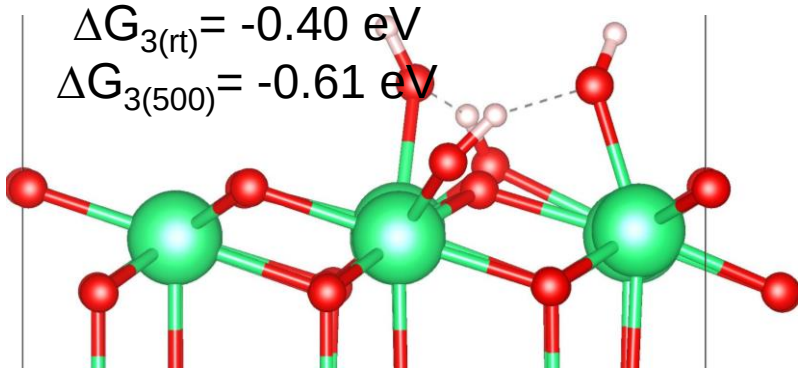

- All possess much **higher energy barrier** than the first water splitting
- **Exothermic reaction for the 2nd Water splitting but water at A3 site tends to desorption**

Summary

- Systematic studied the two DFT+U approaches of the prediction of the ThO_2;
- Provide a balanced consideration on both mechanical (lattice) and electronic (bandgap) properties;
- The ThO_2 (111) surface is hydrophilic and undergoes barrierless water dissociation at RT.
- The “wetted” surface even more attract water;
- However, it requires more energy to overcome the dissociation energy of the 2nd water.

Acknowledgements

- Prof. N. Kaltsoyannis and the group members
- EPSRC: EP/S01019X/1;
- Archer HPC and Grace@UCL and their associated services;

http://www.mub.eps.manchester.ac.uk/kaltsoyannisgroup/

TRANSCEND

Transformative Science and Engineering for Nuclear Decommissioning

Thank you

xiaoyu.han@Manchester.ac.uk

TRANSCEND

Transformative Science and Engineering for Nuclear Decommissioning

Assessment of zirconolite as a suitable waste-form for Pu immobilisation: first/initial results of durability experiments

Clémence Gausse, Ellie Ormerod, Laura J. Gardner, Neil C. Hyatt, Martin C. Stennett and Claire L. Corkhill

NucleUS Immobilisation Science Laboratory, University of Sheffield, United Kingdom

3rd December 2020
Virtual meeting

Radioactive Waste Management

The University Of Sheffield.

Australian Government

ANSTO

Energy
For a Low Carbon Future

Context

- Upon completion of fuel reprocessing, the UK will have a stockpile >140t of PuO_2
- Dual track strategy of immobilisation & reuse by MOX fabrication for LWR

  - Not all Pu will be suitable (Am-241 ingrowth) for MOX

  - Commercial case for MOX utilisation uncertain

- Wasteform selected for Pu immobilisation will need to play a functional role in supporting safe disposal

  - Retaining Pu and its daughters for over 100,000 years

- Hot Isostatic pressing identified as possible thermal treatment for PuO_2 wastes

✓ Uniform incorporation of radionuclides
✓ Batch process (inventory control)
✓ No off-gas production
✓ Minimal secondary wastes produced
✓ Hermetically sealed wasteform
✓ Facilitates high waste-loadings
✓ Significant cost saving

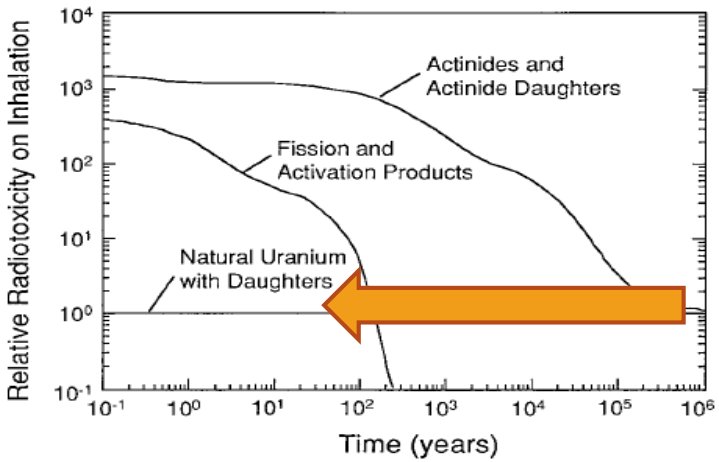

Context

Zirconolite ceramic / glass-ceramic

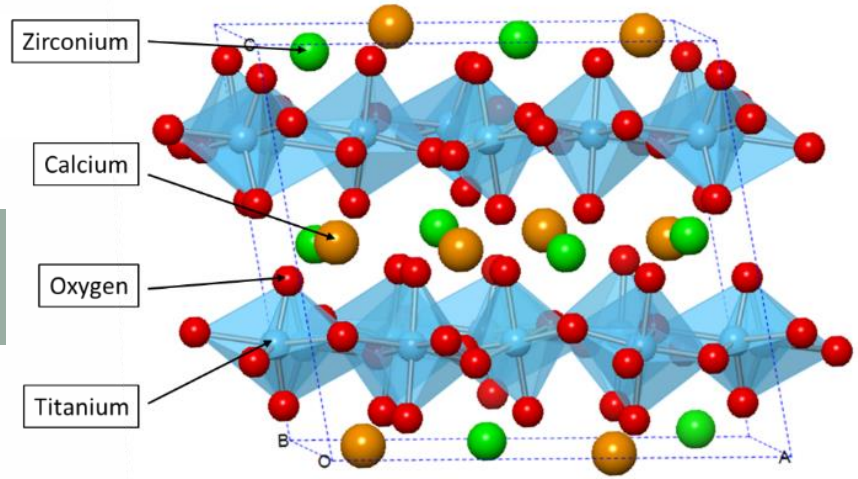

- $CaZrTi_2O_7$
- Natural mineral present in a wide variety of localities in Earth

  - Demonstrates a good chemical flexibility (incorporation of various cations)

  - High durability and radiation tolerance

- Full ceramic suitable for relatively pure Pu-residues
- Glass-ceramic suitable for higher impurity Pu-residues

1. Synthesis & characterisation of the zirconolite ceramic & glass-ceramic

2. Investigate the zirconolite *durability* via dissolution experiments

Synthesis of Ce-zirconolite glass ceramic

- $CaZr_{0.9}Ce_{0.1}Ti_2O_7 : Na_2Al_2Si_6O_{16}$ (70:30 ceramic glass ratio)
- Hot isostatic pressing (HIP) → Uniformly dense samples & void removal

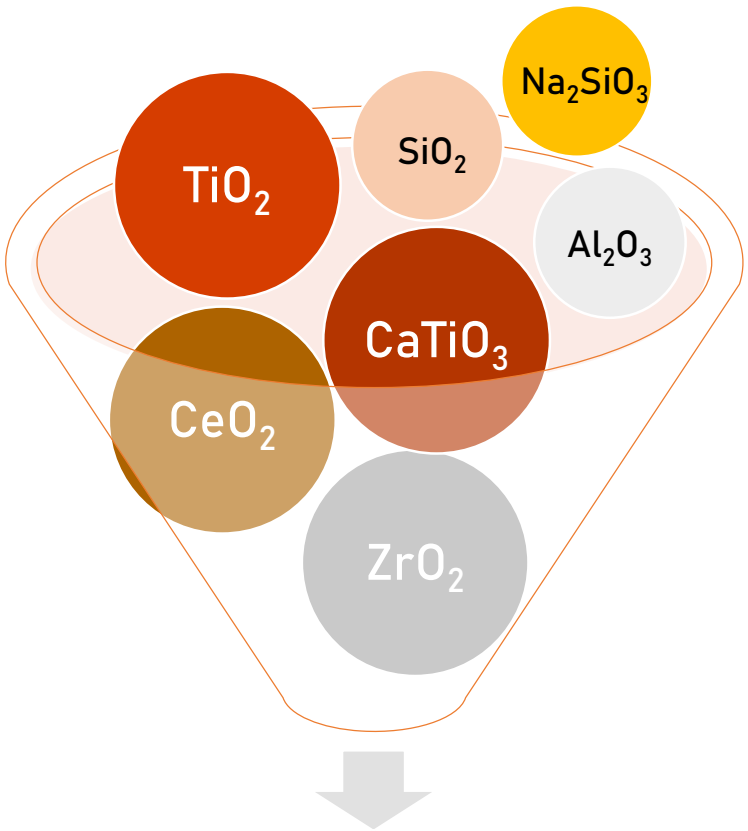

$CaZr_{0.9}Ce_{0.1}Ti_2O_7 : Na_2Al_2Si_6O_{16}$

HIP

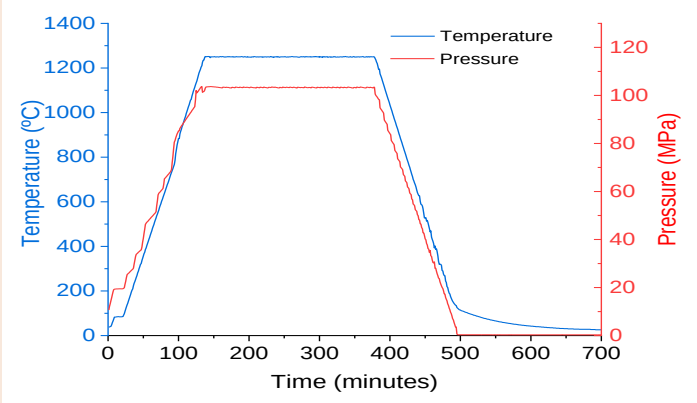

- Max temp 1200°C
- Max pressure 100MPa
- 10 hours
- 20 monoliths
- 3.709 g/cm^3

S.Thornber, PhD thesis, 2018

Characterisation of Ce-zirconolite glass ceramic

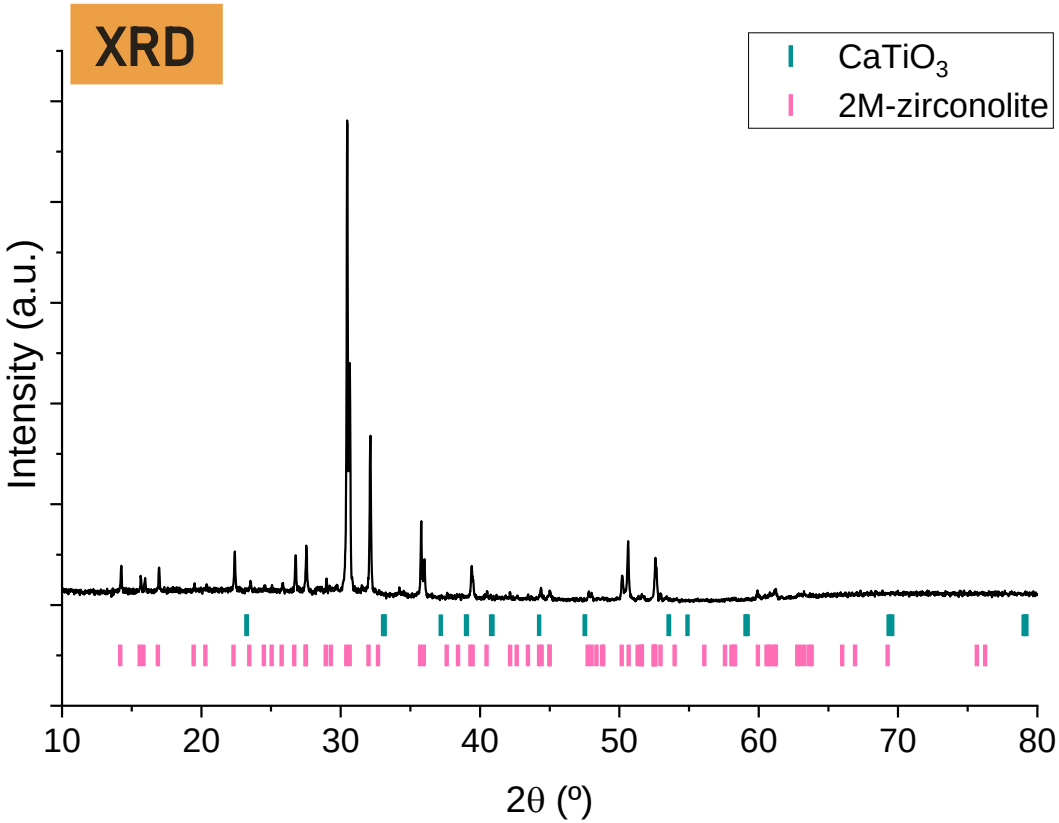

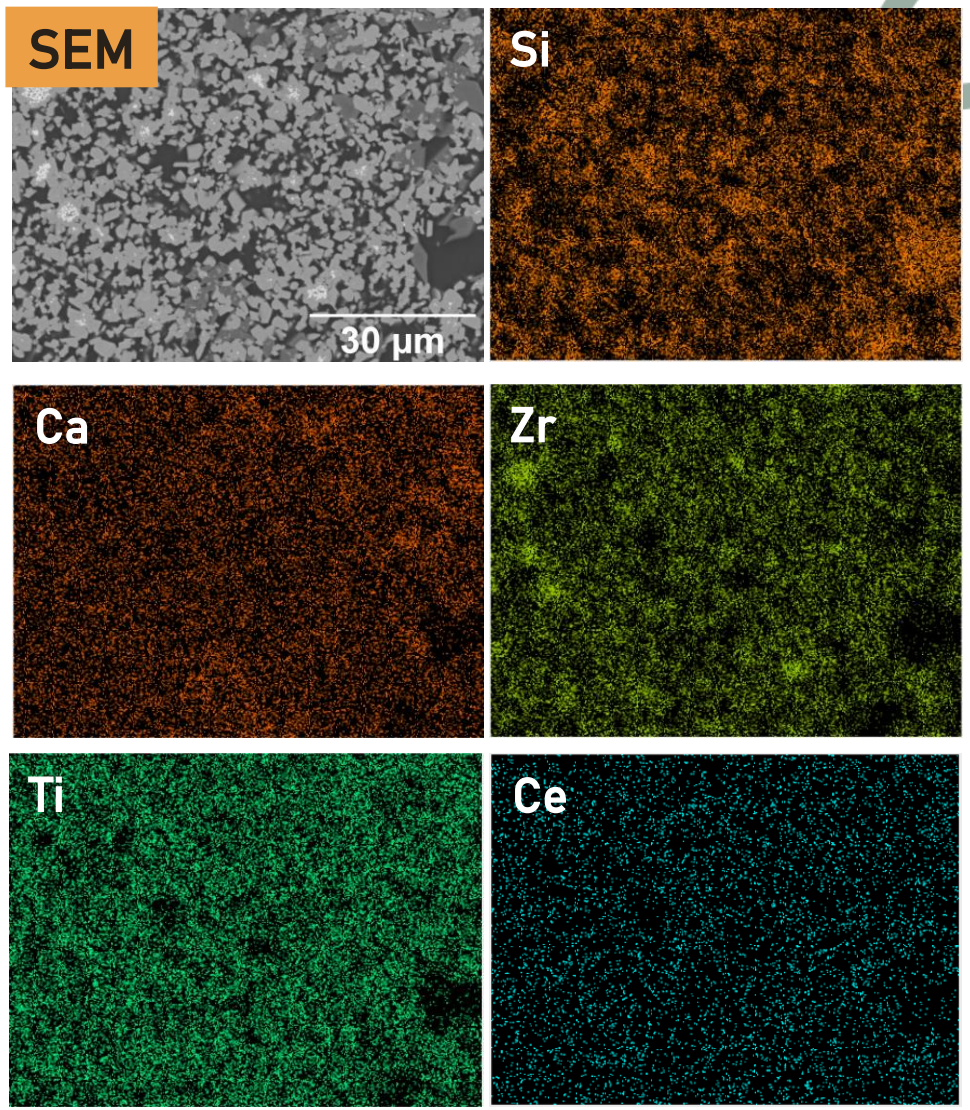

- No evidence of the perovskite $CaTiO_3$ phase on the XRD pattern
- ZrO_2 rich phase & Ca rich phase evidenced on SEM/EDS analyses

Synthesis & characterisation of $Ca_{0.8}Ce_{0.2}Zr_{0.9}Ce_{0.1}Ti_{1.7}Fe_{0.3}O_7$

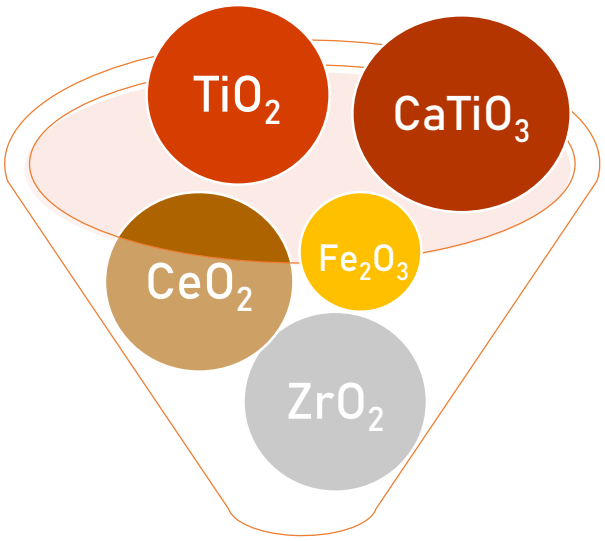

$Ca_{0.8}Ce_{0.3}Zr_{1.0}Ti_{1.7}Fe_{0.4}O_7$

10 mol% ZrO_2 & 10 mol% TiO_2 excess

Avoid in-growth of $(Ca,Ce)TiO_3$

XRD

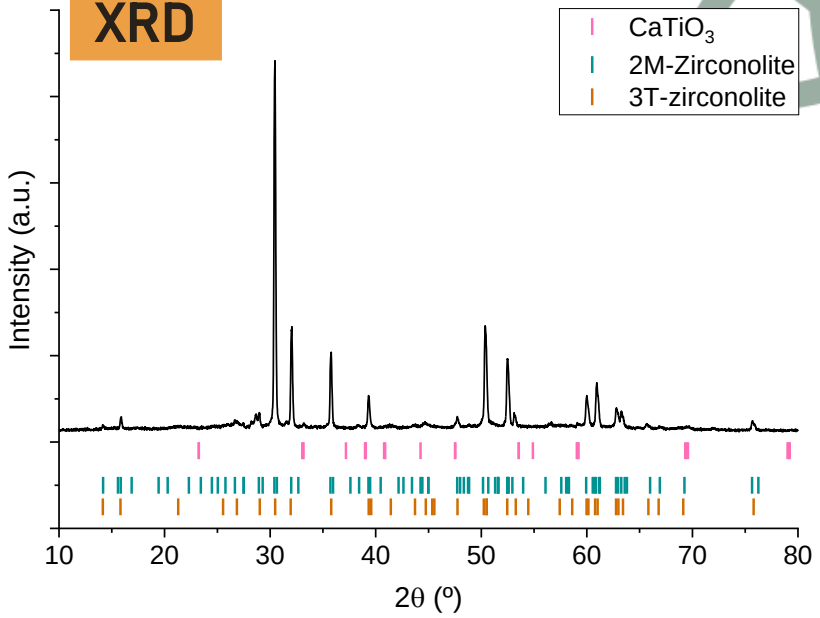

HIP

- Max temp 1350°C
- Max pressure 100MPa
- 10 hours
- 7 monoliths
- 4.734 g/cm³

SEM

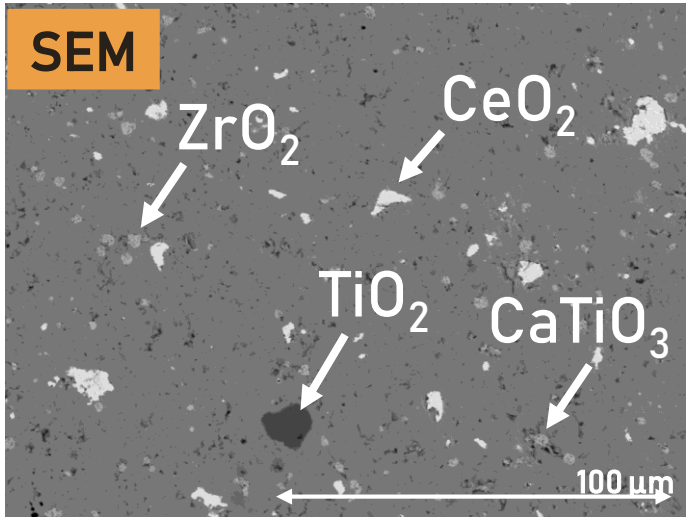

Dissolution experiments methodology

Close to equilibrium

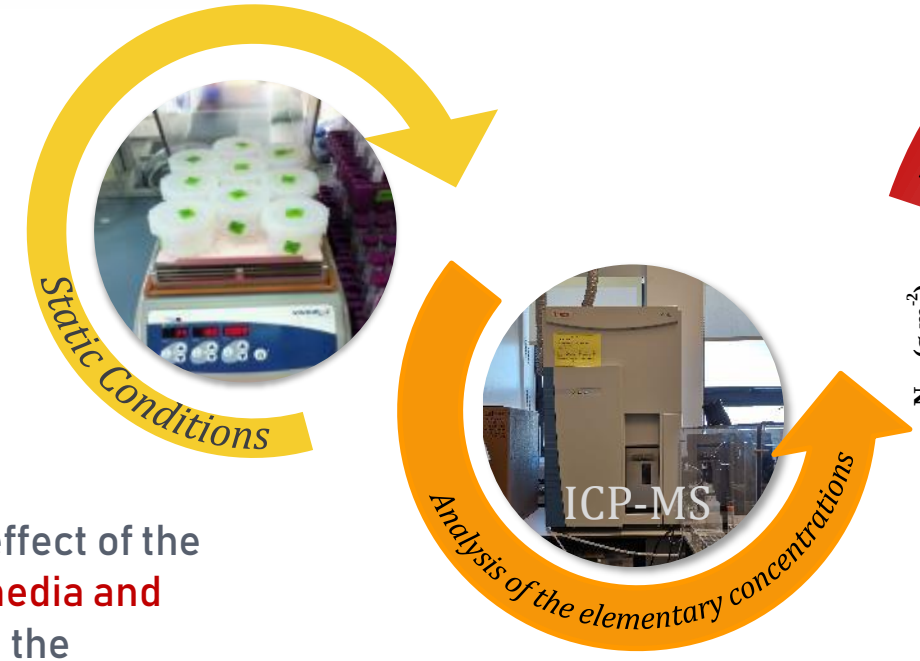

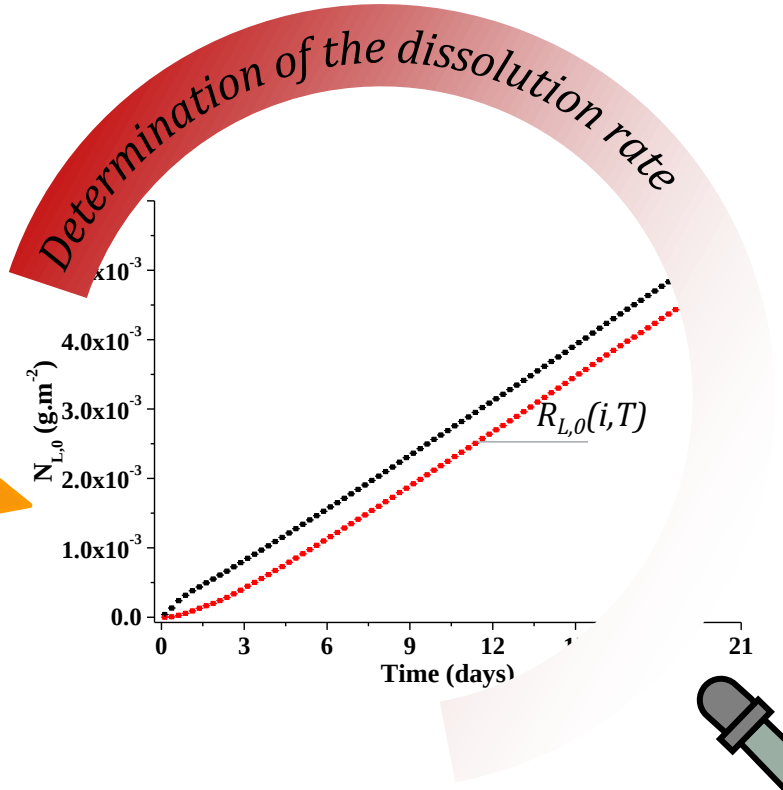

→ Study of the effect of the **dissolution media and saturation** on the normalized dissolution rate

$$R_{L,0}(i,T) = \frac{dN_L(i)}{dt} = \frac{1}{f_i} \times \frac{d}{dt}\left(\frac{C_i \times V}{S}\right)$$

Amount of (E_i) in solution (g.L^{-1})

Effective surface area (m^2)

Mass ratio of (E_i) in the solid

$R_L(i) \approx R_L(j)$	*Congruent dissolution*
$R_L(i) \neq R_L(j)$	*Incongruent dissolution*

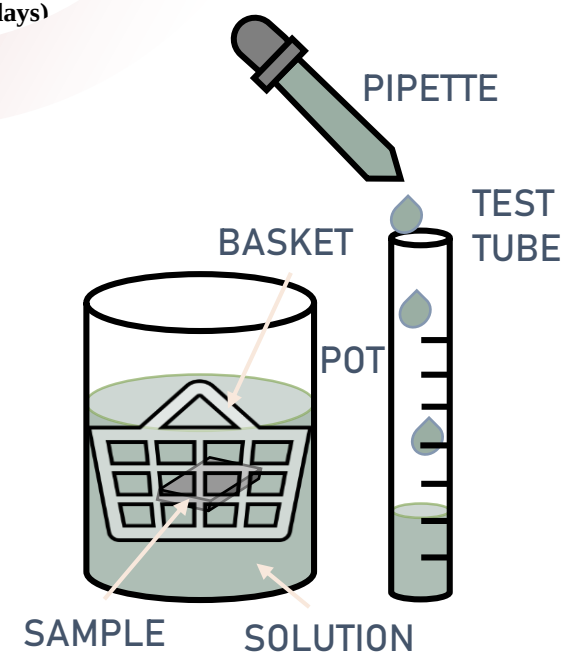

First durability results

19 mM NaCl + 1mM NaHCO3 – 40°C

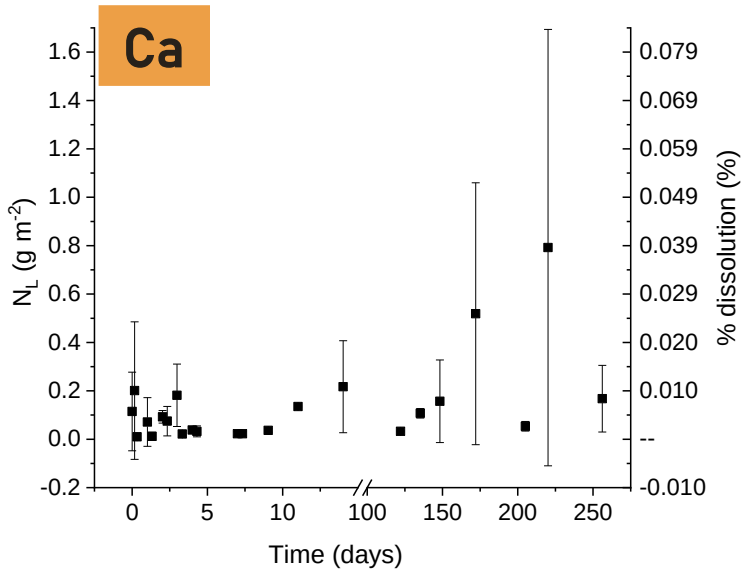

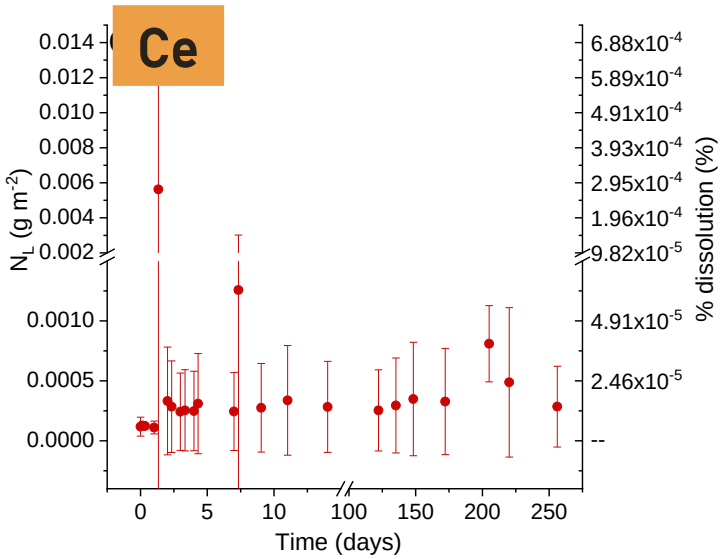

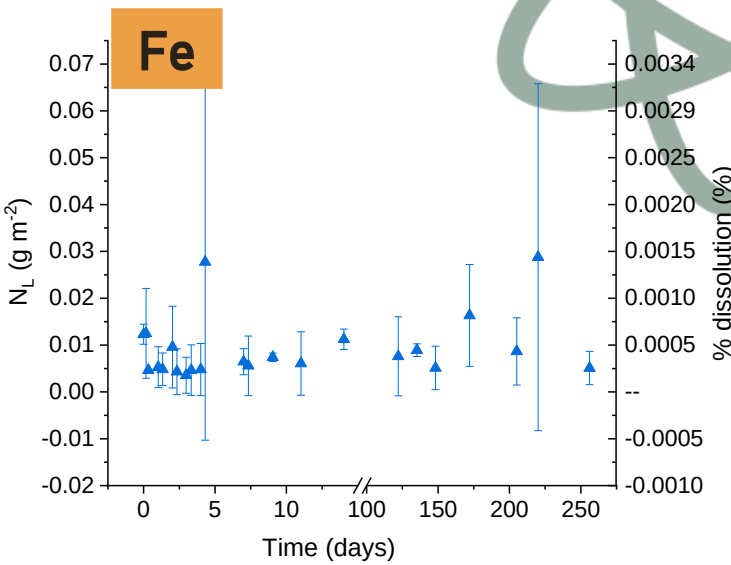

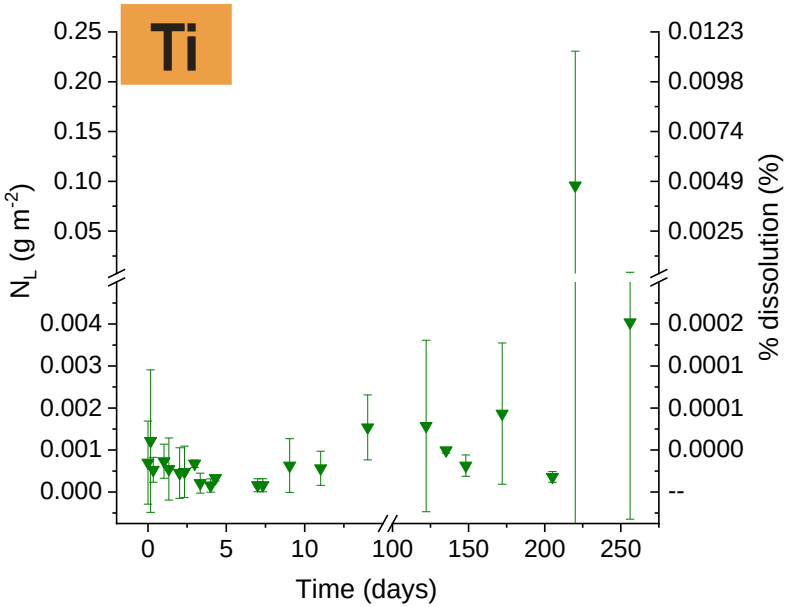

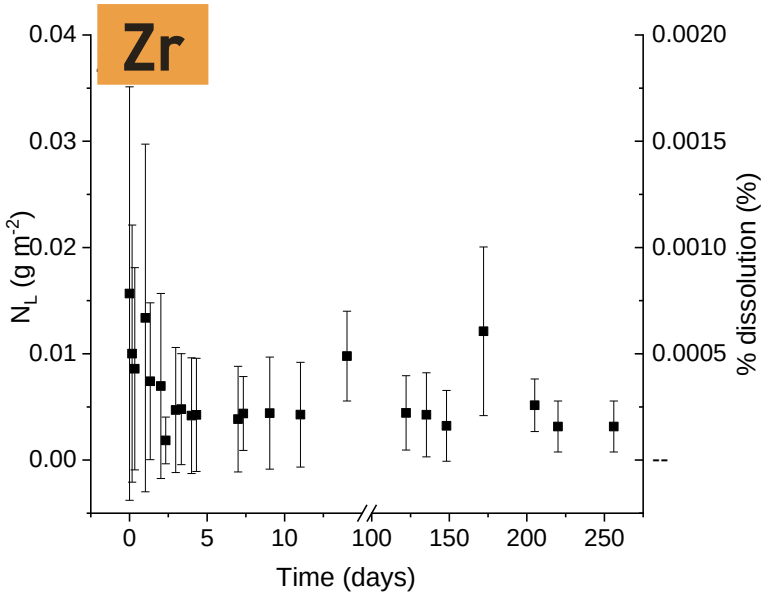

Great durability over time in conditions relevant to geological disposal

SI (TiO_2) = 1.74

Conclusion

1. HIPed zirconolite glass-ceramic & ceramic synthesised

2. HIP resulted in secondary phase formation, but a uniformly dense structure

3. First results in dissolution evidenced a great durability after 256 days

4. Dissolution experiments initiated for zirconolite glass-ceramic

Future work

- Determine the initial amount of secondary phases
- Synthesis & characterisation of HIPed U-doped zirconolite glass-ceramic
- Initiate static and dynamic dissolution experiments at different temperatures and acidity

TRANSCEND

HADES

Thank you!

Special thanks to:

Laura Gardner
Lewis Blackburn
Dan Bailey
Amber Mason
Paul Heath
Claire Corkhill
ISL team

We acknowledge financial support from the Radioactive waste management and EPSRC under grant number EP/156044-11/1. This research utilised the HADES/MIDAS facility at the University of Sheffield established with financial support from EPSRC and BEIS, under grant EP/T011424/1.

HENRY ROYCE INSTITUTE

Radioactive Waste Management

The University Of Sheffield.

Australian Government

ANSTO

NucleUS
Immobilisation Science Laboratory